GEORGE P.L. WALKER
ELICITATION INTERVIEW FOR PVHA PROJECT

VOLCANIC/TECTONIC SETTING

The presence of volcanoes in the region of interest (discussed below) indicates that a melting anomaly is present in the underlying mantle. Melting anomalies are characteristic of the Basin and Range province. These anomalies can occur from a section of mantle that is hotter than usual, or from an unusually shallow section of mantle in which melt is generated by the lowering of external pressure or from the presence of water in the mantle. Melting anomalies are accompanied locally by volcanism. The Basin and Range province has been subject to large-scale extension, with volcanism a direct result. In addition, a kind of mantle plume likely underlies the region (mantle plumes have dimensions of about 1000 to 2000 km), and scores of melting anomalies can be associated with a single plume.

The Crater Flat area is a volcanic field, but is not well defined relative to many other fields in the world. Structural control is indicated by the alignment of Makani, Red, Black, and Little Cones, but it is difficult to assess the extent to which orientation is a function of structure or the shape of the melting anomaly. Melting anomalies have a minimum size, comparable to the local thickness of the lithosphere (probably a few tens of kilometers in the region of interest). Within a melting anomaly there may be local areas, or "nodes," where there are higher magma generation rates and a higher potential for future volcanism. The NNE-trending Death Valley-Pancake Range (DV-PR) volcanic belt proposed by Smith et al. (1990) could trace the form of a melting anomaly, or it may be a tectonic line of some type (e.g., a major deep-seated fault). This belt, which extends from Death Valley to Lunar Crater, has been operative for the past 12 my, and appears to have a few "nodes," or fields, of more active volcanism due, most likely, to higher magma generation rates. There is no need to fill in the "gaps" between nodes of a melting anomaly through time. A ~10 my time frame is a typical lifetime for a melting anomaly, although they may also last much longer, such as the Hawaiian hotspot anomaly that has been active for at least 80 my.

The volcanism in the Crater Flat area is of monogenetic type. At the scale of the ascent of basaltic dikes, the recurrence of an eruption at the same location is purely random. Once a dike has cooled, there is no advantage for a new dike to follow the same path as the earlier dike, but there is some probability that it will coincide with it randomly. In general, however, the occurrence of

polygenetic volcanism is due to an advantage in the ascent of magma at the same location and utilizing the same conduit (or pathway). The physical model for polygenetic volcanism should attempt to explain this advantage (G. Walker presentation at PVHA Workshop 4, summary notes).

EVENT DEFINITION

Temporal Aspects

A volcanic event is equivalent to a volcanic eruption, consisting of the ascent of magma, and one or more episodes of surface eruption, followed by crystallization of the basaltic dike. Observation of this process elsewhere suggests that it lasts, at most, ten to a few tens of years. Among historical eruptions in monogenetic fields and flood basalts, that of Heimaey (Iceland) lasted about one month, and those of Laki (Iceland, 1783) and Capelinhos (Faial, Azores, 1957-58) about one year. Eruptions that lasted several years include Lanzarote (Canary Islands, 1730-36), Paricutin (Mexico, 1943-52), and El Jorullo (Mexico, 1759-74). At Krafla (Iceland) in 1978-84, a series of short rifting and eruptive episodes punctuated the general period of strong ground deformation that lasted from 1978 to 1984, and can be regarded collectively as a single magmatic event. There also are a few basaltic volcanoes (e.g., Stromboli and Etna) that show persistent activity spread over centuries; such volcanoes are rare.

Spatial Aspects

Dikes in monogenetic fields are typically less than 3 km long. Looking at modern fields, one can find alignments of cones that extend for 3 km or more. It is not clear whether these alignments are related to one dike or to a set of dikes. Areas of flood-basalt volcanism, such as Iceland and the eastern Snake River Plain, where 30-km-long dikes occur, are not good analogs to the Yucca Mountain area because of their much higher magma generation and eruption rates. There are, however, monogenetic volcanic fields where dikes exceed 3 km. Perhaps the best example is Lanzarote (Canary Islands), where a crater row 14 km long formed in the eruption of 1730-36. It is conceivable, but unlikely, that an event in the region of interest might extend over dimensions as large as this.

Geochemical Affinity

The geochemical and mineralogical affinity among volcanic deposits are clearly very important in identifying volcanic events.

Note: *The elements of the PVHA model are summarized in the form of a logic tree in Figure GW-1.*

REGION OF INTEREST

The region of interest is the area defined as the DV-PR volcanic belt by Smith et al. (1990). This belt, which extends from Death Valley to Lunar Crater, has shown persistent activity over the past 12 my and contains nodes of activity, such as Crater Flat and Lunar Crater, where volcanism has been more concentrated and is likely to continue to be active.

Within the DV-PR belt, a node of volcanism identified as the Crater Flat volcanic zone (CFVZ) (defined by Crowe and Perry, 1989) is particularly significant for this hazard analysis (Figures GW-2 and GW-3). Over the past 4.6 my, no significant changes in the volume or position of eruptions in the CFVZ have occurred and all eruptions have occurred within the zone. Over this time period, there is no strong evidence to indicate whether the volcanic system in the region is waning or waxing.

SPATIAL MODELS

Three alternative models are used to assess the future locations of volcanic activity in the Yucca Mountain area. These models and their weights are as follows:

Zonation	(0.1)
Field Shape	(0.4)
Spatial Smoothing	(0.5)

In the zonation approach, two zones are identified that are interpreted to have different rates of occurrence. These zones are the CFVZ, which is extended to include the Amargosa Valley aeromagnetic anomalies, and the background zone that is drawn to represent the "node" within the DV-PR volcanic belt (Figure GW-2).

The "field shape" approach is that developed by Sheridan (1992). In this model, the volcanic field defined by centers having ages less than 4.6 Ma follows a bivariate Gaussian distribution. It is assumed that the centers in the CFVZ are realizations of this distribution.

The spatial smoothing approach is generally that presented in Connor and Hill (1995), whereby the observed locations of volcanoes are smoothed with an Epanechnikov smoothing operator to assess the probability of future events. An important constraint on the approach is that 90% of the

probability density is assumed to occur within the CFVZ. This reflects the fact that the locus of volcanic activity over the past 5 my has been primarily within the CFVZ.

EVENT COUNTS

Based on the definition of volcanic "events" given earlier, the number of events and their uncertainties are assessed for each of the centers in the CFVZ (Table GW-1). The number of events is assessed for the past 5 my, which is judged to be the time period of most relevance to estimates of future hazard.

Lathrop Wells

Multiple events may have occurred at Lathrop Wells, but 1 event is most likely. The scoria blanket observed around the cone to the SE, S, SW, W, and NW appears to be continuous and provides evidence of only one eruption (the steep cone slopes are unstable and the sequence is difficult to decipher, so these observations were made beyond the base of the cone). Paleomagnetic data are consistent with a single event; other age-dating methods have large uncertainties because the rocks are so young. Geochemical differences between stratigraphic units are small and not considered to be strong evidence for multiple events, as the geochemical "noise" level in cinder cones is not yet sufficiently well established to assess the significance of small chemical variations. Scoria mounds on the E side of the cone are believed to be sections of collapsed cone rafted on lava, and not evidence of separate vents. At both the north and south ends of the principal cone, however, there is evidence of primary vents associated with in situ cones; these features define a 1.5-km NNW-trending fissure through the principal cone. Fitting of scoria mounds to linear fissures conceivably could represent 2 or 3 events additional to the main one.

The following event counts and their relative weights are assigned for the Lathrop Wells center: 1 (0.9), 2 (0.07), 3 (0.02), and 4 (0.01).

Sleeping Butte

Hidden Cone and Little Black Peak could represent 1 event with their 3-km spacing, or they could be separate events. To the south at the 3.7 Ma area of Crater Flat and at Lathrop Wells, the fissures have a NS strike. If this is the dominant fissure or dike trend in the region, Hidden Cone and Little Black Peak would most likely be separate events. Alternatively, but less likely, they could be connected by a NE-trending dike.

The event counts and their relative weights for the Sleeping Butte area: 1 (0.4), and 2 (0.6).

1.0 Ma Crater Flat

One, 3, or 4 events are represented at northern Crater Flat, where 4 cones dated at 1.0 Ma occur near a straight line trending NNE. This lineation could be the surface expression of a dike, but what appear to be eruptive fissures at Red Cone and Lathrop Wells have a more nearly NNW trend. A dike following a convenient fracture may make side steps, forming an en echelon pattern, but these steps are usually on the order of a few meters apart. The 1.5-km distance between Red and Black cones seems too large to be associated with a side-stepping dike. Red and Black cones could be 1 or 2 events, but are most likely to be separate events. Either interpretation can be made from the similar K-Ar age dates, or the variable geochemistry. The presence of amphibole at Black Cone and not at Red Cone weakly supports the interpretation of separate events. If there was evidence of a dike connecting Red and Black cone, it would strengthen the single-event interpretation. Little Cones is located 3 km from Red Cone, and it is possible that a single dike connects the two features. The small, secondary cone at Little Cones, which is considered to be part of the event that formed the larger cone, is located along the trend of this possible dike. Makani Cone is most likely a separate event because of the distance that separates it from Black Cone. If all of the cones are considered to be part of the same event, they could be related to "tension-gashes" in a NNW-trending strike-slip system.

These scenarios are considered: 1 event involving all four cones; 3 events consisting of Little Cones, Red and Black cones together, and Makani Cone; and four events (assumes Little Cones is 1 event).

The following event counts and their relative weights are assigned for northern Crater Flat: 1 (0.1), 3 (0.35), and 4 (0.55).

Buckboard Mesa

Several of the features appear to be consistent with a single event. There is a main cinder cone, the geochemical analyses show a reasonably tight clustering of values, and the volume is not implausibly large for a single eruption. This area was not field checked by the author, so he has not formed an independent position.

The following event counts and their relative weights are based primarily on the Crowe et al. (1995) assessment for Buckboard Mesa: 1 (0.75), and 2 (0.25).

3.7 Ma Crater Flat

At least two dikes can be observed in the northern part of the 3.7 Ma area and, because more than one dike is not usually associated with a single event, multiple events are likely represented. In the southern part of the area, the larger volumes suggest several events; however, the author has not made a field visit.

Based on the limited information available, the following event counts and their relative weights for the 3.7 Ma area are: 2 (0.5), 3 (0.25), 4 (0.20), 5 (0.05).

Amargosa Valley

Two to 6 events may be present in the Amargosa Valley based on interpretation of the aeromagnetic anomalies; 3 events are most likely. The minimum of 2 events is based on the basalts encountered in wells (anomalies B and D on the aeromagnetic map presented by V. Langenheim at PVHA Workshop 1); the 3-event scenario includes anomaly C, which has a strong dipolar signature. Anomalies E, F, and G are small and less likely to represent events, as they could be ancient features related to the rugged relief on the top of basement rock. It is difficult to evaluate if anomalies F and G represent 1 or 2 events. In addition to anomalies B, C, D, and E, the 5-event scenario includes anomalies F and G as a single event, and the 6 event scenario includes them as 2 separate events. Anomaly A, at the southern end of the 1.0 Ma Crater Flat basalts, is not considered to represent a separate event because it may be part of the larger anomaly related to the Tertiary volcanics.

The following event counts and their relative weights are assigned to the Amargosa Valley area: 2 (0.3), 3 (0.4), 5 (0.15), and 6 (0.15).

Thirsty Mesa

This area was visited but not field checked carefully by the author, so he has not formed an independent position and will follow the interpretations of Crowe et al. (1995). It is noted that the volumes at Thirsty Mesa are not implausibly large to have been associated with a single event.

The following event counts and their relative weights are based primarily on the Crowe et al. (1995) assessment for Thirsty Mesa: 1 (0.85), 2 (0.09), and 3 (0.06).

RATES OF OCCURRENCE

Using the event counts discussed above, the rates of occurrence are calculated for use in the PVHA. These rates are calculated for the post-4.6 Ma time period and for each of the 2 source zones (see summary in Table GW-2).

The selected time period for the rate estimates is from 4.6 Ma to the present. If more recent time periods are used, there are too few points to provide meaningful rate estimates. If older time periods are used (e.g., 10 Ma) changes in tectonics and volumes of volcanics have occurred that can lead to problems in assessing rates. Over the past 4.6 my there have not been significant changes in volumes, the location of volcanism has persisted within the CFVZ without evidence of migration, and there is no significant evidence for waxing or waning of volcanism from the data available.

The rates within the CFVZ are assessed using the counts within northern (1.0 Ma) Crater Flat, 3.7 Ma area, Lathrop Wells, Thirsty Mesa, Sleeping Butte, and Amargosa Valley. The background zone is the "node" of the DV-PR belt. The rate for the background zone comes from the counts at Buckboard Mesa.

Undetected Events

There is no evidence for undetected or buried events in the CFVZ, but in many other volcanic areas in the world there is ample evidence of these features. What could be referred to as "abortive eruptions" have been observed in many tectonic environments. Earthquake swarms of the type that presage eruptions have been recorded in areas where underground magma movements were suspected on the basis of ground deformation. The geologic record includes features such as sill swarms that provide evidence of large-scale subsurface magma movements. Most large sill swarms were emplaced in non-lithified sediments just above basement rock, an area that is typically coincident with the level of neutral buoyancy (LNB). LNB occurrence in an area is an important control, as is magma viscosity, with more viscous magmas like andesites less likely to reach the surface. In active volcanic areas, abortive eruptions could compose up to 50% of the total number of events. Possible examples include: Krafla in northern Iceland, which experienced major rifting events in 1978-84, but only small lava flows were erupted; Rabaul in Papua New Guinea, which had an intense earthquake swarm peaking in 1983, but no eruption (an eruption did, however, occur in 1995); Long Valley in California, which experienced a seismic crisis in 1982; and recent earthquake swarms off Sao Miguel in the Azores. Kilauea volcano in Hawaii also experiences dike injection events commonly without eruption, the event in the Southwest Rift Zone in August 1981 being a fine example.

To account for the possibility of undetected events in assessing the rates for the PVHA, and considering possible analogues, the following factors should be used to multiply the counts derived from observed/interpreted events:

	Cumulative
1 x counts	(0.3)
2 x counts	(0.5)
5 x counts	(1.0)

TEMPORAL MODELS

A homogeneous Poisson temporal model is used to describe the distribution in time of volcanic event occurrence. In terms of a time-series analysis, there is definite evidence for temporal clustering of events. However, given the small numbers of events, we are not able to reject the hypothesis that the rate is uniform over the past 4.6 my. Further, the 4.6 my time period is selected to maximize the number of events that can be used for the analysis, while minimizing the variations in volume and location.

EVENT GEOMETRIES

Dike lengths associated with future events are as long as about 3 km. There is uncertainty in the tail of the dike length distribution (i.e., if the 1.0 Ma basalts in Crater Flat represent 1 event, then dike lengths up to 12 km are allowable). Dike lengths are controlled by the intensity of melting anomalies and associated magma generation rates. The CFVZ is considered to be a low intensity field. On a spectrum of intensity, monogenetic fields such as Crater Flat are on one end, and flood basalt fields, such as in the eastern Snake River Plain, are on the other end. In monogenetic fields that are appropriate analogues for the CFVZ (e.g., El Jorullo in Mexico, active in the 1700s), dikes are no more than about 3 km in length. The cumulative distribution of length is: 2 km (0.5), 3 km (0.9), and 12 km (0.95). For small monogenetic volcanic fields, like those of the Yucca Mountain region, the maximum dike length would be in the range of 15 to 20 km. Both maximum values should be used with equal weight. The dike is likely to be centered on the "event." Therefore, a triangular distribution is used for the event location on the dike.

Note: *At the request of Dr. Walker, a smooth interpolation function was fit to his discrete cumulative density estimates for dike length. The resulting cumulative distributions and density functions are shown on Figure GW-4.*

Data on dike orientations collected recently in Scotland indicates that dikes follow fractures and other zones of weakness with a wide variety of trends. The magnitude of stress differences may control these orientations. Observations of a N-trending fissure system at Red Cone, N-trending dikes at the 3.7 Ma area, and the NNW-trend of fissures at Red Cone and Lathrop Wells are not

consistent with the regional direction of least horizontal compressional stress, N60W (after Stock and Healey, 1988). They are consistent, however, with the NNE-trend of the DV-PR zone. The tension pattern at the top of the crust may be different from the pattern at depth. In Crater Flat, for example, the deep dikes may trend NE as tension gashes but finger upwards toward the surface and form shallow dikes that trend NNW. Future dike orientations in the YMR are assessed to have a bimodal distribution centered on N20W±30 (2σ) and N40E±30 (2σ) with equal frequency.

Dike widths can be estimated using a length to width ratio of about 1,000/1. Width to length ratios are dependent on the elastic properties of rock and the rate of cooling. The longer the dike, the greater the width of the dike. Ballooning of dikes near the ground surface may occur from erosion of dike walls through mechanical or thermal effects.

HYDROMAGMATIC ACTIVITY

A wide variety of hydromagmatic eruptions have been observed around the world, including small steam explosions, huge-volume phreato-magmatic eruptions, maar-type eruptions, etc. Hydromagmatic eruptions inland from the coast are most common in areas having a good regional aquifer and shallow water table. The author disagrees with the interpretation that some of the ashes at Lathrop Wells are hydrovolcanic. Therefore, there is not a single example of hydrovolcanism in the entire region, suggesting a very low probability of future occurrence. An assessment is made that the estimate of M. Sheridan (presentation at PVHA Workshop 4) of 1 or 2 hydrovolcanic events per 100 events is reasonable.

TYPE OF ERUPTIONS

Volcanism in the area of interest is consistent with monogenetic field analogues, and future volcanism will most likely erupt small volumes (0.1 to 0.2 km^3) of slightly alkalic basalts. The record of volcanism in the area of interest indicates some mildly explosive volcanism, including Strombolian activity typical of monogenetic field analogues, so this pattern is likely to continue. Lavas will be more viscous than Hawaiian tholeiite, but fairly fluid. There is no evidence for a bimodal composition of lavas; therefore, the probability of rhyolite appearing in the region is small (<0.05).

George P. L Walker MAY 9, 1996.

REFERENCES

Connor, C.B., and Hill, B.E., 1995, Three nonhomogeneous Poisson models for the probability of basaltic volcanism: application to the Yucca Mountain region, Nevada, USA: Journal of Geophysical Research, v. 100, no. B6, p. 10,107-10,125.

Crowe, B.M., and Perry, F.V., 1989, Volcanic probability calculations for the Yucca Mountain site: estimation of volcanic rates: Proceedings, Nuclear Waste Isolation in the Unsaturated Zone, Focus '89, American Nuclear Society, p. 326-334.

Crowe, B.M., Perry, F.V., Geissman, J., McFadden, L., Wells, S., Murrell, M., Poths, J., Valentine, G.A., Bowker, L., and Finnegan, K., 1995, Status of volcanism studies for the Yucca Mountain site characterization projects: Los Alamos National Laboratory Report LA-12908-MS, March.

Sheridan, M.F., 1992, A Monte Carlo technique to estimate the probability of volcanic dikes: Proceedings, High-Level Radioactive Waste Management, v. 2, p. 2033-2038.

Smith, E.I., Feuerbach, D.L., Nauman, T.R., and Faulds, J.E., 1990, The area of most recent volcanism near Yucca Mountain, Nevada: implications for volcanic risk assessment: Proceedings, High-Level Radioactive Waste Management, v. 1, p. 81-90.

Stock, J.M., and Healey, J.H., 1988, Geological and hydrologic investigations of a potential nuclear waste disposal site at Yucca Mountain, southern Nevada, *in* M.D. Carr and J.C. Yount (eds.), Geologic and Hydrologic Investigations of a Potential Nuclear Waste Disposal Site at Yucca Mountain, Southern Nevada: U.S. Geological Survey Bulletin 1790, p. 87-93.

TABLE GW-1
GEORGE P.L. WALKER - EVENT COUNTS

LOCATION	COUNTS (CONES)	WEIGHT	NOTES
Lathrop Wells	1 2 3 4	(0.9) (0.07) (0.02) (0.01)	BC: Black Cone LC: Little Cones M: Makani Cone RC: Red Cone
Sleeping Butte	1 2	(0.4) (0.6)	
1.0 Ma Crater Flat	1 (all) 3 (LC, RC+BC, M) 4 (LC, RC, BC, M)	(0.1) (0.35) (0.55)	
Buckboard Mesa	1 2	(0.75) (0.25)	
3.7 Ma Crater Flat	2 3 4 5	(0.5) (0.25) (0.20) (0.05)	
Amargosa Valley	2 3 5 6	(0.3) (0.4) (0.15) (0.15)	
Thirsty Mesa	1 2 3	(0.85) (0.09) (0.06)	

TABLE GW-2
GEORGE P.L. WALKER - RATES OF OCCURRENCE

TIME PERIOD	COUNT METHOD FOR ZONES	NOTES
Post 4.6 Ma (1.0)	- CFVZ zone: NCF, 3.7, LW, TM, SB, AV - Background Node: BM	NCF: Northern (1.0 Ma) Crater Flat 3.7: 3.7 Ma Crater Flat LW: Lathrop Wells TM: Thirsty Mesa SB: Sleeping Butte AV: Amargosa Valley BM: Buckboard Mesa

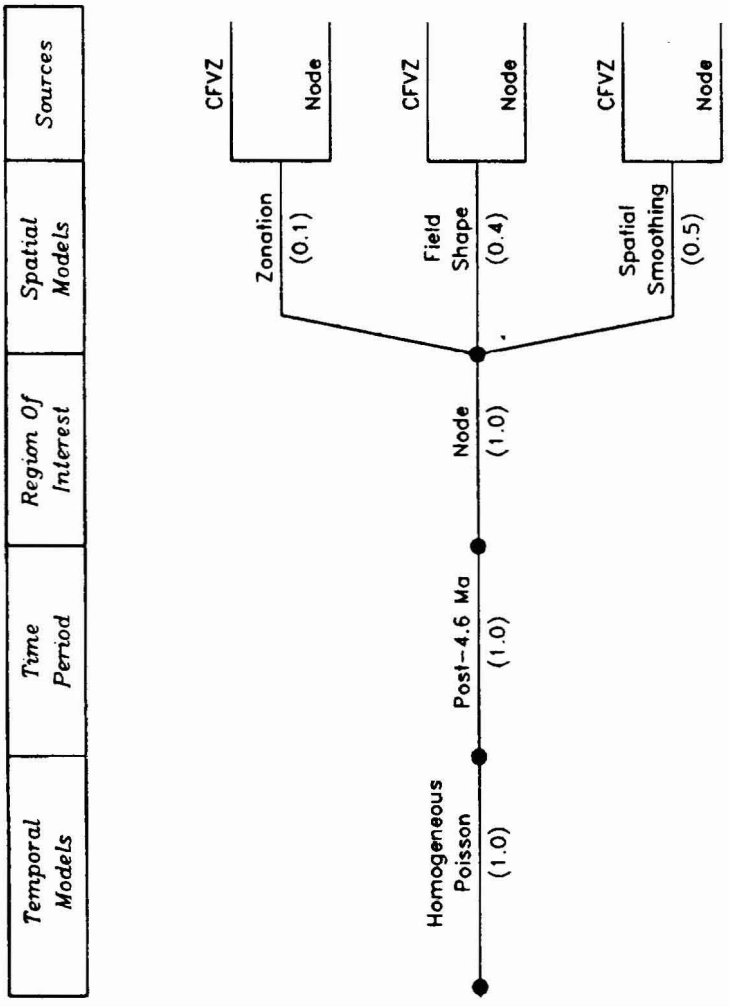

Figure GW-1 PVHA model logic tree developed by George P.L. Walker.

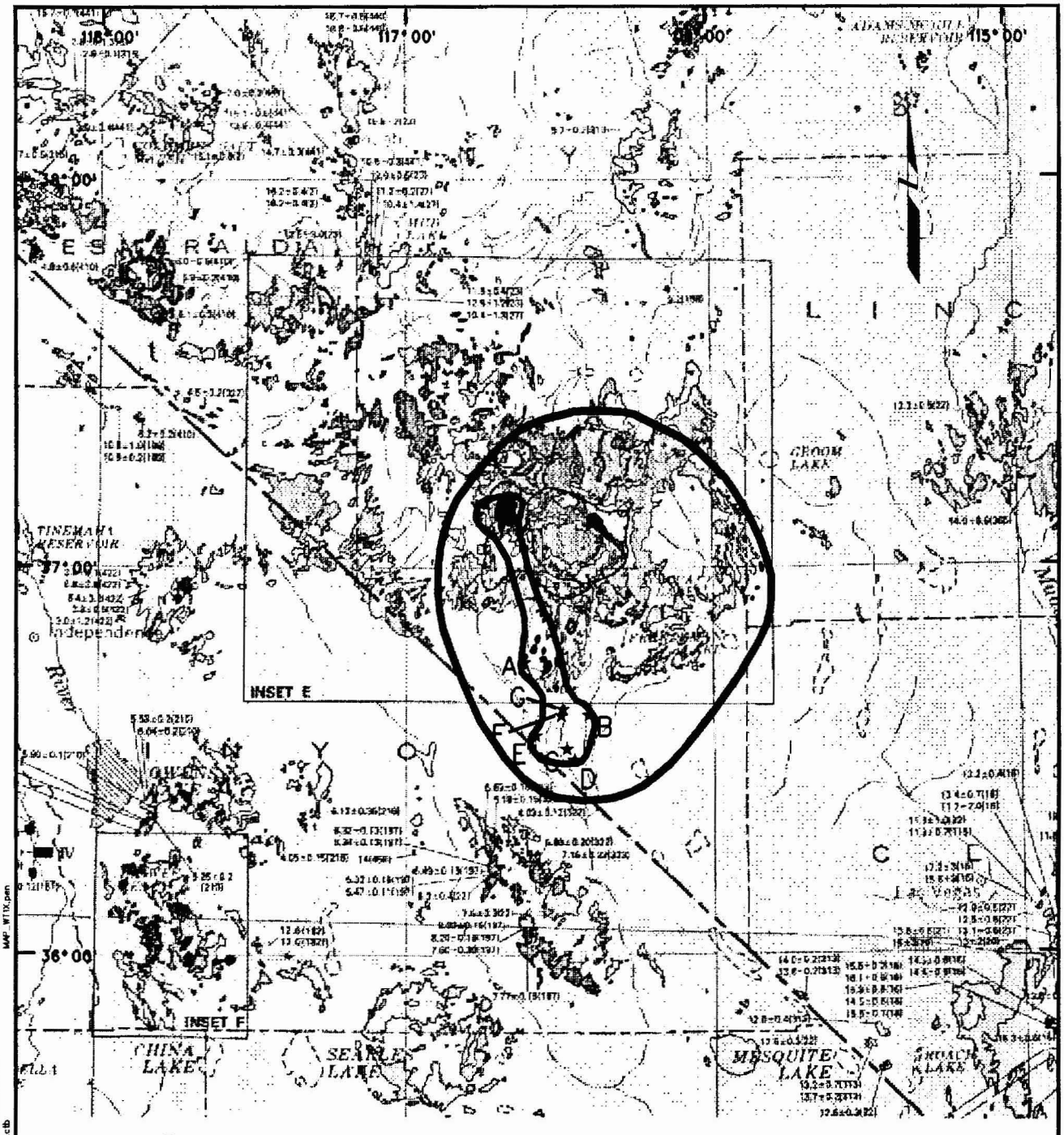

GEOMATRIX

GEORGE P.L. WALKER
REGIONAL BACKGROUND AND
CRATER FLAT VOLCANIC ZONES

Figure GW-2

PVHA Project

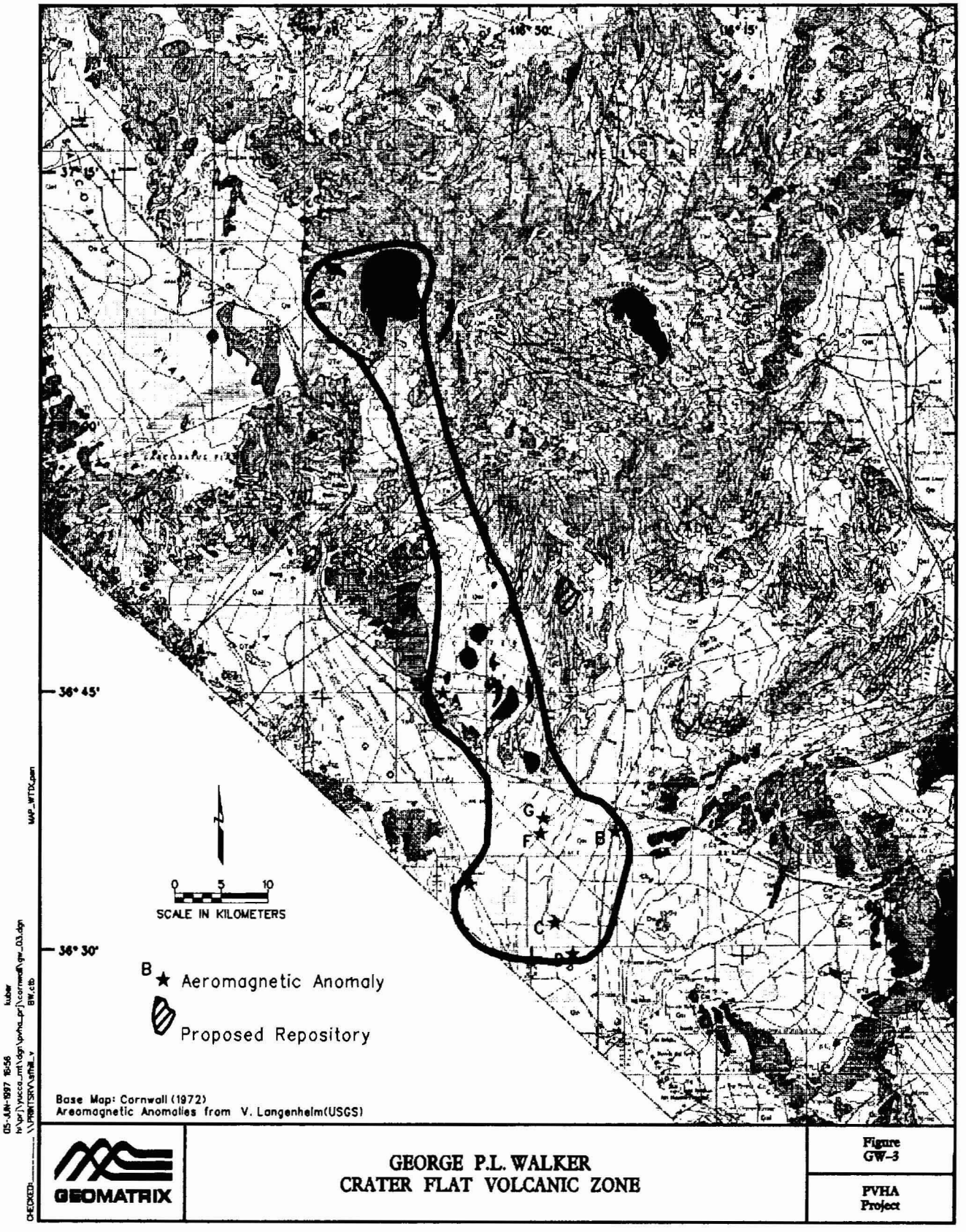
116° 30'
116° 15'
37° 15'
36° 45'
36° 30'
G
F
B
C
0 5 10
SCALE IN KILOMETERS
B ★ Aeromagnetic Anomaly
Proposed Repository
Base Map: Cornwall (1972)
Areomagnetic Anomalies from V. Langenhelm(USGS)
GEOMATRIX
GEORGE P.L. WALKER
CRATER FLAT VOLCANIC ZONE
Figure GW-3
PVHA Project

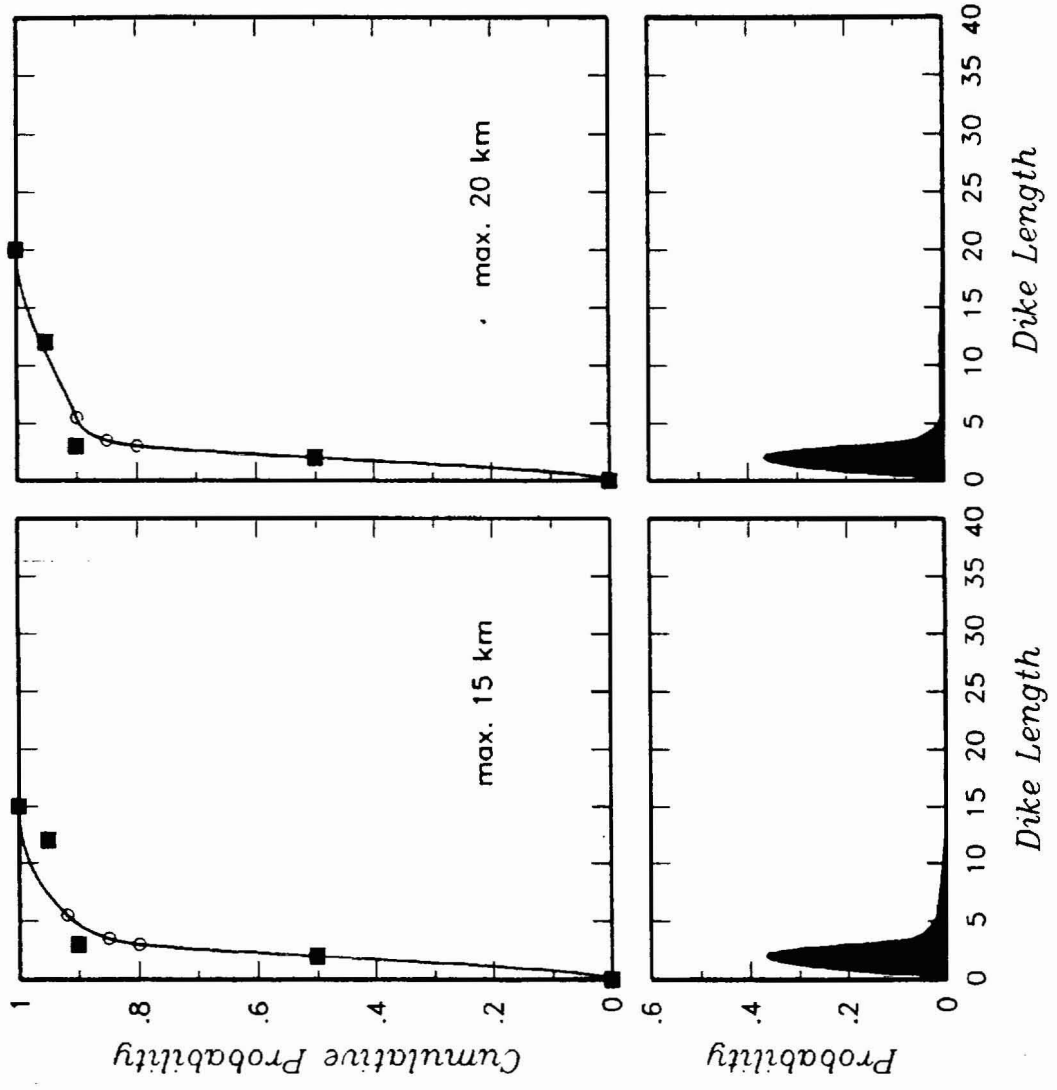

Figure GW-4 Dike length distribution developed by George P.L. Walker.

APPENDIX F

DETAILS OF HAZARD FORMULATION

APPENDIX F
DETAILS OF HAZARD FORMULATION

This appendix presents additional details of the mathematical formulations used to compute the volcanic hazard.

TEMPORAL MODELS

Two basic types of temporal models were used to represent the rate of volcanic events, the homogeneous Poisson process and the nonhomogeneous Weibull process.

The homogeneous Poisson process specifies that the probability distribution for the number of events, n, occurring in time period t is given by:

$$P(n) = \frac{(\lambda t)^n e^{-\lambda t}}{n!} \qquad \text{(F-1)}$$

where λ is the mean rate of occurrence of events. The maximum likelihood estimate for the mean rate, $\hat{\lambda}$, give the observation of N events in time period T is just N/T (e.g. Benjamin and Cornell, 1970). Weichert (1980) developed an approach for defining confidence intervals for the parameter λ. Specifically, the upper, $\lambda_{U(\alpha)}$, and lower, $\lambda_{L(\alpha)}$, points of a (1-α)100% confidence interval for λ based on N events are given by:

$$\lambda_{U(\alpha)} = \hat{\lambda} \cdot \frac{\chi^2(N+0.5, 1-\alpha/2)}{N}$$
$$\lambda_{L(\alpha)} = \hat{\lambda} \cdot \frac{\chi^2(N, \alpha/2)}{N} \qquad \text{(F-2)}$$

where $\chi^2(n,\alpha)$ defines the α probability point of the chi^2 distribution with n degrees of freedom.

The Weibull process is a nonhomogeneous Poisson process in which the rate parameter $\lambda(t)$ changes monotonically with time following a particular functional form: (e.g. Ho, 1991):

$$\lambda(t) = \frac{\beta}{\theta}\left(\frac{t}{\theta}\right)^{\beta-1} \quad \text{for } t \geq 0 \qquad \text{(F-3)}$$

where t is time measured from t_0 when the process "starts", and β and θ are parameters. Application of this model to evaluating the rate of volcanism is described by Ho (1991, 1992). The data used to estimate the parameters β and θ consist of the number of volcanic events, N, that have occurred during time interval T and the age dates for each event. Defining T_i as the age date of the i^{th} event (e.g., 1 Ma) and defining $T=t_0$ as the age date for the beginning of the process (e.g., 5 Ma), then the maximum likelihood estimates for the parameters of the Weibull process are given by the relationships (Crow, 1974):

$$\beta = \frac{N}{\sum_{i=1}^{N} \ln(T/t_i)} \qquad \theta = T/N^{1/\beta} \qquad \text{(F-4)}$$

where $t_i=T-T_i$ is the time interval from the start of the process to the i^{th} event. Crow (1982) tabulates confidence interval factors for the Weibull process. The homogeneous Poisson and Weibull process 90-percent confidence intervals are compared on Figure F-1 for data sets of 2 to 20 events. The two confidence intervals are similar in width.

SPATIAL MODELS

Linear Gradient for a Homogeneous Zone Boundary The locally homogeneous spatial model assumes that the spatial density of events $f(x,y)$ is uniform within a zone and equal to $1/A$, where A is the area of the zone. Thus the integral of the spatial density over the zone area equals unity

$$\int\int_Z f(x,y)\,dx\,dy = \int\int_Z \frac{dx\,dy}{A} = \frac{A}{A} = 1 \qquad \text{(F-5)}$$

In this model there is an abrupt step in the spatial density function at the edge of the zone. An alternative is to assume that $f(x,y)$ decreases linearly from 1/A at the zone boundary to zero over a distance h. Within the transition zone the spatial density is given by

$$f_T(x,y) = \frac{(h-d)/h}{A} \qquad \text{(F-6)}$$

where d is the distance from the zone boundary and is confined to the range of 0 to h. However, the effective area of the zone has now expanded by A_T, the area of the transition zone. Thus, the integral of the spatial density over the effective area of the zone, $A+A_T$ will exceed unity, requiring renormalization to produce a proper density function. The renormalization factor is the integral

of $f(x,y)$ over the entire effective region of the zone. For zones in which the transition region lies along one side, the normalization factor is approximately equal to the area within the zone plus one-half of the area within the transition region. Thus the spatial density becomes

$$f(x,y) \cong \frac{1}{A + A_T/2} \quad for\ (x,y)\ within\ A$$
$$f(x,y) \cong \frac{(h-d)/h}{A + A_T/2} \quad for\ (x,y)\ within\ A_T \qquad \text{(F-7)}$$

The method used to compute the volcanic hazard directly calculated the normalization factor by numerically integrating the spatial density over the zone and transition areas and then renormalized the spatial density function to unity.

Gaussian Field Parameters Two approaches were used to define the parameters of a Gaussian field model for the spatial density defined by the relationship

$$f(x,y) = \frac{e^{-[(x-\mu)^T \Sigma^{-1}(x-\mu)]/2}}{2\pi|\Sigma|^{1/2}} \qquad \text{(F-8)}$$

where x is the location of point (x,y), μ is the location of the center of the field (mean of x and y for all events) and Σ is the covariance matrix of the x and y locations of observed events in the field. If the field parameters are to be estimated from the n observed events then the maximum likelihood estimators are (Johnson and Wichern, 1992):

$$\mu = \frac{1}{n}\sum_{i=1}^{n} x_i$$
$$\Sigma = \frac{1}{n}\sum_{i=1}^{n} (x_i-\mu)^T(x_i-\mu) \qquad \text{(F-9)}$$

where x_i is the location of the i^{th} event in the field. The five parameters of the field are the mean of the x and y locations, μ_x and μ_y, and the covariances of the x and y locations, σ^2_x, σ^2_y, and σ^2_{xy}. The asymptotic covariance of the estimated field mid point μ is equal to Σ/n. The asymptotic covariance for the parameters of Σ are computed using the relationship given by (Searle, 1971)

$$var(c_i,c_j) = 2\left(Trace\left[\Sigma^{-1}\frac{\partial\Sigma}{\partial c_i}\Sigma^{-1}\frac{\partial\Sigma}{\partial c_j}\right]\right)^{-1} \qquad \text{(F-10)}$$

where c_i and c_j refer to the three components of the covariance matrix σ_x^2, σ_y^2, and σ_{xy}^2. These estimates were used to establish ranges for the field parameters. The relative likelihood of a particular set of field parameters, μ^j and Σ^j, being the "correct" model that generated the observed set of events was computed by (Johnson and Wichern, 1992):

$$L(\mu^j,\Sigma^j) = \frac{e^{-\sum_{i=1}^{n}(x_i-\mu^j)^T(\Sigma^j)^{-1}(x_i-\mu^j)}}{(2\pi)^n|\Sigma^j|^{n/2}} \qquad \text{(F-11)}$$

Three values for each of the five parameters were selected, the maximum likelihood value and ±one standard error of estimation. Equation **(F-11)** was then used to compute the likelihood of the 243 possible parameter sets and the resulting values normalized to sum to unity to define a discrete probability distribution for the field parameters.

The alternative approach to specifying a Gaussian field was to define a source zone boundary to correspond to a specified density ellipse of the Gaussian field. The ellipse that encloses 100(1-α) percent of the density of the field satisfies the relationship (Johnson and Wichern, 1992)

$$(x-\mu)^T\Sigma^{-1}(x-\mu) \le \chi^2(2,\alpha) \qquad \text{(F-12)}$$

where $\chi^2(2,\alpha)$ defines the upper α probability point of the chi distribution with 2 degrees of freedom. Given a source zone boundary and a specified value of α, Equation **(F-12)** was used to find the field parameters that minimized the mean square error between $(x-\mu)^T\Sigma^{-1}(x-\mu)$ calculated at points along the zone boundary and the corresponding value for $\chi^2(2,\alpha)$.

Kernel Density Estimation Equations **(3-10)** and **(3-11)** of Section 3.1.4 define axisymmetric kernel densities for Epanechnikov and Gaussian kernels, respectively. Silverman (1986) indicates that one can generalize the kernels to have an anisotropic shape. Defining the aspect ratio of the kernel, R^k, to be the ratio of the long axis to the short axis, $R^k \le 1$, and defining the azimuth of the long axis of the kernel to be ϕ, then the coordinate system of the spatial grid can be rotated through angle ϕ and the kernel density estimates computed by the relationship

$$K^E(d_i') = \frac{2}{\pi|\Sigma_k|^{1/2}}\left[1-d_i'^T\Sigma_k^{-1}d_i'\right] \quad \text{for } d_i'^T\Sigma_k^{-1}d_i' < 1$$

$$= 0 \quad \text{otherwise} \qquad \text{(F-13)}$$

for the Epanechnikov kernel and by the relationship

$$K^{G}(d_i') = \frac{e^{-d_i'^{T}\Sigma_k^{-1}d_i'}}{2\pi|\Sigma_k|^{1/2}} \quad \text{(F-14)}$$

for the Gaussian kernel. The vector d_i' defines the relative coordinates between point (x,y) and event i in the transform rotated coordinate system and Σ_k is a covariance matrix of the kernel in the rotated coordinate system given by

$$\Sigma_k = \begin{bmatrix} h^2 & 0 \\ 0 & (R_k h)^2 \end{bmatrix} \quad \text{(F-15)}$$

As discussed in Section 3.1.4, the value of the smoothing parameter h was either specified directly or was specified by defining a zone boundary as the approximate $100(1-\alpha)$ percentile density contour for the local field. A nonlinear optimization routine was then used to find the value of h that minimized the difference between the zone boundary and the specified density contour computed using kernel density estimation. The process is illustrated on Figure F-2.

A source zone is defined containing a number of events. A trial value of h is selected, for example 5 km, and the 95 percent density contour of a kernel density function is computed. This is denoted by the stippled area. The measure of the error is taken to be the area between the computed density contour and the zone boundary. This includes both the stippled area outside of the source zone boundary and the area inside the source zone that is outside of the computed 95 percent density contour, and is shown on Figure F-2 by the area filled with open circles. In the left hand plot of Figure F-2 there is very little area outside of the zone boundary but a large area of mismatch inside the zone. The process is repeated for a second value of h. The middle plot shows the results for h equal to 10 km. Now the zone is nearly filled by the 95 percent density contour, but there is a large area inside of the 95 percent density contour that lies outside of the source zone. Using a minimization algorithm, the value of h that minimizes the area of mismatch is found to be 7.4 km. The result 95 percent density contour is shown in the right hand plot of Figure F-2. These results were obtained using a Gaussian kernel. Repeating the process with an Epanechnikov kernel yields a best fit value of h equal to 18.9 km. This value is approximately 2.5 times the best fit h for the Gaussian kernel, consistent with the discussion by Silverman (1986) about the ratio of smoothing parameters that produce similar results using the two different kernels.

REFERENCES

Benjamin, J.R, and Cornell, C.A., 1970, Probability, Statistics, and Decision for Civil Engineers: McGraw-Hill, New York.

Crow, L.H., 1974, Reliability analysis of complex repairable systems: *in* Proschan, F., and Serfling, R.J. (eds.), Reliability and Biometry: SIAM, Philadelphia, Penn., p. 392-410.

Crow, L.H., 1982, Confidence interval procedures for the Weibull process with applications for reliability growth: Technometrics, v. 24, p. 67-72.

Ho, C.-H., 1991, Time trend analysis of basaltic volcanism for the Yucca Mountain site: Journal of Volcanology and Geothermal Research, v. 46, p. 61-72.

Ho, C.-H., 1992, Risk assessment for the Yucca Mountain high-level nuclear waste repository site: estimation of volcanic disruption: Mathematical Geology, v. 24, no. 4, p. 347-364.

Johnson, R.A., and Wichern, D.W., 1992, Applied Multivariate Statistical Analysis: 3rd Edition, Prentice Hall, New Jersey.

Searle, S.R., 1971, Linear Models: John Wiley and Sons, New York.

Silverman, B.W., 1986, Density Estimation for Statistics and Data Analysis: Monographs on Statistics and Applied Probability 26: Chapman and Hall, New York.

Weichert, D.H., 1980, Estimation of the earthquake recurrence parameters for unequal observation periods for different magnitudes: Bulletin of the Seismological Society of America, v. 70, p. 1337-1346.

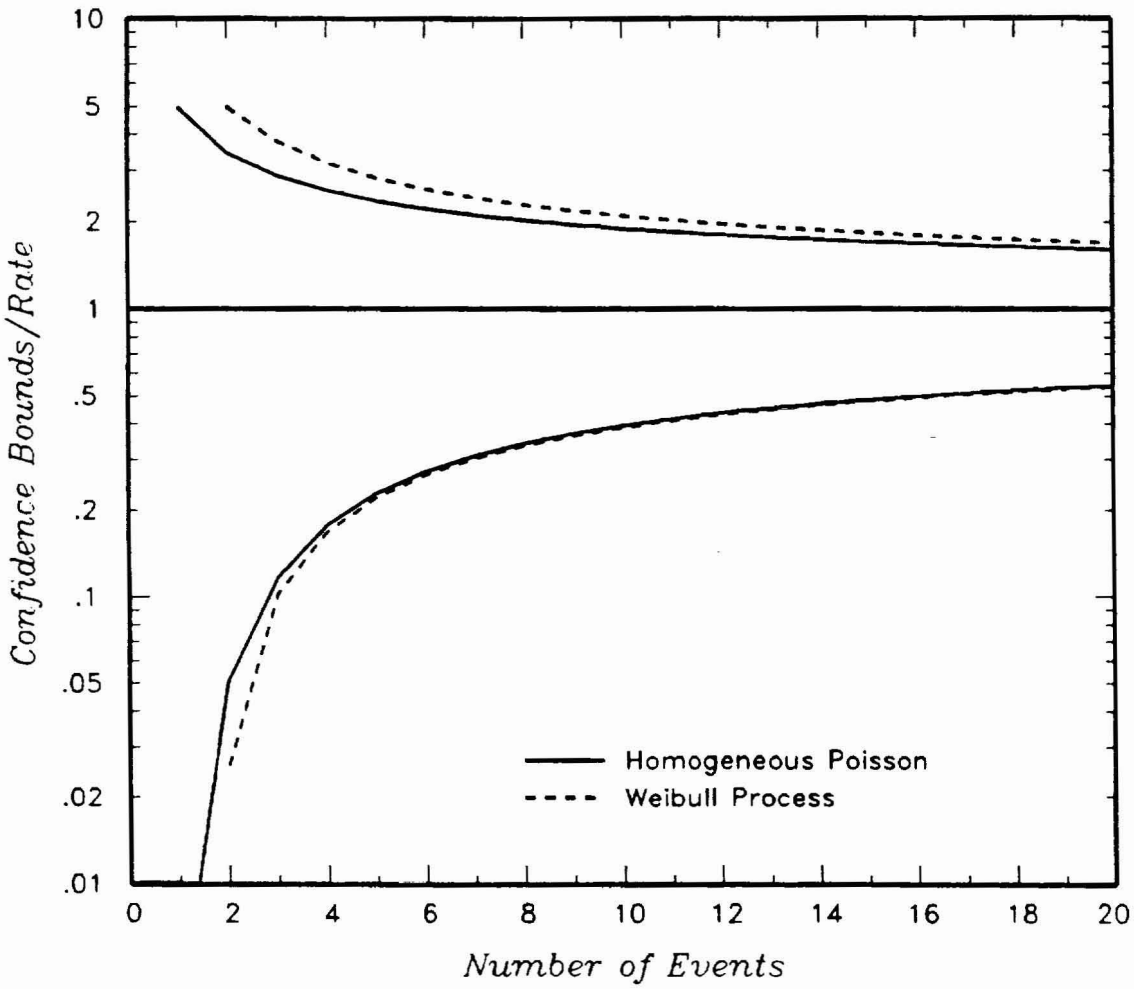

Figure F-1 Ninety-percent confidence intervals for the homogeneous Poisson and Weibull process models as a function of the number of data points.

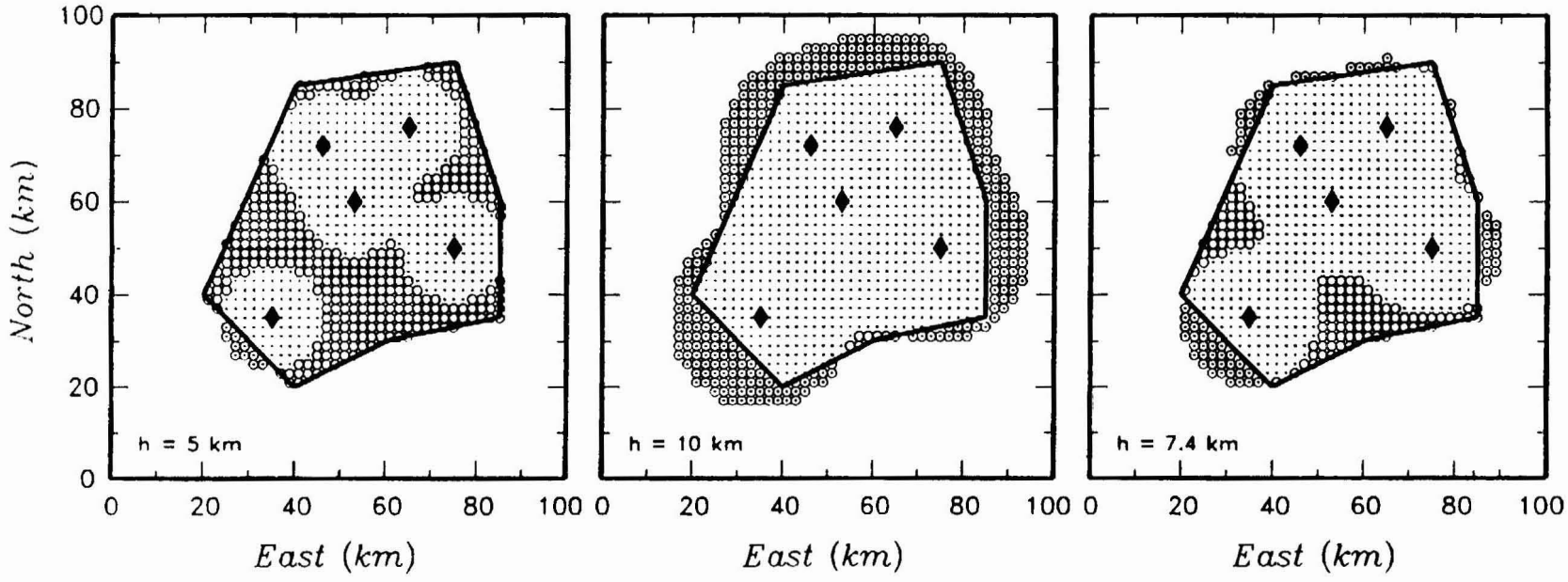

Figure F-2 Illustration of the procedure used to determine the smoothing parameter, *h*, for the kernel density estimation by minimizing the area of mismatch between a zone boundary and a specified density contour computed from the data. The solid triangles represent the data points and the small dots define the 95-percent density contour computed from the data using the indicated values of *h* and a Gaussian kernel. The open circles define the area of mismatch (when they are outside of the zone boundary they contain a dot within them).

APPENDIX G
PROBABILISTIC VOLCANIC HAZARD ANALYSIS CALCULATION ILLUSTRATIONS

APPENDIX G

TABLE OF CONTENTS

APPENDIX G
PROBABILISTIC VOLCANIC HAZARD ANALYSIS EXAMPLE CALCULATION

This appendix presents the approach used for the probabilistic volcanic hazard calculation and illustrates this approach with examples of the type of calculations performed.

The measure of volcanic hazard used in this study was the annual frequency of intersection of the repository, ν_I. The basic formulation for calculating ν_I is given by equation **(3-4)** in the main text:

$$\nu_I(t) = \int\int_R \lambda(t) \cdot f(x,y) \cdot P_I(x,y)\, dx\, dy \qquad \textbf{(3-4)}$$

where $\nu_I(t)$ indicates that ν is a function of time, with t equal to 0 representing the present. Also, as discussed in Sections 3 and 4 of the main text, the volcanic experts treated $\nu(t)_I$ as an uncertain quantity dependent on a number of parameters, designated herein by the vector Θ. The experts specified discrete distributions for the parameters through the use of logic trees, resulting in discrete parameter sets, θ_k, with a specified probability of being the "correct" parameter set, $P(\Theta=\theta_k)$. The frequency of intersection was calculated for each possible parameter set. The results of these calculations formed a discrete distribution for the frequency of intersection. The expected value or mean of this distribution was used as the estimate of the volcanic hazard.

The calculation of $\nu_I(t|\theta_k)$ was performed by discretizing the region of interest, R, on a grid with spacing Δx and Δy and replacing equation **(3-4)** by the equivalent summation:

$$\nu_I(t|\theta_k) = \sum_{i=1}^{N_x} \sum_{j=1}^{N_y} \lambda(t) \cdot f(x_i,y_j) \cdot P_I(x_i,y_k) \cdot \Delta x \cdot \Delta y \qquad \textbf{(G-1)}$$

Calculation of equation **(G-1)** was performed in two steps using the variety of approaches outlined in Section 3.1 and Appendix F. The first step was to calculate the conditional probability of intersection, $P_I(x_i,y_j)$, for each point in the gridded site region. Then the rate parameter $\lambda(t)$ and the discrete spatial mass density, $f(x_i,y_j)$ were calculated following the approaches specified by the expert, and the resulting values multiplied by the conditional probability of intersection and summed over all points in the grid.

G.1 CALCULATION OF THE CONDITIONAL PROBABILITY OF INTERSECTION

The conditional probability of intersection is calculated using the discrete form of Equation **(3-17)**:

$$P_I(x_i,y_j) = \sum_{l=1}^{N_L} P(L=l)\cdot P[\phi_1(x_i,y_j,l)\le\phi\le\phi_2(x_i,y_j,l)] \qquad \textbf{(G-2)}$$

where $P(L=l)$ is the discrete probability mass function for the length of an event (represented as a linear dike) extending from the grid point toward the repository and $P[\phi_1(x_i,y_j,l \le \phi \le \phi_2(x_i,y_j,l]$ is the probability that the dike azimuth lies between ϕ_1 and ϕ_2 (see Figure 3-12). The discrete probability mass function for event length was calculated from a total dike length distribution specified by the expert. The probability distribution for dike azimuth was assumed to be a normal distribution with mean, μ_ϕ, and standard deviation, σ_ϕ, specified by the expert. The distribution for ϕ was assumed to be doubly truncated at $\mu_\phi \pm 90°$.

Figure G-1, part (a) shows an example distribution for total dike length, TL, specified as uniform between 0 and a maximum length of 10 km. The expert then specified a symmetric probability density function for the location of the point event on the dike, Ω (varying from $0\cdot TL$ to $1\cdot TL$). Part (b) of Figure G-1 shows an example of a uniform density function for event location, Ω. The probability mass function for event length was then calculated from the expert-specified distributions using a computer program **DCPELD**(v1.0). Two event length distributions were calculated, the preferred distribution assuming a randomly placed dike and a second distribution assuming that the dike is centered on the point event. The probability mass function is a compound distribution [see Benjamin and Cornell (1970) p. 306-307] and is calculated by the formula:

$$P(L=l) = \sum_{\Omega} P(TL=tl)\cdot P(\Omega=\omega \mid l=tl\cdot\omega) \qquad \textbf{(G-3)}$$

Program **DCPELD** works by discretizing the cumulative distribution into intervals specified by $tl \pm \Delta tl/2$ and the event location distribution into intervals of $\omega \pm \Delta\omega/2$. For the case of the event centered dike, all of the probability mass for Ω is placed on $\omega = 0.5$. The program then forms a discrete distribution for event length with intervals $l \pm \Delta l/2$. All possible combinations of the discrete values of tl and ω are calculated and the probability $P(Tl=tl)\cdot P(\Omega=\omega)$ is added to the probability mass for the event length interval $l=tl\cdot\omega$. After completing all combinations, the probability mass function for l is summed to form a cumulative mass function.

The following is a listing of example input and output files for program **DCPELD**.

Input File: **DCPELD.IN**

```
examp.scd                          input discrete cumul. dist. for total dike length
1 .005 'u'                         Δtl=Δl, Δω, type of distribution for Ω ('u' = uniform)
examp.dld                          output file name
q                                  q to quit
```

Input File: **EXAMP.SCD**

```
Example Dike Length Distribution  10 Max        Label for distribution
   11                                           number of mass points
    0.0    0.0                                  tl, P(TL≤tl)
    1.0    0.1
    2.0    0.2
    3.0    0.3
    4.0    0.4
    5.0    0.5
    6.0    0.6
    7.0    0.7
    8.0    0.8
    9.0    0.9
   10.0    1.0
```

Output File: **EXAMP.DLD**

```
Example Dike Length Distribution  10 Max        Label for distribution
   11                                           number of mass points
    0.000    0.995000005E-01    0.204448403E+00  l, P(L≤l|event centered dike), P(L≤l|randomly placed dike)
    1.000    0.299499989E+00    0.433895228E+00
    2.000    0.499499977E+00    0.596842047E+00
    3.000    0.699499965E+00    0.718122209E+00
    4.000    0.899499953E+00    0.810235703E+00
    5.000    0.100000000E+01    0.879849198E+00
    6.000    0.100000000E+01    0.931129354E+00
    7.000    0.100000000E+01    0.966933327E+00
    8.000    0.100000000E+01    0.989344436E+00
    9.000    0.100000000E+01    0.999949998E+00
   10.000    0.100000000E+01    0.100000000E+01
```

The resulting cumulative mass functions for event length are plotted on part (c) of Figure G-1.

The calculation of $P_f(x_i,y_j)$ was performed by computer program **CPDI**(v1.0). The inputs to this program are the coordinates defining the outline of the proposed repository, the discrete probability distribution for event length, and the dike azimuth distribution parameters μ_ϕ and σ_ϕ. The program calculates three values for $P_f(x_i,y_j)$, one assuming point events with a finite radius, one assuming that the dikes are centered on the event, and one assuming that the dikes are randomly placed on the event.

The following is an example calculation using **CPDI**. Figure G-2 shows an example repository foot print and the points of the calculation grid with $\Delta x = \Delta y = 5$ km. The event cumulative length distributions calculated with using program **DCPELD** are rediscretized at the same intervals $l \pm \Delta l/2$. At each grid point the following set of calculations are made. For a given value of l the two angles of intersection, ϕ_1 and ϕ_2 (see Figure 3-12), are calculated. The probability mass $P[\phi_1(x_i,y_j,l \le \phi \le \phi_2(x_i,y_j,l]$ is calculated by the expression:

$$P(\phi_1 \le \phi \le \phi_2) = F_T\left(\frac{\phi_2 - \mu_\phi}{\sigma_\phi}\right) - F_T\left(\frac{\phi_1 - \mu_\phi}{\sigma_\phi}\right) \quad \text{(G-4)}$$

where $F_T()$ is the standard normal distribution doubly truncated at $\mu_\phi \pm 90°$. The probability $P(L=l) \cdot P[\phi_1(x_i, y_j, l) \le \phi \le \phi_2(x_i, y_j, l)]$ is then added to $P_1(x_i, y_j)$. The process is repeated for all values of l.

The following is a listing of example input and output files for program **CPDI**.

Input File: CPDI.IN

```
n                              y or n for binary output
examp.cpi                      output file name
Example 10 km Max              output label
examp.rep                      repository outline coordinates (km)
0.25 1                         size of point events, # header records in event length dist. file
examp.dld                      event length distribution file (output of DCPELD listed above)
1 45 30 1.0 0.1                # of azimuth dist., μφ, σφ, fraction of population, repeated for multiple means) ,
                                     azimuth discretization increment°
525 575 5 4050 4100 5          start of x grid, end of x grid, Δx, start of y grid, end of y grid, Δy
q                              q to stop
```

Input File: EXAMP.REP

```
Example Repository             Repository file label
   5                           # of vertices
   547.5  4082.5               x, y coordinates (km) of vertices
   547.5  4077.5
   552.5  4077.5
   552.5  4082.5
   547.5  4082.5
```

Output File: EXAMP.DLD

```
Example 10 km Max                                                    Output file label
   10    525.00    575.00      5.00   10   4050.00    4100.00      5.00   grid parameters
   525.000  4050.000  0.0000000E+00  0.0000000E+00  0.0000000E+00         x_i, y_j, P_1(x_i,y_j) for point event,
   525.000  4055.000  0.0000000E+00  0.0000000E+00  0.0000000E+00                event centered dike, and
   525.000  4060.000  0.0000000E+00  0.0000000E+00  0.0000000E+00                randomly placed dike
   525.000  4065.000  0.0000000E+00  0.0000000E+00  0.0000000E+00
   525.000  4070.000  0.0000000E+00  0.0000000E+00  0.0000000E+00
   525.000  4075.000  0.0000000E+00  0.0000000E+00  0.0000000E+00
   525.000  4080.000  0.0000000E+00  0.0000000E+00  0.0000000E+00
   525.000  4085.000  0.0000000E+00  0.0000000E+00  0.0000000E+00
   525.000  4090.000  0.0000000E+00  0.0000000E+00  0.0000000E+00
   525.000  4095.000  0.0000000E+00  0.0000000E+00  0.0000000E+00
   525.000  4100.000  0.0000000E+00  0.0000000E+00  0.0000000E+00
   530.000  4050.000  0.0000000E+00  0.0000000E+00  0.0000000E+00
   530.000  4055.000  0.0000000E+00  0.0000000E+00  0.0000000E+00
   530.000  4060.000  0.0000000E+00  0.0000000E+00  0.0000000E+00
   530.000  4065.000  0.0000000E+00  0.0000000E+00  0.0000000E+00
   530.000  4070.000  0.0000000E+00  0.0000000E+00  0.0000000E+00
   530.000  4075.000  0.0000000E+00  0.0000000E+00  0.0000000E+00
   530.000  4080.000  0.0000000E+00  0.0000000E+00  0.0000000E+00
   530.000  4085.000  0.0000000E+00  0.0000000E+00  0.0000000E+00
   530.000  4090.000  0.0000000E+00  0.0000000E+00  0.0000000E+00
   530.000  4095.000  0.0000000E+00  0.0000000E+00  0.0000000E+00
   530.000  4100.000  0.0000000E+00  0.0000000E+00  0.0000000E+00
```

535.000	4050.000	0.0000000E+00	0.0000000E+00	0.0000000E+00
535.000	4055.000	0.0000000E+00	0.0000000E+00	0.0000000E+00
535.000	4060.000	0.0000000E+00	0.0000000E+00	0.0000000E+00
535.000	4065.000	0.0000000E+00	0.0000000E+00	0.0000000E+00
535.000	4070.000	0.0000000E+00	0.0000000E+00	0.0000000E+00
535.000	4075.000	0.0000000E+00	0.0000000E+00	0.0000000E+00
535.000	4080.000	0.0000000E+00	0.0000000E+00	0.0000000E+00
535.000	4085.000	0.0000000E+00	0.0000000E+00	0.0000000E+00
535.000	4090.000	0.0000000E+00	0.0000000E+00	0.0000000E+00
535.000	4095.000	0.0000000E+00	0.0000000E+00	0.0000000E+00
535.000	4100.000	0.0000000E+00	0.0000000E+00	0.0000000E+00
540.000	4050.000	0.0000000E+00	0.0000000E+00	0.0000000E+00
540.000	4055.000	0.0000000E+00	0.0000000E+00	0.0000000E+00
540.000	4060.000	0.0000000E+00	0.0000000E+00	0.0000000E+00
540.000	4065.000	0.0000000E+00	0.0000000E+00	0.0000000E+00
540.000	4070.000	0.0000000E+00	0.0000000E+00	0.0000000E+00
540.000	4075.000	0.0000000E+00	0.0000000E+00	0.2430110E-02
540.000	4080.000	0.0000000E+00	0.0000000E+00	0.3836453E-02
540.000	4085.000	0.0000000E+00	0.0000000E+00	0.2421387E-03
540.000	4090.000	0.0000000E+00	0.0000000E+00	0.0000000E+00
540.000	4095.000	0.0000000E+00	0.0000000E+00	0.0000000E+00
540.000	4100.000	0.0000000E+00	0.0000000E+00	0.0000000E+00
545.000	4050.000	0.0000000E+00	0.0000000E+00	0.0000000E+00
545.000	4055.000	0.0000000E+00	0.0000000E+00	0.0000000E+00
545.000	4060.000	0.0000000E+00	0.0000000E+00	0.0000000E+00
545.000	4065.000	0.0000000E+00	0.0000000E+00	0.0000000E+00
545.000	4070.000	0.0000000E+00	0.0000000E+00	0.2430110E-02
545.000	4075.000	0.0000000E+00	0.7194468E-01	0.1028100E+00
545.000	4080.000	0.0000000E+00	0.1697034E+00	0.1484004E+00
545.000	4085.000	0.0000000E+00	0.1495051E-02	0.3450712E-02
545.000	4090.000	0.0000000E+00	0.0000000E+00	0.2421387E-03
545.000	4095.000	0.0000000E+00	0.0000000E+00	0.0000000E+00
545.000	4100.000	0.0000000E+00	0.0000000E+00	0.0000000E+00
550.000	4050.000	0.0000000E+00	0.0000000E+00	0.0000000E+00
550.000	4055.000	0.0000000E+00	0.0000000E+00	0.0000000E+00
550.000	4060.000	0.0000000E+00	0.0000000E+00	0.0000000E+00
550.000	4065.000	0.0000000E+00	0.0000000E+00	0.0000000E+00
550.000	4070.000	0.0000000E+00	0.0000000E+00	0.3836453E-02
550.000	4075.000	0.0000000E+00	0.1697034E+00	0.1484004E+00
550.000	4080.000	0.1000000E+01	0.1000000E+01	0.1000000E+01
550.000	4085.000	0.0000000E+00	0.1697034E+00	0.1484004E+00
550.000	4090.000	0.0000000E+00	0.0000000E+00	0.3836453E-02
550.000	4095.000	0.0000000E+00	0.0000000E+00	0.0000000E+00
550.000	4100.000	0.0000000E+00	0.0000000E+00	0.0000000E+00
555.000	4050.000	0.0000000E+00	0.0000000E+00	0.0000000E+00
555.000	4055.000	0.0000000E+00	0.0000000E+00	0.0000000E+00
555.000	4060.000	0.0000000E+00	0.0000000E+00	0.0000000E+00
555.000	4065.000	0.0000000E+00	0.0000000E+00	0.0000000E+00
555.000	4070.000	0.0000000E+00	0.0000000E+00	0.2421387E-03
555.000	4075.000	0.0000000E+00	0.1495051E-02	0.3450712E-02
555.000	4080.000	0.0000000E+00	0.1697034E+00	0.1484004E+00
555.000	4085.000	0.0000000E+00	0.7194468E-01	0.1028100E+00
555.000	4090.000	0.0000000E+00	0.0000000E+00	0.2430110E-02
555.000	4095.000	0.0000000E+00	0.0000000E+00	0.0000000E+00
555.000	4100.000	0.0000000E+00	0.0000000E+00	0.0000000E+00
560.000	4050.000	0.0000000E+00	0.0000000E+00	0.0000000E+00
560.000	4055.000	0.0000000E+00	0.0000000E+00	0.0000000E+00
560.000	4060.000	0.0000000E+00	0.0000000E+00	0.0000000E+00
560.000	4065.000	0.0000000E+00	0.0000000E+00	0.0000000E+00
560.000	4070.000	0.0000000E+00	0.0000000E+00	0.0000000E+00
560.000	4075.000	0.0000000E+00	0.0000000E+00	0.2421387E-03
560.000	4080.000	0.0000000E+00	0.0000000E+00	0.3836453E-02
560.000	4085.000	0.0000000E+00	0.0000000E+00	0.2430110E-02
560.000	4090.000	0.0000000E+00	0.0000000E+00	0.0000000E+00
560.000	4095.000	0.0000000E+00	0.0000000E+00	0.0000000E+00
560.000	4100.000	0.0000000E+00	0.0000000E+00	0.0000000E+00
565.000	4050.000	0.0000000E+00	0.0000000E+00	0.0000000E+00
565.000	4055.000	0.0000000E+00	0.0000000E+00	0.0000000E+00

565.000	4060.000	0.0000000E+00	0.0000000E+00	0.0000000E+00
565.000	4065.000	0.0000000E+00	0.0000000E+00	0.0000000E+00
565.000	4070.000	0.0000000E+00	0.0000000E+00	0.0000000E+00
565.000	4075.000	0.0000000E+00	0.0000000E+00	0.0000000E+00
565.000	4080.000	0.0000000E+00	0.0000000E+00	0.0000000E+00
565.000	4085.000	0.0000000E+00	0.0000000E+00	0.0000000E+00
565.000	4090.000	0.0000000E+00	0.0000000E+00	0.0000000E+00
565.000	4095.000	0.0000000E+00	0.0000000E+00	0.0000000E+00
565.000	4100.000	0.0000000E+00	0.0000000E+00	0.0000000E+00
570.000	4050.000	0.0000000E+00	0.0000000E+00	0.0000000E+00
570.000	4055.000	0.0000000E+00	0.0000000E+00	0.0000000E+00
570.000	4060.000	0.0000000E+00	0.0000000E+00	0.0000000E+00
570.000	4065.000	0.0000000E+00	0.0000000E+00	0.0000000E+00
570.000	4070.000	0.0000000E+00	0.0000000E+00	0.0000000E+00
570.000	4075.000	0.0000000E+00	0.0000000E+00	0.0000000E+00
570.000	4080.000	0.0000000E+00	0.0000000E+00	0.0000000E+00
570.000	4085.000	0.0000000E+00	0.0000000E+00	0.0000000E+00
570.000	4090.000	0.0000000E+00	0.0000000E+00	0.0000000E+00
570.000	4095.000	0.0000000E+00	0.0000000E+00	0.0000000E+00
570.000	4100.000	0.0000000E+00	0.0000000E+00	0.0000000E+00
575.000	4050.000	0.0000000E+00	0.0000000E+00	0.0000000E+00
575.000	4055.000	0.0000000E+00	0.0000000E+00	0.0000000E+00
575.000	4060.000	0.0000000E+00	0.0000000E+00	0.0000000E+00
575.000	4065.000	0.0000000E+00	0.0000000E+00	0.0000000E+00
575.000	4070.000	0.0000000E+00	0.0000000E+00	0.0000000E+00
575.000	4075.000	0.0000000E+00	0.0000000E+00	0.0000000E+00
575.000	4080.000	0.0000000E+00	0.0000000E+00	0.0000000E+00
575.000	4085.000	0.0000000E+00	0.0000000E+00	0.0000000E+00
575.000	4090.000	0.0000000E+00	0.0000000E+00	0.0000000E+00
575.000	4095.000	0.0000000E+00	0.0000000E+00	0.0000000E+00
575.000	4100.000	0.0000000E+00	0.0000000E+00	0.0000000E+00

G.2 CALCULATION OF FREQUENCY OF INTERSECTION

The remaining variables needed for the calculation of the frequency of intersection, $\nu_i(t|\theta_k)$, are the rate parameter $\lambda(t)$ and the discrete spatial mass density, $f(x_i,y_j)$.

G.2.1 Event Rate Calculation

The event rate parameter is calculated using two approaches. If the temporal process is assumed to be homogeneous, then the rate parameter is calculated by the maximum likelihood estimate N/T, where N is the number of volcanic events that have occurred in time T. If the nonhomogeneous Weibull process is assumed to apply, then the rate parameter is calculated using Equation **(F-3)** with the maximum likelihood estimates of the parameters of Equation **(F-3)** given by Equation **(F-4)**. Statistical uncertainty in the estimate of the rate parameter was specified by a three-point discrete distribution with the maximum likelihood estimate assigned a probability of 0.63 and the 5th and 95th percentiles of the sampling distribution assigned a probability of 0.185. The 5th and 95th percentiles of the sampling distribution for the homogeneous process are given by Equation **(F-2)**. The 5th and 95th percentiles of the sampling distribution for the Weibull process are tabulated in Crow (1982). Both of these approaches were implemented in the various computer programs used to calculate the spatial density function.

G.2.2 Spatial Density Calculation

Three basic types of spatial models are used to calculate the spatial density function, $f(x_i,y_j)$, a source zone within which $f(x_i,y_j)$ is assumed to be uniform, a bivariate Gaussian distribution modeling a volcanic field, and a nonparametric kernel density function. Separate computer programs were used to perform each type of spatial density calculation and the summation defined by Equation **(G-1)**. Each of these programs has the same general structure in that they account for the uncertainty in the numbers of volcanic events, the uncertainty in the number of hidden events, and the statistical uncertainty in the rate parameter.

Calculation of Frequency of Intersection for Uniform Volcanic Zone. Figure G-3 shows an example volcanic source zone in which seven events have been identified to have occurred post 5 Ma. These events are separated into a northern center with three events and a southern center with four events. The calculation of the frequency of intersection for a uniform source zone was performed using program **UZVH**(v1.0). The program performs the following operations. First, it reads in the conditional probability of intersection values for the computation grid (the output of program **CPDI**). Then it reads in the source zone boundary(s). The source zones can consist of several disjoint pieces and can include holes. The zones can also have gradual edges with a linear decrease in the spatial density over a specified distance. The approximate zone area within the calculation grid is determined by the number of grid points within the zone boundary multiplying by the grid unit area ($\Delta x \cdot \Delta y$). The spatial density, $f(x_i,y_j)$, in then set equal to the inverse of the zone area. The program then reads in the discrete distributions for the volcanic event counts at each of the volcanic centers that lie within the source zone. Using nested loops, the program calculates all possible combinations of event counts within the source zone. For each possible event count a three point distribution for the rate parameter is calculated for either a homogeneous or nonhomogeneous process (Section G.2.1 above). The program then performs the summation of Equation **(G-1)** for each rate parameter, resulting in three possible values for the frequency of intersection, given a specific set of events. If a distribution for hidden event factors is specified, then frequencies of intersection are calculated for each hidden event factor. The program calculates the exact mean hazard and creates a discrete distribution for the frequency of intersection by placing each individual calculated value into discrete intervals equally spaced on a log scale with 100 intervals per log decade.

The following is a listing of example input and output files for program **UZVH** using the example shown of Figure G-3. Two sets of inputs and outputs are presented, one with no uncertainty in the event counts and one with uncertainty in the event counts.

Input File: **UZVH.IN**

```
uz.in                   first individual source zone input file (no uncertainty in event counts)
uzue.in                 second individual source zone input file (uncertainty in event counts)
q                       q to quit
```

Input File: UZ.IN

```
.\cpdi\examp.cpi                    output of program CPDI
Example Zone 5m years - homogeneous label for first calculation
uz-h                                output file name
1                                   number of zones
Example Zone                        zone name
1                                   number of enclosed zone segments
'examp.z' 1 0 0                     zone file name, zone factor (-1 means remove piece), western ramp distance,
                                        eastern ramp distance (these allow for a gradual decrease in the
                                        spatial density)
1 1  LN                             # of event counts at 1st center, probability of each event count
'X'                                 file name with first event count at 1st center (X indicates no
                                        events at this center within this source zone)
 1 1 NWCF                           # of event counts at 2nd center, probability of each event count
'nvc.3'                             file name with first event count at 2nd center
  1 1   SECF                        # of event counts at 3rd center, probability of each event count
'svc.4'                             file name with first event count at 3rd center
   1 1   AG                         # of event counts at 4th center, probability of each event count
'X'                                 file name with first event count at 4th center
    1 1     SB                      # of event counts at 5th center, probability of each event count
'X'                                 file name with first event count at 5th center
     1 1      TM                    # of event counts at 6th center, probability of each event count
'X'                                 file name with first event count at 6th center
      1 1      BM                   # of event counts at 7th center, probability of each event count
'X'                                 file name with first event count at 7th center
     t 5000000 1.0 0 1 1.0 1.0      t for homogeneous, time period, rate factor, # of additional centers within
                                        zone, # of hidden event factors, hidden event factor, probability
for
                                        factor (pairs repeated for each factor)
Example Zone 5m years - nonhomogeneous label for next calculation
uz-w                                output file name
1                                   number of zones
Example Zone                        zone name
1                                   number of enclosed zone segments
'examp.z' 1 0 0                     zone file name, zone factor (-1 means remove piece),
                                        western ramp distance, eastern ramp distance (these allow
                                        for a gradual decrease in the spatial density)
1 1  LN                             # of event counts at 1st center, probability of each event count
'X'                                 file name with first event count at 1st center (X indicates no
                                        events at this center within this source zone)
 1 1 NWCF                           # of event counts at 2nd center, probability of each event count
'nvc.3'                             file name with first event count at 2nd center
  1 1   SECF                        # of event counts at 3rd center, probability of each event count
'svc.4'                             file name with first event count at 3rd center
   1 1   AG                         # of event counts at 4th center, probability of each event count
'X'                                 file name with first event count at 4th center
    1 1     SB                      # of event counts at 5th center, probability of each event count
'X'                                 file name with first event count at 5th center
     1 1      TM                    # of event counts at 6th center, probability of each event count
'X'                                 file name with first event count at 6th center
      1 1      BM                   # of event counts at 7th center, probability of each event count
'X'                                 file name with first event count at 7th center
     f 5000000 1.0 0 1 1.0 1.0      f for nonhomogeneous, time period, rate factor, # of additional centers
within
                                        zone, # of hidden event factors, hidden event factor, probability
for
                                        factor (pairs repeated for each factor)
```

Input File: EXAMP.Z

```
Example Zone                Zone Label
   18                       # of zone boundary vertices
   532.5  4062.5            x, y of zone boundary vertex
   532.5  4067.5
```

```
532.5  4072.5
532.5  4077.5
532.5  4082.5
532.5  4087.5
535.0  4087.5
537.5  4085.0
540.0  4082.5
542.5  4080.0
545.0  4077.5
547.5  4075.0
547.5  4070.0
547.5  4062.5
547.5  4062.5
542.5  4062.5
537.5  4062.5
532.5  4062.5
```

Input File: NVC.3

```
North Center 3 events                  label for file
3 0                                    # of mapped events, # of hidden events
534.0 4077.0  0.5                      x, y, age (Ma) of first event
535.0 4082.0  1.0                      x, y, age (Ma) of second event
538.0 4080.0  1.5                      ...
```

Input File: SVC.3 (same format as NVC.3)

```
South Center 4 events
4 0
535.0 4067.0  3.0
537.5 4065.0  3.5
542.5 4070.0  4.0
545.0 4068.0  4.5
```

The program produces three output files for each calculation.

Output File: UZ-H.OUT

```
Example Zone 5m years - homogeneous
 Source              SUM1          SUM2          SUM3          mambda     mbeta  sbeta
Example Zone     0.0000E+00  0.6058E-02  0.9390E-02  0.1509E-05  0.000  0.000
```

This lists the sum of $f(x_i,y_j) \cdot P_j(x_i,y_j)$ over the source zone for the three event representations (point event, event-centered dike, and randomly placed dike), the mean value of $\lambda(t=0)$, and the mean and standard error of the β parameter of the Weibull process (if used).

Output File: UZ-H.HAZ

```
Example Zone 5m years - homogeneous
    3
     1  0.0000000E+00  0.0000000E+00  0.0000000E+00  0.0000000E+00  0.0000000E+00  0.0000000E+00  0.0000000E+00
0.0000000E+00  0.0000000E+00  0.0000000E+00  0.0000000E+00  0.0000000E+00  0.0000000E+00  0.0000000E+00
     2  0.9145091E-08  0.2239166E-16  0.0000000E+00  0.0000000E+00  0.0000000E+00  0.0000000E+00  0.0000000E+00
0.0000000E+00  0.0000000E+00  0.0000000E+00  0.0000000E+00  0.0000000E+00  0.0000000E+00  0.2239166E-16
     3  0.1417393E-07  0.5378866E-16  0.0000000E+00  0.0000000E+00  0.0000000E+00  0.0000000E+00  0.0000000E+00
0.0000000E+00  0.0000000E+00  0.0000000E+00  0.0000000E+00  0.0000000E+00  0.0000000E+00  0.5378866E-16
```

This file contains three main lines of output, one for each type of event representations (1 - point event, 2 - event-centered dike, 3 - randomly placed dike). Each line contains the mean frequency of intersection, the variance in the frequency of intersection, and the breakdown of the variance into the components associated with each type of uncertainty. The last component is the variance in the hazard due to the statistical distribution for the rate parameter.

Output File: UZ-H.DST

```
Example Zone 5m years - homogeneous
    3
    1
 0.0000E+00 0.1000E+01
    3
 0.2630E-08 0.1850E+00 0.8511E-08 0.6300E+00 0.1778E-07 0.1850E+00
    3
 0.4074E-08 0.1850E+00 0.1318E-07 0.6300E+00 0.2754E-07 0.1850E+00
```

This file contains three blocks of output. Each block is the discrete distribution for frequency of intersection calculated for all of the alternative parameter values defined in the input file. In this example, there are only three alternatives, corresponding to the three-point distribution for the rate parameter. Only one value (0) is shown for the point event representation because the value of the conditional probability of intersection is zero everywhere within the source zone.

The corresponding output files for the nonhomogeneous case are:

Output File: UZ-W.OUT

```
Example Zone 5m years - nonhomogeneous
 Source              SUM1        SUM2        SUM3       mambda    mbeta  sbeta
Example Zone     0.0000E+00  0.6058E-02  0.9390E-02  0.1656E-05  1.042  0.000
```

Note that the mean value of $\lambda(t=0)$ is larger than for the homogeneous case because $\beta > 1$.

Output File: UZ-W.HAZ

```
Example Zone 5m years - nonhomogeneous
    3
     1   0.0000000E+00   0.0000000E+00   0.0000000E+00   0.0000000E+00   0.0000000E+00   0.0000000E+00   0.0000000E+0
0.0000000E+00  0.0000000E+00  0.0000000E+00  0.0000000E+00  0.0000000E+00  0.0000000E+00
     2   0.1003296E-07   0.3502814E-16   0.2237134E-23   0.2237134E-23   0.2237134E-23   0.2237134E-23   0.2237134E-23
0.2237134E-23  0.2237134E-23  0.2237134E-23  0.2237134E-23  0.2237134E-23  0.3502814E-16
     3   0.1555003E-07   0.8414365E-16   0.3728359E-23   0.3728359E-23   0.3728359E-23   0.3728359E-23   0.3728359E-23
0.3728359E-23  0.3728359E-23  0.3728359E-23  0.3728359E-23  0.3728359E-23  0.8414365E-16
```

Output File: UZ-W.DST

```
Example Zone 5m years - nonhomogeneous
    3
    1
 0.0000E+00 0.1000E+01
    3
 0.2692E-08 0.1850E+00 0.8913E-08 0.6300E+00 0.2138E-07 0.1850E+00
    3
 0.4169E-08 0.1850E+00 0.1380E-07 0.6300E+00 0.3311E-07 0.1850E+00
```

The second input file contains an example with uncertainty in the event counts.

Input File: UZUE.IN

```
.\cpdi\examp.cpi                          output of program CPDI
Example Zone 5m years uncertain events - homogeneous      label for first calculation
uzue-h                                    output file name
1                                         number of zones
Example Zone                              zone name
1                                         number of enclosed zone segments
'examp.z' 1 0 0                           zone file name, zone factor (-1 means remove piece),
                                                western ramp distance, eastern ramp distance (these allow
```

```
                                        for a gradual decrease in the spatial density)
1 1  LN                                 # of event counts at 1st center, probability of each event count
'X'                                     file name with first event count at 1st center (X indicates no
                                            events at this center within this source zone)
 2 .3 .7 NWCF                           # of event counts at 2nd center, probability of each event count
'nvc.2'                                 file name with first event count at 2nd center
'nvc.3'                                 file name with second event count at 2nd center
  2 .4 .6   SECF                        # of event counts at 3rd center, probability of each event count
'svc.2'                                 file name with first event count at 3rd center
'svc.4'                                 file name with second event count at 3rd center
   1 1   AG                             # of event counts at 4th center, probability of each event count
'X'                                     file name with first event count at 4th center
    1 1     SB                          # of event counts at 5th center, probability of each event count
'X'                                     file name with first event count at 5th center
     1 1      TM                        # of event counts at 6th center, probability of each event count
'X'                                     file name with first event count at 6th center
      1 1      BM                       # of event counts at 7th center, probability of each event count
'X'                                     file name with first event count at 7th center
     t 5000000 1.0 0 1 1.0 1.0          t for homogeneous, time period, rate factor, # of additional
                                            centers within zone, # of hidden event factors, hidden
                                        event factor, probability for factor (pairs repeated for
                                            each factor)
Example Zone 5m years uncertain events - nonhomogeneous    label for next calculation
uzue-w                                  output file name
1                                       number of zones
Example Zone                            zone name
1                                       number of enclosed zone segments
'examp.z' 1 0 0                         zone file name, zone factor (-1 means remove piece), western ramp distance,
                                            eastern ramp distance (these allow for a gradual decrease in the
                                            spatial density)
1 1  LN                                 # of event counts at 1st center, probability of each event count
'X'                                     file name with first event count at 1st center (X indicates no
                                            events at this center within this source zone)
 2 .3 .7 NWCF                           # of event counts at 2nd center, probability of each event count
'nvc.2'                                 file name with first event count at 2nd center
'nvc.3'                                 file name with second event count at 2nd center
  2 .4 .6   SECF                        # of event counts at 3rd center, probability of each event count
'svc.2'                                 file name with first event count at 3rd center
'svc.4'                                 file name with second event count at 3rd center
   1 1   AG                             # of event counts at 4th center, probability of each event count
'X'                                     file name with first event count at 4th center
    1 1     SB                          # of event counts at 5th center, probability of each event count
'X'                                     file name with first event count at 5th center
     1 1      TM                        # of event counts at 6th center, probability of each event count
'X'                                     file name with first event count at 6th center
      1 1      BM                       # of event counts at 7th center, probability of each event count
'X'                                     file name with first event count at 7th center
     f 5000000 1.0 0 1 1.0 1.0          f for nonhomogeneous, time period, rate factor, # of additional
                                            centers within zone, # of hidden event factors, hidden
                                        event factor, probability for factor (pairs repeated for
                                            each factor)
```

The additional input files not listed above are:

Input File: NVC.2

```
North Center 2 events
2 0
534.0 4077.0  0.5
538.0 4080.0  1.5
```

Input File: SVC.2

```
South Center 2 events
2 0
```

```
535.0 4067.0  3.0
545.0 4068.0  4.5
```

The corresponding output files for the homogeneous case are:

Output File: UZUE-H.OUT

```
Example Zone 5m years uncertain events - homogeneous
 Source              SUM1        SUM2        SUM3       mambda    mbeta  sbeta
Example Zone     0.0000E+00  0.6058E-02  0.9390E-02  0.1290E-05  0.000  0.000
```

Output File: UZUE-H.HAZ

```
Example Zone 5m years uncertain events - homogeneous
    3
     1  0.0000000E+00  0.0000000E+00  0.0000000E+00  0.0000000E+00  0.0000000E+00  0.0000000E+00  0.0000000E+00
0.0000000E+00  0.0000000E+00  0.0000000E+00  0.0000000E+00  0.0000000E+00  0.0000000E+00  0.0000000E+00
     2  0.7815300E-08  0.2074333E-16  0.0000000E+00  0.3068350E-18  0.1402733E-17  0.0000000E+00  0.0000000E+00
0.0000000E+00  0.0000000E+00  0.0000000E+00  0.0000000E+00  0.0000000E+00  0.0000000E+00  0.1903377E-16
     3  0.1211289E-07  0.4982909E-16  0.0000000E+00  0.7370798E-18  0.3369605E-17  0.3702531E-24  0.3702531E-24
0.3702531E-24  0.3702531E-24  0.3702531E-24  0.3702531E-24  0.3702531E-24  0.3702531E-24  0.4572243E-16
```

Note that additional components of variance appear. (The extremely small variance components, of the order of 10^{-24} are a result of numerical round off error during single precision arithmetic.)

Output File: UZUE-W.DST

```
Example Zone 5m years uncertain events -
    3
    1
 0.0000E+00 0.1000E+01
   12
 0.8710E-09 0.2220E-01 0.1380E-08 0.5180E-01 0.1995E-08 0.3330E-01 0.2630E-08 0.7770E-01 0.4898E-08 0.7560E-01
 0.6026E-08 0.1764E+00 0.7244E-08 0.1134E+00 0.8511E-08 0.2646E+00 0.1259E-07 0.2220E-01 0.1445E-07 0.5180E-01
 0.1622E-07 0.3330E-01 0.1778E-07 0.7770E-01
   12
 0.1349E-08 0.2220E-01 0.2138E-08 0.5180E-01 0.3090E-08 0.3330E-01 0.4074E-08 0.7770E-01 0.7586E-08 0.7560E-01
 0.9333E-08 0.1764E+00 0.1122E-07 0.1134E+00 0.1318E-07 0.2646E+00 0.1950E-07 0.2220E-01 0.2239E-07 0.5180E-01
 0.2512E-07 0.3330E-01 0.2754E-07 0.7770E-01
```

Note that the distributions now contain 12 values, 4 possible sets of event counts times 3 rates per event count.

The corresponding output files for the nonhomogeneous case are:

Output File: UZUE-W.OUT

```
Example Zone 5m years uncertain events - nonhomogeneous
 Source              SUM1        SUM2        SUM3       mambda    mbeta  sbeta
Example Zone     0.0000E+00  0.6058E-02  0.9390E-02  0.1487E-05  1.093  0.127
```

Note that there is now uncertainty in β due to the uncertainty in the event counts.

Output File: UZUE-W.HAZ

```
Example Zone 5m years uncertain events - nonhomogeneous
    3
     1  0.0000000E+00  0.0000000E+00  0.0000000E+00  0.0000000E+00  0.0000000E+00  0.0000000E+00  0.0000000E+00
0.0000000E+00  0.0000000E+00  0.0000000E+00  0.0000000E+00  0.0000000E+00  0.0000000E+00  0.0000000E+00
     2  0.9008075E-08  0.3558571E-16  0.5046430E-24  0.1227629E-17  0.1951847E-18  0.1643379E-23  0.1643379E-23
0.1643379E-23  0.1643379E-23  0.1643379E-23  0.1643379E-23  0.1643379E-23  0.1643379E-23  0.3416290E-16
     3  0.1396157E-07  0.8548303E-16  0.0000000E+00  0.2948996E-17  0.4688485E-18  0.1553743E-23  0.1553743E-23
0.1553743E-23  0.1553743E-23  0.1553743E-23  0.1553743E-23  0.1553743E-23  0.1553743E-23  0.8206520E-16
```

Output File: **UZUE-W.DST**

```
Example Zone 5m years uncertain events -
    3
    1
 0.0000E+00 0.1000E+01
   12
 0.8913E-09 0.2220E-01 0.1738E-08 0.5180E-01 0.1778E-08 0.3330E-01 0.2692E-08 0.7770E-01 0.5248E-08 0.7560E-01
 0.6761E-08 0.1134E+00 0.7762E-08 0.1764E+00 0.8913E-08 0.2646E+00 0.1698E-07 0.2220E-01 0.1738E-07 0.3330E-01
 0.2138E-07 0.7770E-01 0.2188E-07 0.5180E-01
   12
 0.1380E-08 0.2220E-01 0.2692E-08 0.5180E-01 0.2754E-08 0.3330E-01 0.4169E-08 0.7770E-01 0.8128E-08 0.7560E-01
 0.1047E-07 0.1134E+00 0.1202E-07 0.1764E+00 0.1380E-07 0.2646E+00 0.2630E-07 0.2220E-01 0.2692E-07 0.3330E-01
 0.3311E-07 0.7770E-01 0.3388E-07 0.5180E-01
```

Calculation of Frequency of Intersection for Bivariate Gaussian Field. The second approach to estimating the spatial density of volcanic events, $f(x,y)$, was to assume that the events within a volcanic field are distributed following a bivariate Gaussian distribution. Two approaches were used to define the parameters of this distribution. The first was to assume that a specified source zone boundary approximates a specified density contour of the field. Equation **(F-12)** defines the coordinates of a specified density ellipse for a bivariate Gaussian distribution. The computer program **FITFIELD**(v1.0) was used to find the parameters of the equivalent Gaussian field that minimize the mean square error between $(x-\mu)^T\Sigma^{-1}(x-\mu)$ calculated at points along the zone boundary and the corresponding value for $\chi^2(2,\alpha)$, where $1-\alpha$ is the specified density contour. The minimization is performed using minimization routines given in Press et al. (1992).

Figure G-4 shows an example of fitting a bivariate Gaussian field to the volcanic source zone shown on Figure G-3, assuming that it represents an approximate 95 percent density contour. The input and output files to program **FITFIELD** are:

Input File: **FITFIELD.IN**

```
Fit Gaussian Fit to Example Zone Chi2=95%        Label for calculation
5.99 20 .01                                      χ²(2,α), max # iterations, stopping tolerance
1 '*'                                            # headers in zone file, format
examp.z                                          zone boundary file (listed above)
```

Output File: **FITFIELD.OUT**

```
 Fit Gaussian Fit to Example Zone Chi2=95%

 INITIAL FLOATING PARAMETERS :
 -----------

   C( 1) =     0.5387500000E+03                  starting parameters calculated using zone vertices
   C( 2) =     0.4073333250E+04
   C( 3) =     0.9244791980E+01
   C( 4) =     0.2135416980E+02
   C( 5) =    -0.3211805580E+01

 Maximum tolerance =     0.9999999780E-02
```

```
Direction Set: Powell algorithm

Iteration No.=     1 MSE =   0.366829E+01        first iteration results
C=   0.5387E+03  0.4073E+04  0.1659E+02  0.2943E+02 -0.6677E+01

Iteration No.=     2 MSE =   0.345864E+01
C=   0.5384E+03  0.4072E+04  0.1486E+02  0.3080E+02 -0.6275E+01

Iteration No.=     3 MSE =   0.336030E+01
C=   0.5386E+03  0.4072E+04  0.1411E+02  0.3208E+02 -0.6171E+01


FINAL RESULT :
------------
  Iteration Number =     4 MSE =   0.3273E+01    final results
   CHI2      Mean X      Mean Y      sigmaX2     sigmaY2      sigmaXY
  5.990     538.957    4071.693      12.966      34.955       -5.975
```

The field parameters are then used to calculate the spatial density associated with the field. The rate term, $\lambda(t=0)$ is calculated in the same was as for the homogeneous source zone using the events within the zone boundary. The annual frequency of intersection is calculated using program **PFGVH**(v1.0). The program performs the following operations. First, it reads in the conditional probability of intersection values for the computation grid (the output of program **CPDI**). Then it reads in the field parameters calculated by program **FITFIELD** and calculates the spatial density, $f(x_i,y_j)$, using Equation **(3-9)**. The program then follows the structure of **UZVH**, reading in the discrete distributions for the volcanic event counts at each of the volcanic centers that lie within the source zone and using nested loops to calculate all possible combinations of event counts associated with the field. For each possible event count a three point distribution for the rate parameter is calculated for either a homogeneous or nonhomogeneous process (Section G.2.1 above). The program then performs the summation of Equation **(G-1)** for each rate parameter, resulting in three possible values for the frequency of intersection, given a specific set of events. If a distribution for hidden event factors is specified, then frequencies of intersection are calculated for each hidden event factor. The program calculates the exact mean hazard and creates a discrete distribution for the frequency of intersection by placing each individual calculated value into discrete intervals equally spaced on a log scale with 100 intervals per log decade.

The following is a listing of example input and output files for program **PFGVH** using the example shown of Figure G-4. The example presents only calculations for the homogeneous temporal model. Results for the nonhomogeneous Weibull process are obtained in exactly the same manner as in the use of program **UZVH**.

Input File: PFGVH.IN

```
pfg.in                          first individual source zone input file
q                               q to quit
```

Input File: pfg.IN

```
.\cpdi\examp.cpi                        output file from program CPDI
95% Gaussian field fit to Example Zone - homogeneous      field calculation label
pf-h                                    output file name
1                                       # of fields
Example Zone                            field label
  538.957    4071.693      12.966      34.955      -5.975 field parameters (from program FITFIELD)
1 1  LN                                 remaining parameters are the same as described above for input file
'X'                                             UZ.IN used in program UZVH
 1 1 NWCF
'nvc.3'
  1 1   SECF
'svc.4'
   1 1   AG
'X'
    1 1     SB
'X'
     1 1      TM
'X'
      1 1      BM
'X'
     t 5000000 1.0 0 1 1.0 1.0
```

As before, the program produces three output files for each calculation.

Output File: PF-H.OUT

```
95% Gaussian field fit to Example Zone - homogeneous
 Source              SUM1         SUM2         SUM3        mambda    mbeta  sbeta
Example Zone     0.1089E-03  0.3334E-02  0.4700E-02  0.1509E-05  0.000  0.000
```

Output File: PF-H.HAZ

```
95% Gaussian field fit to Example Zone - homogeneous
    3
     1   0.1643792E-09   0.7234425E-20   0.0000000E+00   0.0000000E+00   0.0000000E+00   0.0000000E+00   0.0000000E+00
0.0000000E+00  0.0000000E+00  0.0000000E+00  0.0000000E+00  0.0000000E+00  0.7234425E-20
     2   0.5033139E-08   0.6782474E-17   0.0000000E+00   0.0000000E+00   0.0000000E+00   0.0000000E+00   0.0000000E+00
0.0000000E+00  0.0000000E+00  0.0000000E+00  0.0000000E+00  0.0000000E+00  0.6782474E-17
     3   0.7094505E-08   0.1347580E-16   0.4018061E-24   0.4018061E-24   0.4018061E-24   0.4018061E-24   0.4018061E-24
0.4018061E-24  0.4018061E-24  0.4018061E-24  0.4018061E-24  0.4018061E-24  0.1347580E-16
```

Output File: PF-H.DST

```
95% Gaussian field fit to Example Zone -
    3
    3
 0.4786E-10 0.1850E+00 0.1549E-09 0.6300E+00 0.3236E-09 0.1850E+00
    3
 0.1445E-08 0.1850E+00 0.4677E-08 0.6300E+00 0.9772E-08 0.1850E+00
    3
 0.2042E-08 0.1850E+00 0.6607E-08 0.6300E+00 0.1380E-07 0.1850E+00
```

The second approach calculates the parameters of the bivariate Gaussian distribution directly from the observed volcanic events. Equation **(F-9)** is used to calculate the maximum likelihood estimates of the field parameters from the observed events in a field. Statistical uncertainty in the field parameters is modeled in the hazard calculation by defining three values for each parameter, the maximum likelihood value and $\pm 1\sigma$ [calculated using Equation **(F-10)**]. The result is 3^5=243 possible sets of field parameters. Equation **(F-11)** is used to calculate the likelihood value for each set of parameters and these likelihoods are normalized to form a joint probability distribution for the field parameters.

This approach to calculating the spatial density and the resulting frequency of intersection is implemented in program **FPFGVH**(v1.0). Figure G-5 shows the example volcanic events from Figure G-3 and the maximum likelihood bivariate Gaussian distribution fit to the seven event locations. The program performs the following operations. First, it reads in the conditional probability of intersection values for the computation grid (the output of program **CPDI**). Then it reads in the discrete distributions for the volcanic event counts at each of the volcanic centers associated with the field. The program then uses nested loops to calculate all possible combinations of event counts associated with the field. For each possible event count a bivariate Gaussian field is fit to the event locations and distributions for the field parameters are calculated. Each set of field parameters is used to calculate the spatial density for future events associated with the field. These spatial densities are combined with the three point distribution for the rate parameter calculated as described above. The program then performs the summation of Equation **(G-1)** for each rate parameter and field parameter set, resulting in 3^6=729 possible values for the frequency of intersection, given a specific set of events. Hidden event factors are then included in the same manner as in the calculations described above.

The following is a listing of example input and output files for program **FPFGVH** using the example shown of Figure G-5. The example presents only calculations for the homogeneous temporal model. Results for the nonhomogeneous Weibull process are obtained in exactly the same manner as in the use of program **UZVH**.

Input File: **FPFGVH.IN**

```
fpf.in                          first individual source zone input file
q                               q to quit
```

Input File: **fpf.IN**

```
.\cpdi\examp.cpi                        output file from program CPDI
Gaussian Field fitted to events - homogeneous     calculation label
fpf-h                                   output file name
1                                       number of fields
Example Zone                            field label
   538.143  4072.714    14.765    39.918    -9.888  7     default field parameters calculated from a selected
```

```
                                                                    set of events, usually the most likely,
                                                                    and used when the number of events is too
                                                                    few to estimate the field parameters (<3),
                                                                    maximum aspect ratio for the field
1 1  LN                                          the remaining parameters are the same as those in the input to the
                                                       above programs
'X'
 1 1 NWCF
'nvc.3'
  1 1   SECF
'svc.4'
   1 1   AG
'X'
    1 1     SB
'X'
     1 1      TM
'X'
      1 1      BM
'X'
     t 5000000 1.0 0 1 1.0 1.0
```

As before, the program produces three output files for each calculation.

Output File: **FPF-H.OUT**

```
Gaussian Field fitted to events - homogeneous
 Source              SUM1        SUM2        SUM3       mambda     mbeta  sbeta  Mean ar sig ar
Example Zone     0.7040E-03  0.4875E-02  0.6049E-02  0.1509E-05  0.000  0.000  1.955  0.000
```

Note that the output file lists the statistics of the aspect ratios for the fitted fields (based on the maximum likelihood fits).

Output File: **FPF-H.HAZ**

```
Gaussian Field fitted to events - homogeneous
    3
     1   0.1062704E-08   0.4299878E-17   0.0000000E+00   0.0000000E+00   0.0000000E+00   0.0000000E+00   0.0000000E+00
0.0000000E+00  0.0000000E+00  0.3153261E-17  0.1979248E-25  0.1979248E-25  0.1146616E-17
     2   0.7357951E-08   0.7342884E-16   0.2568802E-22   0.0000000E+00   0.0000000E+00   0.0000000E+00   0.0000000E+00
0.0000000E+00  0.0000000E+00  0.4648722E-16  0.0000000E+00  0.0000000E+00  0.2694160E-16
     3   0.9130597E-08   0.9166999E-16   0.7797159E-22   0.0000000E+00   0.0000000E+00   0.0000000E+00   0.0000000E+00
0.0000000E+00  0.0000000E+00  0.5470306E-16  0.8440318E-24  0.8440318E-24  0.3696686E-16
```

Note that the partition of the total variance that is due to the uncertainty in the field parameters is given by the fourth from the end value.

Output File: **FPF-H.HAZ**

```
Gaussian Field fitted to events - homoge
    3
  316
 0.0000E+00 0.5465E-01 0.1047E-11 0.5545E-02 0.1072E-11 0.3378E-02 0.1096E-11 0.8543E-02 0.1122E-11 0.7872E-05
 0.1148E-11 0.4887E-05 0.1175E-11 0.4747E-02 0.1202E-11 0.5533E-02 0.1230E-11 0.2807E-04 0.1259E-11 0.2618E-03
 0.1288E-11 0.8707E-03 0.1318E-11 0.1104E-04 0.1380E-11 0.9698E-03 0.1413E-11 0.4863E-06 0.1445E-11 0.1065E-02
 0.1479E-11 0.1881E-04 0.1514E-11 0.7134E-05 0.1549E-11 0.3576E-05 0.1585E-11 0.1918E-02 0.1622E-11 0.2539E-03
 0.1660E-11 0.8622E-06 0.1698E-11 0.2445E-02 0.1778E-11 0.4158E-04 0.1820E-11 0.8500E-03 0.1905E-11 0.2131E-04
 0.1950E-11 0.1026E-02 0.1995E-11 0.9426E-04 0.2042E-11 0.3758E-04 0.2089E-11 0.1208E-02 0.2188E-11 0.4379E-03
 0.2239E-11 0.5633E-03 0.2291E-11 0.1656E-05 0.2399E-11 0.4335E-05 0.2455E-11 0.7548E-03 0.2512E-11 0.5430E-04
 0.2570E-11 0.7402E-05 0.2630E-11 0.7526E-04 0.2692E-11 0.6117E-05 0.2754E-11 0.2496E-03 0.2884E-11 0.6257E-05
 0.3020E-11 0.2288E-04 0.3090E-11 0.2936E-05 0.3162E-11 0.1944E-04 0.3311E-11 0.1957E-05 0.3631E-11 0.3393E-04
 0.3715E-11 0.4863E-06 0.3802E-11 0.2169E-06 0.3981E-11 0.1273E-05 0.4074E-11 0.3502E-02 0.4169E-11 0.3117E-02
 0.4266E-11 0.2174E-05 0.4467E-11 0.4114E-02 0.4571E-11 0.1796E-05 0.4677E-11 0.4228E-06 0.4786E-11 0.4718E-02
 0.4898E-11 0.3930E-03 0.5495E-11 0.2264E-04 0.5623E-11 0.2863E-04 0.5754E-11 0.7958E-04 0.5888E-11 0.1432E-02
 0.6310E-11 0.3245E-03 0.6761E-11 0.3287E-02 0.7244E-11 0.3585E-02 0.7413E-11 0.8481E-03 0.7586E-11 0.1118E-02
```

0.7762E-11 0.8937E-04 0.7943E-11 0.2862E-04 0.8318E-11 0.1208E-02 0.8913E-11 0.3326E-03 0.9120E-11 0.1053E-03
0.9550E-11 0.1155E-03 0.1000E-10 0.3055E-02 0.1072E-10 0.8406E-05 0.1122E-10 0.9579E-02 0.1148E-10 0.5430E-04
0.1202E-10 0.3244E-02 0.1230E-10 0.2898E-04 0.1288E-10 0.1440E-05 0.1318E-10 0.1221E-01 0.1349E-10 0.1176E-03
0.1413E-10 0.2450E-03 0.1479E-10 0.1250E-03 0.1549E-10 0.8258E-04 0.1622E-10 0.3810E-03 0.1660E-10 0.6958E-03
0.1698E-10 0.4399E-02 0.1738E-10 0.2822E-07 0.1778E-10 0.4702E-03 0.1820E-10 0.5439E-02 0.1862E-10 0.3036E-07
0.1905E-10 0.3393E-04 0.1950E-10 0.1091E-01 0.1995E-10 0.2828E-03 0.2042E-10 0.8666E-04 0.2138E-10 0.1874E-01
0.2188E-10 0.2888E-02 0.2239E-10 0.2862E-02 0.2570E-10 0.6522E-05 0.2630E-10 0.4228E-06 0.2692E-10 0.5895E-02
0.2754E-10 0.3452E-04 0.2951E-10 0.3058E-02 0.3020E-10 0.1169E-01 0.3090E-10 0.6291E-03 0.3162E-10 0.3966E-03
0.3236E-10 0.3208E-02 0.3311E-10 0.5998E-04 0.3388E-10 0.1541E-02 0.3467E-10 0.1257E-02 0.3631E-10 0.1134E-01
0.3715E-10 0.1019E-03 0.3981E-10 0.3531E-02 0.4074E-10 0.8304E-04 0.4169E-10 0.2192E-03 0.4365E-10 0.4419E-02
0.4467E-10 0.3478E-03 0.4571E-10 0.8580E-03 0.4677E-10 0.3218E-02 0.4786E-10 0.6040E-03 0.4898E-10 0.1210E-03
0.5012E-10 0.6018E-03 0.5129E-10 0.2556E-02 0.5248E-10 0.5265E-03 0.5370E-10 0.9609E-07 0.5495E-10 0.1601E-02
0.5623E-10 0.4583E-03 0.5754E-10 0.2092E-01 0.5888E-10 0.1034E-06 0.6310E-10 0.3492E-02 0.6457E-10 0.8631E-03
0.6761E-10 0.2251E-01 0.6918E-10 0.2662E-02 0.7413E-10 0.4460E-03 0.7586E-10 0.3208E-02 0.7943E-10 0.1195E-02
0.8128E-10 0.6566E-02 0.8511E-10 0.8114E-02 0.9120E-10 0.2450E-03 0.9333E-10 0.1052E-01 0.9550E-10 0.1104E-01
0.9772E-10 0.2142E-02 0.1000E-09 0.1276E-02 0.1023E-09 0.1092E-01 0.1047E-09 0.5169E-03 0.1072E-09 0.9965E-02
0.1096E-09 0.8962E-03 0.1122E-09 0.2822E-07 0.1148E-09 0.1889E-02 0.1175E-09 0.1246E-02 0.1202E-09 0.5419E-02
0.1230E-09 0.3036E-07 0.1259E-09 0.1114E-02 0.1288E-09 0.1021E-03 0.1349E-09 0.1129E-02 0.1380E-09 0.2469E-02
0.1413E-09 0.7239E-02 0.1445E-09 0.7420E-03 0.1479E-09 0.1116E-01 0.1514E-09 0.2057E-02 0.1549E-09 0.4121E-03
0.1622E-09 0.1409E-02 0.1698E-09 0.2599E-02 0.1778E-09 0.4194E-02 0.1820E-09 0.1221E-01 0.1862E-09 0.2168E-02
0.1950E-09 0.4254E-05 0.1995E-09 0.6238E-02 0.2042E-09 0.2555E-02 0.2089E-09 0.5085E-02 0.2138E-09 0.4527E-02
0.2188E-09 0.9064E-02 0.2239E-09 0.2941E-02 0.2291E-09 0.1104E-04 0.2344E-09 0.2943E-03 0.2399E-09 0.3024E-02
0.2455E-09 0.5376E-03 0.2512E-09 0.9435E-02 0.2570E-09 0.1164E-02 0.2630E-09 0.2145E-01 0.2692E-09 0.1545E-02
0.2754E-09 0.3952E-02 0.2818E-09 0.2192E-03 0.2884E-09 0.1395E-02 0.3020E-09 0.1549E-01 0.3090E-09 0.1095E-01
0.3162E-09 0.5544E-02 0.3236E-09 0.2277E-03 0.3311E-09 0.4536E-03 0.3388E-09 0.1602E-01 0.3467E-09 0.2400E-02
0.3715E-09 0.4244E-02 0.3802E-09 0.7432E-02 0.3890E-09 0.8646E-03 0.4074E-09 0.1770E-02 0.4169E-09 0.3007E-02
0.4266E-09 0.1007E-02 0.4365E-09 0.1653E-02 0.4467E-09 0.1206E-01 0.4571E-09 0.2937E-02 0.4677E-09 0.3248E-02
0.5012E-09 0.3422E-02 0.5248E-09 0.3748E-03 0.5370E-09 0.2441E-02 0.5495E-09 0.1537E-01 0.5623E-09 0.3036E-03
0.5754E-09 0.1345E-02 0.5888E-09 0.4369E-02 0.6026E-09 0.5674E-02 0.6310E-09 0.4845E-03 0.6457E-09 0.1015E-01
0.6761E-09 0.1889E-01 0.7079E-09 0.2022E-02 0.7244E-09 0.8066E-02 0.7413E-09 0.1206E-02 0.7586E-09 0.1413E-02
0.7762E-09 0.6577E-02 0.7943E-09 0.1859E-01 0.8128E-09 0.1257E-02 0.8318E-09 0.2035E-02 0.8511E-09 0.3828E-02
0.8710E-09 0.1711E-02 0.8913E-09 0.1132E-01 0.9120E-09 0.2965E-03 0.9333E-09 0.5320E-02 0.9550E-09 0.3180E-02
0.9772E-09 0.1269E-01 0.1000E-08 0.2653E-02 0.1023E-08 0.8750E-02 0.1047E-08 0.1205E-02 0.1072E-08 0.1133E-02
0.1096E-08 0.2319E-02 0.1148E-08 0.2593E-02 0.1175E-08 0.1186E-02 0.1202E-08 0.2325E-02 0.1230E-08 0.9763E-02
0.1259E-08 0.2290E-02 0.1288E-08 0.1227E-02 0.1318E-08 0.1684E-01 0.1349E-08 0.1835E-02 0.1413E-08 0.4229E-02
0.1445E-08 0.6615E-02 0.1514E-08 0.1420E-02 0.1622E-08 0.1185E-01 0.1660E-08 0.1480E-02 0.1698E-08 0.9335E-02
0.1738E-08 0.9171E-03 0.1778E-08 0.1034E-02 0.1820E-08 0.1489E-02 0.1862E-08 0.1018E-01 0.1905E-08 0.2469E-02
0.1950E-08 0.8866E-03 0.1995E-08 0.5086E-03 0.2042E-08 0.4243E-02 0.2089E-08 0.1149E-02 0.2138E-08 0.1964E-02
0.2188E-08 0.1264E-01 0.2291E-08 0.3148E-02 0.2344E-08 0.8525E-03 0.2399E-08 0.6877E-02 0.2455E-08 0.1339E-02
0.2512E-08 0.2192E-03 0.2570E-08 0.2867E-02 0.2630E-08 0.2732E-03 0.2692E-08 0.7708E-02 0.2754E-08 0.2372E-02
0.2818E-08 0.3331E-02 0.2884E-08 0.2412E-02 0.2951E-08 0.8865E-03 0.3020E-08 0.3812E-02 0.3162E-08 0.2872E-02
0.3236E-08 0.2719E-02 0.3311E-08 0.7020E-02 0.3388E-08 0.7080E-02 0.3548E-08 0.4750E-02 0.3631E-08 0.1246E-02
0.3802E-08 0.7222E-02 0.3890E-08 0.3939E-02 0.3981E-08 0.2659E-02 0.4169E-08 0.2259E-02 0.4266E-08 0.8392E-02
0.4571E-08 0.3228E-03 0.4677E-08 0.3389E-02 0.4786E-08 0.7377E-03 0.4898E-08 0.2048E-04 0.5012E-08 0.5020E-03
0.5129E-08 0.1413E-02 0.5248E-08 0.3638E-04 0.5623E-08 0.3049E-02 0.5754E-08 0.1355E-02 0.5888E-08 0.1419E-02
0.6166E-08 0.7082E-03 0.6457E-08 0.5687E-03 0.6607E-08 0.4961E-03 0.6761E-08 0.6875E-03 0.6918E-08 0.2520E-02
0.7079E-08 0.8456E-03 0.7244E-08 0.3595E-03 0.7413E-08 0.1285E-02 0.7586E-08 0.2666E-02 0.7762E-08 0.4181E-02
0.7943E-08 0.2350E-02 0.8128E-08 0.1592E-02 0.8318E-08 0.1157E-02 0.8710E-08 0.2643E-02 0.8913E-08 0.6633E-03
0.9120E-08 0.4610E-02 0.9550E-08 0.3019E-02 0.1175E-07 0.6438E-03 0.1259E-07 0.4166E-03 0.1585E-07 0.6594E-03
0.1622E-07 0.1234E-03 0.1660E-07 0.1569E-02 0.1698E-07 0.2192E-03 0.1862E-07 0.7761E-03 0.1950E-07 0.6718E-03
0.1995E-07 0.8865E-03

270

0.4169E-11 0.8939E-04 0.4786E-11 0.1053E-03 0.6026E-11 0.2899E-04 0.1122E-10 0.3044E-03 0.1230E-10 0.1710E-07
0.1259E-10 0.5634E-03 0.1318E-10 0.3585E-03 0.1380E-10 0.3037E-07 0.1514E-10 0.7180E-03 0.1549E-10 0.2823E-07
0.1738E-10 0.9872E-04 0.2042E-10 0.2496E-03 0.2291E-10 0.8939E-04 0.2692E-10 0.1048E-02 0.3162E-10 0.1055E-02
0.3548E-10 0.2899E-04 0.3631E-10 0.9725E-03 0.3802E-10 0.1919E-02 0.4074E-10 0.2496E-03 0.4266E-10 0.1021E-02
0.4467E-10 0.2663E-06 0.4571E-10 0.2445E-02 0.4786E-10 0.9614E-07 0.5495E-10 0.2005E-03 0.6310E-10 0.8501E-03
0.7943E-10 0.5634E-03 0.8128E-10 0.1802E-02 0.8511E-10 0.3212E-02 0.8913E-10 0.3037E-07 0.9333E-10 0.4255E-05
0.9550E-10 0.7180E-03 0.1000E-09 0.5904E-02 0.1096E-09 0.5747E-06 0.1148E-09 0.3312E-02 0.1230E-09 0.5336E-06
0.1259E-09 0.6523E-05 0.1288E-09 0.8510E-03 0.1318E-09 0.2496E-03 0.1349E-09 0.1846E-02 0.1380E-09 0.3479E-02
0.1413E-09 0.9067E-06 0.1445E-09 0.4134E-05 0.1479E-09 0.1796E-05 0.1549E-09 0.1210E-02 0.1585E-09 0.9725E-03
0.1738E-09 0.1038E-04 0.1778E-09 0.1626E-02 0.1820E-09 0.1028E-02 0.1862E-09 0.1104E-04 0.1905E-09 0.3326E-03
0.2089E-09 0.2048E-04 0.2138E-09 0.1998E-02 0.2239E-09 0.2087E-03 0.2344E-09 0.3639E-04 0.2399E-09 0.9725E-03
0.2512E-09 0.3382E-04 0.2570E-09 0.1055E-02 0.2630E-09 0.6137E-02 0.2692E-09 0.2496E-03 0.2754E-09 0.2813E-02
0.2884E-09 0.1021E-02 0.3020E-09 0.1476E-04 0.3162E-09 0.7868E-02 0.3311E-09 0.3585E-02 0.3388E-09 0.2496E-03
0.3467E-09 0.1957E-05 0.3715E-09 0.2025E-03 0.3981E-09 0.3204E-02 0.4074E-09 0.2221E-04 0.4169E-09 0.6298E-03
0.4266E-09 0.6278E-02 0.4365E-09 0.1253E-02 0.4467E-09 0.4595E-05 0.4571E-09 0.3602E-02 0.4677E-09 0.6118E-05
0.4786E-09 0.1103E-03 0.4898E-09 0.7403E-05 0.5012E-09 0.8144E-02 0.5129E-09 0.4339E-02 0.5370E-09 0.1767E-03

0.5495E-09 0.2652E-02 0.5623E-09 0.1167E-03 0.5888E-09 0.5050E-02 0.6166E-09 0.4340E-02 0.6310E-09 0.4255E-05
0.6457E-09 0.1234E-03 0.6607E-09 0.2496E-03 0.6761E-09 0.2403E-02 0.6918E-09 0.3629E-02 0.7079E-09 0.2192E-03
0.7244E-09 0.7250E-03 0.7413E-09 0.3282E-03 0.7586E-09 0.1021E-03 0.7762E-09 0.5356E-02 0.7943E-09 0.1821E-03
0.8128E-09 0.7443E-03 0.8318E-09 0.3890E-02 0.8511E-09 0.2740E-04 0.8710E-09 0.4093E-03 0.8913E-09 0.1242E-01
0.9120E-09 0.1846E-02 0.9333E-09 0.6529E-02 0.9550E-09 0.5477E-03 0.9772E-09 0.6308E-05 0.1000E-08 0.3579E-03
0.1047E-08 0.7654E-02 0.1072E-08 0.1318E-01 0.1096E-08 0.1277E-02 0.1122E-08 0.2660E-02 0.1148E-08 0.1108E-02
0.1175E-08 0.3964E-02 0.1202E-08 0.2310E-02 0.1230E-08 0.1439E-02 0.1259E-08 0.2993E-02 0.1288E-08 0.1091E-01
0.1318E-08 0.1178E-02 0.1349E-08 0.2196E-02 0.1380E-08 0.4382E-02 0.1413E-08 0.6734E-02 0.1445E-08 0.2226E-02
0.1479E-08 0.1221E-01 0.1514E-08 0.6134E-03 0.1585E-08 0.4411E-03 0.1622E-08 0.6738E-02 0.1660E-08 0.1515E-01
0.1698E-08 0.3130E-02 0.1738E-08 0.5440E-02 0.1778E-08 0.1180E-02 0.1820E-08 0.1170E-02 0.1862E-08 0.5153E-02
0.1905E-08 0.9597E-02 0.1950E-08 0.2662E-06 0.1995E-08 0.1142E-01 0.2042E-08 0.4845E-03 0.2089E-08 0.4202E-03
0.2138E-08 0.1522E-02 0.2188E-08 0.1079E-02 0.2239E-08 0.1747E-01 0.2291E-08 0.2870E-02 0.2344E-08 0.4879E-04
0.2399E-08 0.1470E-02 0.2455E-08 0.4404E-02 0.2512E-08 0.1744E-01 0.2570E-08 0.3317E-02 0.2630E-08 0.6438E-03
0.2692E-08 0.1995E-02 0.2754E-08 0.3897E-02 0.2818E-08 0.6913E-02 0.2884E-08 0.1339E-01 0.2951E-08 0.1246E-02
0.3020E-08 0.2399E-01 0.3090E-08 0.6752E-02 0.3162E-08 0.1053E-02 0.3236E-08 0.1570E-02 0.3311E-08 0.1040E-01
0.3388E-08 0.1226E-01 0.3467E-08 0.8472E-02 0.3548E-08 0.2702E-02 0.3631E-08 0.1470E-01 0.3715E-08 0.1393E-01
0.3802E-08 0.3784E-02 0.3890E-08 0.7951E-02 0.3981E-08 0.3037E-02 0.4074E-08 0.1013E-01 0.4169E-08 0.4053E-02
0.4266E-08 0.5532E-02 0.4365E-08 0.1570E-02 0.4467E-08 0.1492E-01 0.4571E-08 0.1126E-01 0.4677E-08 0.4332E-02
0.4786E-08 0.2079E-02 0.4898E-08 0.2190E-02 0.5012E-08 0.5363E-03 0.5129E-08 0.1378E-02 0.5248E-08 0.1662E-01
0.5370E-08 0.7753E-02 0.5495E-08 0.1398E-01 0.5623E-08 0.5971E-02 0.5754E-08 0.4120E-02 0.5888E-08 0.2661E-03
0.6026E-08 0.1794E-01 0.6166E-08 0.1012E-01 0.6310E-08 0.7173E-02 0.6457E-08 0.1779E-02 0.6607E-08 0.4927E-02
0.6761E-08 0.3418E-03 0.6918E-08 0.5400E-02 0.7079E-08 0.3576E-02 0.7244E-08 0.4584E-01 0.7413E-08 0.7084E-02
0.7586E-08 0.2841E-02 0.7762E-08 0.3751E-02 0.7943E-08 0.1454E-01 0.8128E-08 0.2690E-02 0.8318E-08 0.3214E-02
0.8511E-08 0.6362E-02 0.8710E-08 0.3758E-02 0.8913E-08 0.4495E-02 0.9120E-08 0.1600E-01 0.9333E-08 0.1708E-01
0.9550E-08 0.2688E-02 0.9772E-08 0.8341E-02 0.1000E-07 0.4764E-02 0.1023E-07 0.3591E-02 0.1047E-07 0.8412E-03
0.1072E-07 0.4047E-03 0.1096E-07 0.7083E-03 0.1122E-07 0.1803E-01 0.1148E-07 0.7621E-02 0.1175E-07 0.1183E-01
0.1202E-07 0.3088E-02 0.1230E-07 0.5205E-02 0.1259E-07 0.3472E-03 0.1288E-07 0.3972E-02 0.1318E-07 0.2813E-02
0.1349E-07 0.3376E-02 0.1380E-07 0.1154E-01 0.1413E-07 0.2194E-02 0.1479E-07 0.1047E-01 0.1514E-07 0.1292E-01
0.1549E-07 0.4458E-02 0.1585E-07 0.8949E-02 0.1622E-07 0.1133E-02 0.1660E-07 0.1232E-02 0.1698E-07 0.8395E-02
0.1738E-07 0.4590E-02 0.1778E-07 0.9214E-02 0.1820E-07 0.4726E-03 0.1862E-07 0.5086E-03 0.1905E-07 0.3304E-02
0.1950E-07 0.8705E-02 0.1995E-07 0.6104E-02 0.2042E-07 0.1745E-02 0.2089E-07 0.2883E-03 0.2138E-07 0.1063E-01
0.2188E-07 0.1277E-02 0.2239E-07 0.7168E-03 0.2344E-07 0.1552E-02 0.2399E-07 0.5379E-02 0.2455E-07 0.8711E-03
0.2512E-07 0.2659E-02 0.2570E-07 0.1531E-02 0.2630E-07 0.6000E-04 0.2692E-07 0.4283E-02 0.2754E-07 0.2643E-02
0.2818E-07 0.2264E-02 0.2884E-07 0.4201E-03 0.2951E-07 0.6179E-02 0.3090E-07 0.2626E-02 0.3162E-07 0.5580E-02
0.3236E-07 0.1443E-02 0.3311E-07 0.8571E-03 0.3388E-07 0.1553E-02 0.3631E-07 0.2831E-02 0.3715E-07 0.5218E-03
0.3802E-07 0.1993E-02 0.3981E-07 0.2457E-03 0.4074E-07 0.5687E-03 0.4169E-07 0.1145E-02 0.4266E-07 0.6438E-03
0.4467E-07 0.2322E-02 0.4571E-07 0.4947E-03 0.4677E-07 0.2105E-03 0.5012E-07 0.4557E-03 0.5623E-07 0.1228E-02
0.5888E-07 0.1193E-02 0.6026E-07 0.1234E-03 0.6166E-07 0.6718E-03 0.6607E-07 0.2192E-03 0.6761E-07 0.1432E-02
235
0.4365E-10 0.8939E-04 0.4898E-10 0.1053E-03 0.5754E-10 0.2899E-04 0.6310E-10 0.1710E-07 0.6761E-10 0.5861E-07
0.9550E-10 0.5634E-03 0.1148E-09 0.7180E-03 0.1380E-09 0.3044E-03 0.1413E-09 0.9431E-03 0.1445E-09 0.1567E-06
0.1479E-09 0.2496E-03 0.1549E-09 0.3585E-03 0.1622E-09 0.1056E-02 0.1820E-09 0.2499E-03 0.1862E-09 0.9872E-04
0.1905E-09 0.9725E-03 0.1995E-09 0.5822E-07 0.2138E-09 0.1034E-06 0.2188E-09 0.9614E-07 0.2291E-09 0.1021E-02
0.2570E-09 0.1026E-02 0.2818E-09 0.4255E-05 0.2884E-09 0.8939E-04 0.2951E-09 0.2003E-03 0.3020E-09 0.3010E-02
0.3090E-09 0.1919E-02 0.3162E-09 0.5747E-06 0.3311E-09 0.1053E-03 0.3548E-09 0.2310E-02 0.3631E-09 0.2782E-02
0.3802E-09 0.2265E-04 0.3890E-09 0.2899E-04 0.3981E-09 0.8548E-05 0.4169E-09 0.4744E-04 0.4365E-09 0.9753E-03
0.4467E-09 0.4056E-04 0.4571E-09 0.4040E-02 0.4677E-09 0.8897E-05 0.4786E-09 0.8514E-03 0.4898E-09 0.3834E-02
0.5129E-09 0.3594E-02 0.5248E-09 0.9067E-06 0.5495E-09 0.2003E-03 0.5754E-09 0.4528E-02 0.5888E-09 0.8509E-03
0.6166E-09 0.3312E-02 0.6457E-09 0.5634E-03 0.6607E-09 0.3204E-02 0.6918E-09 0.1115E-02 0.7244E-09 0.4763E-02
0.7586E-09 0.4831E-02 0.7762E-09 0.7200E-03 0.7943E-09 0.1019E-03 0.8128E-09 0.3231E-02 0.8318E-09 0.5015E-02
0.8511E-09 0.3576E-05 0.8913E-09 0.1676E-02 0.9120E-09 0.1267E-03 0.9333E-09 0.8304E-04 0.9550E-09 0.4796E-02
0.9772E-09 0.1029E-01 0.1000E-08 0.8855E-03 0.1023E-08 0.1957E-05 0.1047E-08 0.7179E-03 0.1072E-08 0.2037E-03
0.1096E-08 0.1056E-02 0.1148E-08 0.7882E-02 0.1175E-08 0.6261E-02 0.1202E-08 0.3005E-02 0.1230E-08 0.2720E-03
0.1259E-08 0.2035E-02 0.1288E-08 0.1017E-02 0.1318E-08 0.3452E-04 0.1349E-08 0.7672E-03 0.1380E-08 0.6718E-02
0.1413E-08 0.7211E-02 0.1445E-08 0.1100E-02 0.1479E-08 0.5690E-02 0.1514E-08 0.3341E-02 0.1549E-08 0.1061E-01
0.1585E-08 0.3599E-02 0.1660E-08 0.2976E-02 0.1698E-08 0.3715E-02 0.1738E-08 0.2174E-05 0.1778E-08 0.4263E-02
0.1820E-08 0.2310E-02 0.1862E-08 0.1687E-01 0.1905E-08 0.3208E-02 0.1950E-08 0.1333E-02 0.1995E-08 0.4455E-03
0.2042E-08 0.3211E-02 0.2089E-08 0.2295E-03 0.2138E-08 0.1439E-01 0.2188E-08 0.1210E-02 0.2239E-08 0.4606E-02
0.2291E-08 0.5169E-02 0.2344E-08 0.8348E-02 0.2399E-08 0.1876E-01 0.2455E-08 0.1469E-02 0.2512E-08 0.3557E-03
0.2570E-08 0.3332E-02 0.2630E-08 0.1106E-01 0.2692E-08 0.7650E-02 0.2754E-08 0.4092E-02 0.2818E-08 0.5128E-02
0.2884E-08 0.6378E-02 0.2951E-08 0.3052E-02 0.3020E-08 0.4010E-02 0.3090E-08 0.4198E-02 0.3162E-08 0.1140E-01
0.3236E-08 0.2851E-02 0.3311E-08 0.4906E-02 0.3388E-08 0.2901E-02 0.3467E-08 0.4618E-02 0.3548E-08 0.7818E-03
0.3631E-08 0.1819E-02 0.3715E-08 0.1280E-02 0.3802E-08 0.1819E-01 0.3890E-08 0.1566E-01 0.3981E-08 0.5779E-02
0.4074E-08 0.4495E-02 0.4169E-08 0.3051E-02 0.4266E-08 0.1176E-03 0.4365E-08 0.6453E-02 0.4467E-08 0.2747E-01
0.4571E-08 0.1357E-01 0.4677E-08 0.4276E-02 0.4786E-08 0.1124E-01 0.4898E-08 0.1256E-01 0.5012E-08 0.1068E-03
0.5129E-08 0.1220E-01 0.5248E-08 0.2013E-05 0.5370E-08 0.1139E-01 0.5495E-08 0.1348E-01 0.5623E-08 0.4583E-02
0.5754E-08 0.9862E-02 0.5888E-08 0.1274E-01 0.6026E-08 0.1997E-02 0.6166E-08 0.1269E-01 0.6310E-08 0.7402E-02
0.6457E-08 0.1877E-02 0.6607E-08 0.4690E-02 0.6761E-08 0.1529E-02 0.6918E-08 0.1596E-01 0.7079E-08 0.1710E-02

```
0.7244E-08 0.1614E-01 0.7413E-08 0.5621E-02 0.7586E-08 0.1504E-01 0.7762E-08 0.1118E-02 0.7943E-08 0.9316E-02
0.8128E-08 0.2798E-02 0.8318E-08 0.1171E-01 0.8511E-08 0.1595E-02 0.8710E-08 0.8790E-02 0.8913E-08 0.1395E-01
0.9120E-08 0.1959E-01 0.9333E-08 0.2958E-02 0.9550E-08 0.1670E-01 0.9772E-08 0.1309E-01 0.1000E-07 0.1531E-01
0.1023E-07 0.4920E-02 0.1047E-07 0.3221E-02 0.1072E-07 0.5392E-02 0.1096E-07 0.2803E-02 0.1122E-07 0.1299E-01
0.1148E-07 0.1376E-01 0.1175E-07 0.5889E-04 0.1202E-07 0.5226E-02 0.1230E-07 0.5789E-02 0.1259E-07 0.5700E-02
0.1288E-07 0.1413E-01 0.1349E-07 0.1191E-01 0.1413E-07 0.1518E-01 0.1445E-07 0.5560E-02 0.1479E-07 0.4977E-02
0.1514E-07 0.1092E-02 0.1549E-07 0.9164E-02 0.1585E-07 0.3228E-03 0.1622E-07 0.4320E-02 0.1660E-07 0.2415E-01
0.1698E-07 0.6718E-03 0.1738E-07 0.3376E-02 0.1778E-07 0.6113E-02 0.1820E-07 0.1712E-02 0.1862E-07 0.7640E-02
0.1905E-07 0.9165E-02 0.1950E-07 0.3584E-02 0.1995E-07 0.7110E-03 0.2042E-07 0.7255E-02 0.2089E-07 0.1213E-01
0.2138E-07 0.2407E-02 0.2188E-07 0.5658E-02 0.2239E-07 0.5371E-02 0.2291E-07 0.4563E-03 0.2344E-07 0.2179E-02
0.2399E-07 0.9310E-02 0.2455E-07 0.4563E-02 0.2512E-07 0.1306E-04 0.2570E-07 0.3957E-02 0.2630E-07 0.1370E-02
0.2692E-07 0.1021E-02 0.2754E-07 0.2302E-02 0.2818E-07 0.2976E-02 0.2951E-07 0.1121E-01 0.3020E-07 0.5678E-03
0.3090E-07 0.2591E-02 0.3162E-07 0.2684E-02 0.3236E-07 0.1291E-02 0.3311E-07 0.5997E-04 0.3388E-07 0.3019E-02
0.3467E-07 0.6117E-02 0.3548E-07 0.3546E-02 0.3631E-07 0.8456E-03 0.3715E-07 0.9605E-03 0.3802E-07 0.3036E-07
0.3981E-07 0.2014E-02 0.4074E-07 0.3748E-03 0.4169E-07 0.6778E-03 0.4266E-07 0.1617E-02 0.4365E-07 0.1519E-02
0.4571E-07 0.2230E-02 0.4786E-07 0.1061E-02 0.5012E-07 0.4583E-03 0.5129E-07 0.1534E-02 0.5248E-07 0.8090E-03
0.5370E-07 0.6324E-03 0.5495E-07 0.3638E-04 0.5754E-07 0.3381E-04 0.6166E-07 0.2004E-02 0.6607E-07 0.6718E-03
0.6761E-07 0.5399E-03 0.7079E-07 0.8865E-03 0.7244E-07 0.2192E-03 0.7413E-07 0.3418E-03 0.7586E-07 0.2037E-03
```

Note that the distribution file is much larger, reflecting the large number of alternative hazard estimates.

Calculation of Frequency of Intersection for Kernel Density. The third approach to estimating the spatial density of volcanic events, $f(x,y)$, was to use kernel density estimates, defined by Equations **(3-10)** and **(3-11)**. The required parameter is h the smoothing constant. Two approaches were used to define the parameter h. The first was for the expert to directly specify a distribution for h. Figure G-6 shows an example of the spatial density calculated using a Epanechnikov kernel with h set to 10 km. The stippled pattern encompasses the 95 percent density region.

For the case of an expert specified value of h, the annual frequency of intersection is calculated using program **FKVH**(v1.0). First, the program reads in the conditional probability of intersection values for the computation grid (the output of program **CPDI**). Then it reads in the discrete distributions for the volcanic event counts at each of the volcanic centers associated with the field. The program then uses nested loops to calculate all possible combinations of event counts associated with the field. For each possible event count a kernel density estimate of $f(x,y)$ is calculated using the specified kernel type and value of h. These spatial densities are combined with the three point distribution for the rate parameter calculated as described above. The program then performs the summation of Equation **(G-1)** for each rate parameter and spatial density estimate, given a specific set of events. Hidden event factors are then included in the same manner as in the calculations described above.

The following is a listing of example input and output files for program **FKVH** using the example shown of Figure G-6. The example presents only calculations for the homogeneous temporal model. Results for the nonhomogeneous Weibull process are obtained in exactly the same manner as in the use of program **UZVH**.

Input File: **FKVH.IN**

```
fk.in                          first individual source zone input file
q                              q to quit
```

Input File: **fk.IN**

```
.\cpdi\examp.cpi                        output file from program CPDI
Epanechnikov kernel fix h of 10 km - homogeneous  field calculation label
fk-h                                    output file name
1                                       # of fields
Example Zone                            field label
'x' 'e' 10 1 1 0                        zone boundary file for constraint of density function (x indicates no
                                                constraint), kernel type (e - Epanechnikov, g - Gaussian), h for
major
                                                axis, unit variance for major axis of kernel, unit variance for minor
                                                axis, azimuth of major axis
1 1  LN                                 remaining parameters are the same as described above for input file
'X'                                             UZ.IN used in program UZVH
 1 1 NWCF
'nvc.3'
  1 1   SECF
'svc.4'
   1 1   AG
'X'
    1 1     SB
'X'
     1 1      TM
'X'
      1 1      BM
'X'
     t 5000000 1.0 0 1 1.0 1.0
```

As before, the program produces three output files for each calculation.

Output File: **FK-H.OUT**

```
Epanechnikov kernel fix h of 10 km - homogeneous
 Source              SUM1        SUM2        SUM3       mambda    mbeta  sbeta
Example Zone     0.0000E+00  0.6123E-02  0.7261E-02  0.1509E-05  0.000  0.000
```

Output File: **FK-H.HAZ**

```
Epanechnikov kernel fix h of 10 km - homogeneous
    3
     1   0.0000000E+00   0.0000000E+00   0.0000000E+00   0.0000000E+00   0.0000000E+00   0.0000000E+00   0.0000000E+00
0.0000000E+00  0.0000000E+00  0.0000000E+00  0.0000000E+00  0.0000000E+00  0.0000000E+00
     2   0.9241772E-08   0.2286762E-16   0.2999940E-23   0.2999940E-23   0.2999940E-23   0.2999940E-23   0.2999940E-23
0.2999940E-23  0.2999940E-23  0.2999940E-23  0.2999940E-23  0.2999940E-23  0.2286762E-16
     3   0.1096076E-07   0.3216559E-16   0.2459447E-23   0.2459447E-23   0.2459447E-23   0.2459447E-23   0.2459447E-23
0.2459447E-23  0.2459447E-23  0.2459447E-23  0.2459447E-23  0.2459447E-23  0.3216559E-16
```

Output File: **FK-H.DST**

```
Epanechnikov kernel fix h of 10 km - hom
    3
    1
 0.0000E+00 0.1000E+01
    3
 0.2630E-08 0.1850E+00 0.8511E-08 0.6300E+00 0.1820E-07 0.1850E+00
    3
 0.3162E-08 0.1850E+00 0.1023E-07 0.6300E+00 0.2138E-07 0.1850E+00
```

The second approach for selecting the value of the smoothing parameter *h* involves matching a specified density contour of the kernel density function to a volcanic zone boundary in a similar fashion to the method for defining Gaussian field parameters shown on Figure G-4. A range of trial values of *h* are used to calculate a specified density contour of the kernel density estimate. For each value of *h* the area of mismatch is calculated. The area of mismatch is defined as the area within the specified density contour but outside of the zone boundary plus the area within the zone boundary but outside of the specified density contour (see Figure F-2). The selected value of *h* is the one that minimizes the area of mismatch. Figure G-7 shows an example of fitting a 95 percent density contour for an Epanechnikov kernel to the events and source zone boundary shown on Figure G-3. The value of *h* that minimizes the area of mismatch is 5.2 km.

This approach for calculating the annual frequency of intersection is implemented in program **ZBCKVH**(v1.0). First, the program reads in the conditional probability of intersection values for the computation grid (the output of program **CPDI**). Then it reads in the zone boundary and the discrete distributions for the volcanic event counts at each of the volcanic centers associated with the field. The program then uses nested loops to calculate all possible combinations of event counts associated with the field. For each possible event count the value of *h* that minimizes the area of mismatch is found using the minimization routines given in Press et al. (1992). For this value of *h* a spatial density function is calculated and combined with the three point distribution for the rate parameter calculated as described above. The program then performs the summation of Equation **(G-1)** for each rate parameter and the spatial density estimate, given a specific set of events. Hidden event factors are then included in the same manner as in the calculations described above.

The following is a listing of example input and output files for program **ZBCKVH** using the example shown of Figure G-7. The example presents only calculations for the homogeneous temporal model. Results for the nonhomogeneous Weibull process are obtained in exactly the same manner as in the use of program **UZVH**.

Input File: **ZBCKVH.IN**

```
ek.in                          first individual source zone input file
q                              q to quit
```

Input File: **ek.IN**

```
.\cpdi\examp1.cpi              output file from program CPDI (note that a new grid with a 1 km spacing was
calculated
                                        to use in this example to all for a better fit to the zone boundary
95% Epanechnikov kernel fit to Example Zone - homogeneous calculation label
ek95-h                         output file
1                              number of sources
Example Zone                   source label
'examp.z' 'e' 5 0.95 .001 20   zone boundary file (listed in the UZVH example), kernel type (e - Epanechnikov,
```

```
                                        g- Gaussian), starting value of h, density probability for zone boundary,
                                        minimization stopping tolerance, maximum number of iterations
1 1  LN                                 remaining parameters are the same as described above for input file
'X'                                             UZ.IN used in program UZVH
 1 1 NWCF
'nvc.3'
  1 1   SECF
'svc.4'
   1 1   AG
'X'
    1 1     SB
'X'
     1 1      TM
'X'
      1 1      BM
'X'
     t 5000000 1.0 0 1 1.0 1.0
```

As before, the program produces three output files for each calculation.

Output File: **EK95-H.OUT**

```
95% Epanechnikov kernel fit to Example Zone - homogeneous
 Source              SUM1        SUM2        SUM3       mambda    mbeta  sbeta mean H
Example Zone     0.0000E+00  0.3434E-04  0.1321E-02  0.1509E-05  0.000  0.000  5.215  0.000

Note the file lists the statistics of the fitted values of h
```

Output File: **EK95-H.HAZ**

```
95% Epanechnikov kernel fit to Example Zone - homogeneous
    3
     1   0.0000000E+00   0.0000000E+00   0.0000000E+00   0.0000000E+00   0.0000000E+00   0.0000000E+00   0.0000000E+00
0.0000000E+00  0.0000000E+00  0.0000000E+00  0.0000000E+00  0.0000000E+00  0.0000000E+00
     2   0.5183692E-10   0.7194298E-21   0.0000000E+00   0.0000000E+00   0.0000000E+00   0.0000000E+00   0.0000000E+00
0.0000000E+00  0.0000000E+00  0.0000000E+00  0.0000000E+00  0.0000000E+00  0.7194298E-21
     3   0.1994310E-08   0.1064867E-17   0.1084203E-24   0.1084203E-24   0.1084203E-24   0.1084203E-24   0.1084203E-24
0.1084203E-24  0.1084203E-24  0.1084203E-24  0.1084203E-24  0.1084203E-24  0.1064867E-17
```

Output File: **EK95-H.DST**

```
95% Epanechnikov kernel fit to Example Z
    3
    1
 0.0000E+00 0.1000E+01
    3
 0.1585E-10 0.1850E+00 0.4898E-10 0.6300E+00 0.1023E-09 0.1850E+00
    3
 0.5754E-09 0.1850E+00 0.1862E-08 0.6300E+00 0.3890E-08 0.1850E+00
```

G.2.3 Combined Hazard Calculation

The five computer programs described above calculate the frequency of intersection for specific sources and sets of parameters. The final calculation is to combine the contributions from all of the sources and calculate the hazard distribution over all of the possible models and parameters specified by the experts in their volcanic hazard model logic trees, and aggregate the distributions from all experts. This calculation is performed using computer program **VHTREE(v1.0)**. The program consists of a set of nested loops that read in the discrete distributions for models and parameters defined by the experts and laid out in the sequence

presented on Figures 3-15 and 3-16. The program reads as input the weights assigned to the logic tree branches and the output files (with the extensions **.HAZ** and **.DST**) developed by the various calculation modules described above.

The input and output files for an example calculation are described below.

Input File: **VHTREE.IN**

```
Aggregated                                          calculation label
'x' 'x' 'Expert' 'x' 'DLD' 'DAzm' 'TempM' 'TimeP' 'BG' 'SpaceM' 'ZoneM' 'ZoneB' 'AgeD' 'ZEgd' 'H' 'SRBase' 'SRFac' 'LW'
'NWCF' 'SECF' 'AV' 'SB' 'TM' 'BM' 'FP' 'OZEC' 'HE' 'Rate' labels for the levels of the logic tree
1 1                                                 additional level of logic tree not used
 1 1                                                additional level of logic tree not used
  1 1 Experts                                       # of experts, weight assigned to each expert
   1 Source Types                                   additional level of logic tree not used
    1 1  Event Type                                 # of event types, weight assigned to each event type
     1 1  Dike Length Distribution                  # of dike length distributions, weight assigned to each distribution
      1 1  Dike Azimuth Distribution                # of dike azimuth distributions, weight assigned to each distribution
       1 1  Temporal Model                          # of temporal models, weight assigned to each model
        1 1  Time Period                            # of time periods, weight assigned to each time period
         1 1  Backgrounds                           # of regions of interest, weight assigned to region
          5 .2 .2 .2 .2 .2  Spatial Model           # of spatial models, weight assigned to each model
           1 1  Zonation Model                      # of zonation models, weight assigned to each model
            1 1  Zone Boundaries                    # of zone boundary alternatives, weight assigned to each alternative
             1  sources                             # of source for this spatial and zonation model
              1 1 Age Dates                         # of age date sets, weight assigned to each date set
               1 1  Zone Edge                       # of zone edge models, weight assigned to each model
                1 1  H - Smoothing parameter        # of smoothing parameter values, weight assigned to each value
                 1 1  Source Rate Basis             # of approaches to calculating zone event rate, weight assigned to
                                                        each approach
                  1 1  Source Rate Factor           # of source rate factors, weight assigned to each factor
.\haz\uz-h                                          output fine name for first spatial model
           1 1  Zonation Model                      remaining lines give the input for the other spatial models
            1 1  Zone Boundaries
             1  sources
              1 1 Age Dates
               1 1  Zone Edge
                1 1  H - Smoothing parameter
                 1 1  Source Rate Basis
                  1 1  Source Rate Factor
.\haz\pf-h
           1 1  Zonation Model
            1 1  Zone Boundaries
             1  sources
              1 1 Age Dates
               1 1  Zone Edge
                1 1  H - Smoothing parameter
                 1 1  Source Rate Basis
                  1 1  Source Rate Factor
.\haz\fpf-h
           1 1  Zonation Model
            1 1  Zone Boundaries
             1  sources
              1 1 Age Dates
               1 1  Zone Edge
                1 1  H - Smoothing parameter
                 1 1  Source Rate Basis
                  1 1  Source Rate Factor
.\haz\fk-h
           1 1  Zonation Model
            1 1  Zone Boundaries
             1  sources
```

```
             1 1 Age Dates
              1 1  Zone Edge
               1 1  H - Smoothing parameter
                1 1  Source Rate Basis
                 1 1  Source Rate Factor
.\haz\ek95-h
```

The program produces two primary output files.

Output File: VHTREE

```
    total hazard:
Aggregated

  iz            enu             snu        cov

   1  0.2454167E-09  0.1016103E-08      4.140     mean, standard deviation, and coefficient of variation for the three
   2  0.6165958E-08  0.6064549E-08      0.984           event type measures (1 - point event, 2 - event centered
dike,
   3  0.8670821E-08  0.7415725E-08      0.855           3 - randomly placed dike)


 Contributions to Variance in Hazard Rate

                          percent contribution to variance from:
  iz       cov Expert DLD    DAzm   TempM  TimeP  BG     SpaceM ZoneM  ZoneB  AgeD   ZEgd   H
   1     4.140  0.000  0.000  0.000  0.000  0.000  0.000  0.166  0.000  0.000  0.000  0.000  0.000
   2     0.984  0.000  0.000  0.000  0.000  0.000  0.000  0.318  0.000  0.000  0.000  0.000  0.000
   3     0.855  0.000  0.000  0.000  0.000  0.000  0.000  0.301  0.000  0.000  0.000  0.000  0.000
 ************************************************************************

 SRBase SRFac  LW     NWCF   SECF   AV     SB     TM     BM     FP     OZEC   HE     Rate
  0.000  0.000  0.000  0.000  0.000  0.000  0.000  0.000  0.000  0.611  0.000  0.000  0.224
  0.000  0.000  0.000  0.000  0.000  0.000  0.000  0.000  0.000  0.253  0.000  0.000  0.430
  0.000  0.000  0.000  0.000  0.000  0.000  0.000  0.000  0.000  0.199  0.000  0.000  0.500

Breakdown of the total variance into the fraction arising from uncertainty at each level of the logic tree.  In this
example the only uncertainties are in the spatial model, the Gaussian field parameters, and the statistical
uncertainty in the rate estimate.

 Aggregated

 probability levels calculated from distribution

   iz       enu         snu    pl: 0.0500      0.1000      0.1500      0.2000      0.3000      0.4000      0.5000      0.6000
  0.7000      0.8000      0.8500      0.9000      0.9500
    1 0.2463E-09 0.1017E-08 0.0000E+00 0.0000E+00 0.0000E+00 0.0000E+00 0.0000E+00 0.0000E+00 0.0000E+00 0.0000E+00
0.8710E-10 0.1549E-09 0.1995E-09 0.3236E-09 0.1023E-08
    2 0.6158E-08 0.6057E-08 0.5248E-10 0.5248E-10 0.5248E-10 0.1023E-09 0.2512E-08 0.3715E-08 0.4677E-08 0.8511E-08
0.8511E-08 0.8511E-08 0.9772E-08 0.1514E-07 0.1820E-07
    3 0.8674E-08 0.7386E-08 0.8913E-09 0.1862E-08 0.1862E-08 0.2042E-08 0.3715E-08 0.5129E-08 0.6607E-08 0.1023E-07
0.1023E-07 0.1318E-07 0.1380E-07 0.1862E-07 0.2455E-07

Fractiles of the discrete distribution for frequency of intersection
```

Output File: VHTREE.DST

```
Aggregated
   3
  284
 0.0000E+00 0.6109E+00 0.3981E-11 0.1109E-02 0.4074E-11 0.2384E-02 0.4169E-11 0.2059E-02 0.4266E-11 0.2343E-03
 0.4365E-11 0.1941E-03 0.4467E-11 0.2168E-03 0.4571E-11 0.3857E-03 0.4677E-11 0.5483E-03 0.4786E-11 0.1700E-03
 0.4898E-11 0.4262E-05 0.5012E-11 0.2316E-03 0.5129E-11 0.3292E-03 0.5248E-11 0.1130E-03 0.5370E-11 0.8670E-06
 0.5495E-11 0.1510E-03 0.5623E-11 0.7854E-04 0.5888E-11 0.1251E-05 0.6026E-11 0.4576E-05 0.6166E-11 0.4475E-05
```

0.6310E-11 0.3914E-06 0.6607E-11 0.6883E-05 0.6761E-11 0.4338E-07 0.7079E-11 0.2546E-06 0.7244E-11 0.1324E-02
0.7413E-11 0.8228E-03 0.7586E-11 0.4438E-06 0.7762E-11 0.9436E-03 0.7943E-11 0.7860E-04 0.8318E-11 0.4528E-05
0.8511E-11 0.5726E-05 0.8710E-11 0.1592E-04 0.8913E-11 0.2864E-03 0.9333E-11 0.6490E-04 0.9772E-11 0.6574E-03
0.1023E-10 0.8866E-03 0.1047E-10 0.2236E-03 0.1072E-10 0.1787E-04 0.1096E-10 0.5724E-05 0.1122E-10 0.2416E-03
0.1202E-10 0.6652E-04 0.1230E-10 0.2106E-04 0.1259E-10 0.2310E-04 0.1288E-10 0.6110E-03 0.1380E-10 0.1681E-05
0.1413E-10 0.1916E-02 0.1445E-10 0.1086E-04 0.1479E-10 0.6488E-03 0.1514E-10 0.5796E-05 0.1585E-10 0.2880E-06
0.1622E-10 0.2442E-02 0.1660E-10 0.2352E-04 0.1738E-10 0.4900E-04 0.1778E-10 0.2500E-04 0.1862E-10 0.1652E-04
0.1905E-10 0.7620E-04 0.1950E-10 0.1019E-02 0.1995E-10 0.5644E-08 0.2042E-10 0.9404E-04 0.2089E-10 0.1088E-02
0.2138E-10 0.6072E-08 0.2188E-10 0.6786E-05 0.2239E-10 0.2182E-02 0.2291E-10 0.5656E-04 0.2344E-10 0.1733E-04
0.2455E-10 0.3748E-02 0.2512E-10 0.5776E-03 0.2570E-10 0.5724E-03 0.2951E-10 0.1389E-05 0.3020E-10 0.1186E-02
0.3162E-10 0.6116E-03 0.3236E-10 0.2338E-02 0.3311E-10 0.1258E-03 0.3388E-10 0.7932E-04 0.3467E-10 0.6416E-03
0.3548E-10 0.1200E-04 0.3631E-10 0.3082E-03 0.3715E-10 0.2514E-03 0.3890E-10 0.2268E-02 0.3981E-10 0.2038E-04
0.4266E-10 0.7062E-03 0.4365E-10 0.1661E-04 0.4467E-10 0.4384E-04 0.4677E-10 0.8838E-03 0.4786E-10 0.6956E-04
0.4898E-10 0.1716E-03 0.5012E-10 0.6436E-03 0.5129E-10 0.3712E-01 0.5248E-10 0.2420E-04 0.5370E-10 0.1204E-03
0.5495E-10 0.5112E-03 0.5623E-10 0.1053E-03 0.5754E-10 0.1922E-07 0.5888E-10 0.3202E-03 0.6026E-10 0.9166E-04
0.6166E-10 0.4184E-02 0.6310E-10 0.2068E-07 0.6761E-10 0.6984E-03 0.6918E-10 0.1726E-03 0.7244E-10 0.4502E-02
0.7413E-10 0.5324E-03 0.7943E-10 0.8920E-04 0.8128E-10 0.6416E-03 0.8511E-10 0.2390E-03 0.8710E-10 0.2936E-02
0.9120E-10 0.4900E-04 0.9333E-10 0.2104E-02 0.9550E-10 0.2208E-02 0.9772E-10 0.4284E-03 0.1000E-09 0.2552E-03
0.1023E-09 0.2184E-02 0.1047E-09 0.1034E-03 0.1072E-09 0.1993E-02 0.1096E-09 0.1792E-03 0.1122E-09 0.5644E-08
0.1148E-09 0.3778E-03 0.1175E-09 0.2492E-03 0.1202E-09 0.1084E-02 0.1230E-09 0.6072E-08 0.1259E-09 0.2228E-03
0.1288E-09 0.2042E-04 0.1349E-09 0.2258E-03 0.1380E-09 0.4938E-03 0.1413E-09 0.1448E-02 0.1445E-09 0.1484E-03
0.1479E-09 0.2232E-02 0.1514E-09 0.4114E-03 0.1549E-09 0.1261E+00 0.1622E-09 0.2818E-03 0.1698E-09 0.5198E-03
0.1778E-09 0.8388E-03 0.1820E-09 0.2442E-02 0.1862E-09 0.4336E-03 0.1950E-09 0.8508E-06 0.1995E-09 0.1248E-02
0.2042E-09 0.5110E-03 0.2089E-09 0.1017E-02 0.2138E-09 0.9054E-03 0.2188E-09 0.1813E-02 0.2239E-09 0.5882E-03
0.2291E-09 0.2208E-05 0.2344E-09 0.5886E-04 0.2399E-09 0.6048E-03 0.2455E-09 0.1075E-03 0.2512E-09 0.1887E-02
0.2570E-09 0.2328E-03 0.2630E-09 0.4290E-02 0.2692E-09 0.3090E-03 0.2754E-09 0.7904E-03 0.2818E-09 0.4384E-04
0.2884E-09 0.2790E-03 0.3020E-09 0.3098E-02 0.3090E-09 0.2190E-02 0.3162E-09 0.1109E-02 0.3236E-09 0.3705E-01
0.3311E-09 0.9072E-04 0.3388E-09 0.3204E-02 0.3467E-09 0.4800E-03 0.3715E-09 0.8488E-03 0.3802E-09 0.1486E-02
0.3890E-09 0.1729E-03 0.4074E-09 0.3540E-03 0.4169E-09 0.6014E-03 0.4266E-09 0.2014E-03 0.4365E-09 0.3306E-03
0.4467E-09 0.2412E-02 0.4571E-09 0.5874E-03 0.4677E-09 0.6496E-03 0.5012E-09 0.6844E-03 0.5248E-09 0.7496E-04
0.5370E-09 0.4882E-03 0.5495E-09 0.3074E-02 0.5623E-09 0.6072E-04 0.5754E-09 0.2690E-03 0.5888E-09 0.8738E-03
0.6026E-09 0.1135E-02 0.6310E-09 0.9690E-04 0.6457E-09 0.2030E-02 0.6761E-09 0.3778E-02 0.7079E-09 0.4044E-03
0.7244E-09 0.1613E-02 0.7413E-09 0.2412E-03 0.7586E-09 0.2826E-03 0.7762E-09 0.1315E-02 0.7943E-09 0.3718E-02
0.8128E-09 0.2514E-03 0.8318E-09 0.4070E-03 0.8511E-09 0.7656E-03 0.8710E-09 0.3422E-03 0.8913E-09 0.2264E-02
0.9120E-09 0.5930E-04 0.9333E-09 0.1064E-02 0.9550E-09 0.6360E-03 0.9772E-09 0.2538E-02 0.1000E-08 0.5306E-03
0.1023E-08 0.1750E-02 0.1047E-08 0.2410E-03 0.1072E-08 0.2266E-03 0.1096E-08 0.4638E-03 0.1148E-08 0.5186E-03
0.1175E-08 0.2372E-03 0.1202E-08 0.4650E-03 0.1230E-08 0.1953E-02 0.1259E-08 0.4580E-03 0.1288E-08 0.2454E-03
0.1318E-08 0.3368E-02 0.1349E-08 0.3670E-03 0.1413E-08 0.8458E-03 0.1445E-08 0.1323E-02 0.1514E-08 0.2840E-03
0.1622E-08 0.2370E-02 0.1660E-08 0.2960E-03 0.1698E-08 0.1867E-02 0.1738E-08 0.1834E-03 0.1778E-08 0.2068E-03
0.1820E-08 0.2978E-03 0.1862E-08 0.2036E-02 0.1905E-08 0.4938E-03 0.1950E-08 0.1773E-03 0.1995E-08 0.1017E-03
0.2042E-08 0.8486E-03 0.2089E-08 0.2298E-03 0.2138E-08 0.3928E-03 0.2188E-08 0.2528E-02 0.2291E-08 0.6296E-03
0.2344E-08 0.1705E-03 0.2399E-08 0.1375E-02 0.2455E-08 0.2678E-03 0.2512E-08 0.4384E-04 0.2570E-08 0.5734E-03
0.2630E-08 0.5464E-04 0.2692E-08 0.1542E-02 0.2754E-08 0.4744E-03 0.2818E-08 0.6662E-03 0.2884E-08 0.4824E-03
0.2951E-08 0.1773E-03 0.3020E-08 0.7624E-03 0.3162E-08 0.5744E-03 0.3236E-08 0.5438E-03 0.3311E-08 0.1404E-02
0.3388E-08 0.1416E-02 0.3548E-08 0.9500E-03 0.3631E-08 0.2492E-03 0.3802E-08 0.1444E-02 0.3890E-08 0.7878E-03
0.3981E-08 0.5318E-03 0.4169E-08 0.4518E-03 0.4266E-08 0.1678E-02 0.4571E-08 0.6456E-04 0.4677E-08 0.6778E-03
0.4786E-08 0.1475E-03 0.4898E-08 0.4096E-05 0.5012E-08 0.1004E-03 0.5129E-08 0.2826E-03 0.5248E-08 0.7276E-05
0.5623E-08 0.6098E-03 0.5754E-08 0.2710E-03 0.5888E-08 0.2838E-03 0.6166E-08 0.1416E-03 0.6457E-08 0.1137E-03
0.6607E-08 0.9922E-04 0.6761E-08 0.1375E-03 0.6918E-08 0.5040E-03 0.7079E-08 0.1691E-03 0.7244E-08 0.7190E-04
0.7413E-08 0.2570E-03 0.7586E-08 0.5332E-03 0.7762E-08 0.8362E-03 0.7943E-08 0.4700E-03 0.8128E-08 0.3184E-03
0.8318E-08 0.2314E-03 0.8710E-08 0.5286E-03 0.8913E-08 0.1327E-03 0.9120E-08 0.9220E-03 0.9550E-08 0.6038E-03
0.1175E-07 0.1288E-03 0.1259E-07 0.8332E-04 0.1585E-07 0.1319E-03 0.1622E-07 0.2468E-04 0.1660E-07 0.3138E-03
0.1698E-07 0.4384E-04 0.1862E-07 0.1552E-03 0.1950E-07 0.1344E-03 0.1995E-07 0.1773E-03

271

0.7244E-11 0.1788E-04 0.7762E-11 0.2106E-04 0.9120E-11 0.5798E-05 0.1413E-10 0.6088E-04 0.1514E-10 0.3420E-08
0.1549E-10 0.1127E-03 0.1622E-10 0.7170E-04 0.1698E-10 0.6074E-08 0.1820E-10 0.1436E-03 0.1862E-10 0.3700E-01
0.1995E-10 0.1974E-04 0.2344E-10 0.4992E-04 0.2630E-10 0.1788E-04 0.3020E-10 0.2096E-03 0.3388E-10 0.2110E-03
0.3802E-10 0.5798E-05 0.3890E-10 0.1945E-03 0.4074E-10 0.3838E-03 0.4365E-10 0.4992E-04 0.4571E-10 0.2042E-03
0.4786E-10 0.5326E-07 0.4898E-10 0.4890E-03 0.5129E-10 0.1923E-07 0.5248E-10 0.1260E+00 0.5888E-10 0.4010E-04
0.6761E-10 0.1700E-03 0.8511E-10 0.1127E-03 0.8710E-10 0.1003E-02 0.8913E-10 0.6074E-08 0.9333E-10 0.8510E-06
0.9550E-10 0.1436E-03 0.1000E-09 0.1181E-02 0.1023E-09 0.3700E-01 0.1096E-09 0.1149E-06 0.1148E-09 0.6624E-03
0.1230E-09 0.1067E-06 0.1259E-09 0.1305E-05 0.1288E-09 0.1702E-03 0.1318E-09 0.4992E-04 0.1349E-09 0.3692E-03
0.1380E-09 0.6958E-03 0.1413E-09 0.1813E-06 0.1445E-09 0.8268E-06 0.1479E-09 0.3592E-06 0.1549E-09 0.2420E-03
0.1585E-09 0.1945E-03 0.1738E-09 0.2076E-05 0.1778E-09 0.3252E-03 0.1820E-09 0.2056E-03 0.1862E-09 0.2208E-05
0.1905E-09 0.6652E-04 0.2089E-09 0.4096E-05 0.2138E-09 0.3996E-03 0.2239E-09 0.4174E-04 0.2344E-09 0.7278E-05
0.2399E-09 0.1945E-03 0.2512E-09 0.6764E-05 0.2570E-09 0.2110E-03 0.2630E-09 0.1227E-02 0.2692E-09 0.4992E-04
0.2754E-09 0.5626E-03 0.2884E-09 0.2042E-03 0.3020E-09 0.2952E-05 0.3162E-09 0.1574E-02 0.3311E-09 0.7170E-03
0.3388E-09 0.4992E-04 0.3467E-09 0.3914E-06 0.3715E-09 0.4050E-04 0.3981E-09 0.6408E-03 0.4074E-09 0.4442E-05

0.4169E-09 0.1260E-03 0.4266E-09 0.1256E-02 0.4365E-09 0.2506E-03 0.4467E-09 0.9190E-06 0.4571E-09 0.7204E-03
0.4677E-09 0.1224E-05 0.4786E-09 0.2206E-04 0.4898E-09 0.1481E-05 0.5012E-09 0.1629E-02 0.5129E-09 0.8678E-03
0.5370E-09 0.3534E-04 0.5495E-09 0.5304E-03 0.5623E-09 0.2334E-04 0.5888E-09 0.1010E-02 0.6166E-09 0.8680E-03
0.6310E-09 0.8510E-06 0.6457E-09 0.2468E-04 0.6607E-09 0.4992E-04 0.6761E-09 0.4806E-03 0.6918E-09 0.7258E-03
0.7079E-09 0.4384E-04 0.7244E-09 0.1450E-03 0.7413E-09 0.6564E-04 0.7586E-09 0.2042E-04 0.7762E-09 0.1071E-02
0.7943E-09 0.3642E-04 0.8128E-09 0.1489E-03 0.8318E-09 0.7780E-03 0.8511E-09 0.5480E-05 0.8710E-09 0.8186E-04
0.8913E-09 0.2484E-02 0.9120E-09 0.3692E-03 0.9333E-09 0.1306E-02 0.9550E-09 0.1095E-03 0.9772E-09 0.1262E-05
0.1000E-08 0.7158E-04 0.1047E-08 0.1531E-02 0.1072E-08 0.2636E-02 0.1096E-08 0.2554E-03 0.1122E-08 0.5320E-03
0.1148E-08 0.2216E-03 0.1175E-08 0.7928E-03 0.1202E-08 0.4620E-03 0.1230E-08 0.2878E-03 0.1259E-08 0.5986E-03
0.1288E-08 0.2182E-02 0.1318E-08 0.2356E-03 0.1349E-08 0.4392E-03 0.1380E-08 0.8764E-03 0.1413E-08 0.1347E-02
0.1445E-08 0.3745E-01 0.1479E-08 0.2442E-02 0.1514E-08 0.1227E-03 0.1585E-08 0.8822E-04 0.1622E-08 0.1348E-02
0.1660E-08 0.3030E-02 0.1698E-08 0.6260E-03 0.1738E-08 0.1088E-02 0.1778E-08 0.2360E-03 0.1820E-08 0.2340E-03
0.1862E-08 0.1031E-02 0.1905E-08 0.1919E-02 0.1950E-08 0.5324E-07 0.1995E-08 0.2284E-02 0.2042E-08 0.9690E-04
0.2089E-08 0.8404E-04 0.2138E-08 0.3044E-03 0.2188E-08 0.2158E-03 0.2239E-08 0.3494E-02 0.2291E-08 0.5740E-03
0.2344E-08 0.9758E-05 0.2399E-08 0.2940E-03 0.2455E-08 0.8808E-03 0.2512E-08 0.3488E-02 0.2570E-08 0.6634E-03
0.2630E-08 0.7413E-01 0.2692E-08 0.3990E-03 0.2754E-08 0.7794E-03 0.2818E-08 0.1383E-02 0.2884E-08 0.2678E-02
0.2951E-08 0.2492E-03 0.3020E-08 0.4798E-02 0.3090E-08 0.1350E-02 0.3162E-08 0.2106E-03 0.3236E-08 0.3140E-03
0.3311E-08 0.2080E-02 0.3388E-08 0.2452E-02 0.3467E-08 0.1694E-02 0.3548E-08 0.5404E-03 0.3631E-08 0.2940E-02
0.3715E-08 0.2786E-02 0.3802E-08 0.7568E-03 0.3890E-08 0.1590E-02 0.3981E-08 0.6074E-03 0.4074E-08 0.2026E-02
0.4169E-08 0.8106E-03 0.4266E-08 0.1106E-02 0.4365E-08 0.3140E-03 0.4467E-08 0.2984E-02 0.4571E-08 0.2252E-02
0.4677E-08 0.1269E+00 0.4786E-08 0.4158E-03 0.4898E-08 0.4380E-03 0.5012E-08 0.1073E-03 0.5129E-08 0.2756E-03
0.5248E-08 0.3324E-02 0.5370E-08 0.1551E-02 0.5495E-08 0.2796E-02 0.5623E-08 0.1194E-02 0.5754E-08 0.8240E-03
0.5888E-08 0.5322E-04 0.6026E-08 0.3588E-02 0.6166E-08 0.2024E-02 0.6310E-08 0.1435E-02 0.6457E-08 0.3558E-03
0.6607E-08 0.9854E-03 0.6761E-08 0.6836E-04 0.6918E-08 0.1080E-02 0.7079E-08 0.7152E-03 0.7244E-08 0.9168E-02
0.7413E-08 0.1417E-02 0.7586E-08 0.5682E-03 0.7762E-08 0.7502E-03 0.7943E-08 0.2908E-02 0.8128E-08 0.5380E-03
0.8318E-08 0.6428E-03 0.8511E-08 0.2533E+00 0.8710E-08 0.7516E-03 0.8913E-08 0.8990E-03 0.9120E-08 0.3200E-02
0.9333E-08 0.3416E-02 0.9550E-08 0.5376E-03 0.9772E-08 0.3867E-01 0.1000E-07 0.9528E-03 0.1023E-07 0.7182E-03
0.1047E-07 0.1682E-03 0.1072E-07 0.8094E-04 0.1096E-07 0.1417E-03 0.1122E-07 0.3606E-02 0.1148E-07 0.1524E-02
0.1175E-07 0.2366E-02 0.1202E-07 0.6176E-03 0.1230E-07 0.1041E-02 0.1259E-07 0.6944E-04 0.1288E-07 0.7944E-03
0.1318E-07 0.5626E-03 0.1349E-07 0.6752E-03 0.1380E-07 0.2308E-02 0.1413E-07 0.4388E-03 0.1479E-07 0.2094E-02
0.1514E-07 0.2584E-02 0.1549E-07 0.8916E-03 0.1585E-07 0.1790E-02 0.1622E-07 0.2266E-03 0.1660E-07 0.2464E-03
0.1698E-07 0.1679E-02 0.1738E-07 0.9180E-03 0.1778E-07 0.3884E-01 0.1820E-07 0.3709E-01 0.1862E-07 0.1017E-03
0.1905E-07 0.6608E-03 0.1950E-07 0.1741E-02 0.1995E-07 0.1221E-02 0.2042E-07 0.3490E-03 0.2089E-07 0.5766E-04
0.2138E-07 0.2126E-02 0.2188E-07 0.2554E-03 0.2239E-07 0.1434E-03 0.2344E-07 0.3104E-03 0.2399E-07 0.1076E-02
0.2455E-07 0.1742E-03 0.2512E-07 0.5318E-03 0.2570E-07 0.3062E-03 0.2630E-07 0.1200E-04 0.2692E-07 0.8566E-03
0.2754E-07 0.5286E-03 0.2818E-07 0.4528E-03 0.2884E-07 0.8402E-04 0.2951E-07 0.1236E-02 0.3090E-07 0.5252E-03
0.3162E-07 0.1116E-02 0.3236E-07 0.2886E-03 0.3311E-07 0.1714E-03 0.3388E-07 0.3106E-03 0.3631E-07 0.5662E-03
0.3715E-07 0.1044E-03 0.3802E-07 0.3986E-03 0.3981E-07 0.4914E-04 0.4074E-07 0.1137E-03 0.4169E-07 0.2290E-03
0.4266E-07 0.1288E-03 0.4467E-07 0.4644E-03 0.4571E-07 0.9894E-04 0.4677E-07 0.4210E-04 0.5012E-07 0.9114E-04
0.5623E-07 0.2456E-03 0.5888E-07 0.2386E-03 0.6026E-07 0.2468E-04 0.6166E-07 0.1344E-03 0.6607E-07 0.4384E-04
0.6761E-07 0.2864E-03

237

0.4677E-10 0.1788E-04 0.5248E-10 0.2106E-04 0.6166E-10 0.5798E-05 0.6761E-10 0.3420E-08 0.7244E-10 0.1172E-07
0.9550E-10 0.1127E-03 0.1148E-09 0.1436E-03 0.1380E-09 0.6088E-04 0.1413E-09 0.1886E-03 0.1445E-09 0.3134E-07
0.1479E-09 0.4992E-04 0.1549E-09 0.7170E-04 0.1622E-09 0.2112E-03 0.1820E-09 0.4998E-04 0.1862E-09 0.1974E-04
0.1905E-09 0.1945E-03 0.1995E-09 0.1164E-07 0.2138E-09 0.2068E-07 0.2188E-09 0.1923E-07 0.2291E-09 0.2042E-03
0.2570E-09 0.2052E-03 0.2818E-09 0.8510E-06 0.2884E-09 0.1788E-04 0.2951E-09 0.4006E-04 0.3020E-09 0.6020E-03
0.3090E-09 0.3838E-03 0.3162E-09 0.1149E-06 0.3311E-09 0.2106E-04 0.3548E-09 0.4620E-03 0.3631E-09 0.5564E-03
0.3802E-09 0.4530E-05 0.3890E-09 0.5798E-05 0.3981E-09 0.1710E-05 0.4169E-09 0.9488E-05 0.4365E-09 0.1951E-03
0.4467E-09 0.8112E-05 0.4571E-09 0.8080E-03 0.4677E-09 0.1779E-05 0.4786E-09 0.1703E-03 0.4898E-09 0.7668E-03
0.5129E-09 0.7188E-03 0.5248E-09 0.1813E-06 0.5495E-09 0.4006E-04 0.5754E-09 0.3791E-01 0.5888E-09 0.1702E-03
0.6166E-09 0.6624E-03 0.6457E-09 0.1127E-03 0.6607E-09 0.6408E-03 0.6918E-09 0.2230E-03 0.7244E-09 0.9526E-03
0.7586E-09 0.9662E-03 0.7762E-09 0.1440E-03 0.7943E-09 0.2038E-04 0.8128E-09 0.6462E-03 0.8318E-09 0.1003E-02
0.8511E-09 0.7152E-06 0.8913E-09 0.3352E-03 0.9120E-09 0.2534E-04 0.9333E-09 0.1661E-04 0.9550E-09 0.9592E-03
0.9772E-09 0.2058E-02 0.1000E-08 0.1771E-03 0.1023E-08 0.3914E-06 0.1047E-08 0.1436E-03 0.1072E-08 0.4074E-04
0.1096E-08 0.2112E-03 0.1148E-08 0.1576E-02 0.1175E-08 0.1252E-02 0.1202E-08 0.6010E-03 0.1230E-08 0.5440E-04
0.1259E-08 0.4070E-03 0.1288E-08 0.2034E-03 0.1318E-08 0.6904E-05 0.1349E-08 0.1534E-03 0.1380E-08 0.1344E-02
0.1413E-08 0.1442E-02 0.1445E-08 0.2200E-03 0.1479E-08 0.1138E-02 0.1514E-08 0.6682E-03 0.1549E-08 0.2122E-02
0.1585E-08 0.7198E-03 0.1660E-08 0.5952E-03 0.1698E-08 0.7430E-03 0.1738E-08 0.4348E-06 0.1778E-08 0.8526E-03
0.1820E-08 0.4620E-03 0.1862E-08 0.1294E+00 0.1905E-08 0.6416E-03 0.1950E-08 0.2666E-03 0.1995E-08 0.8910E-04
0.2042E-08 0.3764E-01 0.2089E-08 0.4590E-04 0.2138E-08 0.2878E-02 0.2188E-08 0.2420E-03 0.2239E-08 0.9212E-03
0.2291E-08 0.1034E-02 0.2344E-08 0.1670E-02 0.2399E-08 0.3752E-02 0.2455E-08 0.2938E-03 0.2512E-08 0.7114E-04
0.2570E-08 0.6664E-03 0.2630E-08 0.2212E-02 0.2692E-08 0.1530E-02 0.2754E-08 0.8184E-03 0.2818E-08 0.1026E-02
0.2884E-08 0.1276E-02 0.2951E-08 0.6104E-03 0.3020E-08 0.8020E-03 0.3090E-08 0.8396E-03 0.3162E-08 0.3928E-01
0.3236E-08 0.5702E-03 0.3311E-08 0.9812E-03 0.3388E-08 0.5802E-03 0.3467E-08 0.9236E-03 0.3548E-08 0.1564E-03
0.3631E-08 0.3638E-03 0.3715E-08 0.2560E-03 0.3802E-08 0.3638E-02 0.3890E-08 0.4013E-01 0.3981E-08 0.1156E-02
0.4074E-08 0.3790E-01 0.4169E-08 0.6102E-03 0.4266E-08 0.2352E-04 0.4365E-08 0.1291E-02 0.4467E-08 0.5494E-02
0.4571E-08 0.2714E-02 0.4677E-08 0.8552E-03 0.4786E-08 0.2248E-02 0.4898E-08 0.2512E-02 0.5012E-08 0.2136E-04

0.5129E-08 0.2440E-02 0.5248E-08 0.4026E-06 0.5370E-08 0.2278E-02 0.5495E-08 0.2696E-02 0.5623E-08 0.9166E-03
0.5754E-08 0.1972E-02 0.5888E-08 0.2548E-02 0.6026E-08 0.3994E-03 0.6166E-08 0.2538E-02 0.6310E-08 0.1480E-02
0.6457E-08 0.3754E-03 0.6607E-08 0.1269E+00 0.6761E-08 0.3058E-03 0.6918E-08 0.3192E-02 0.7079E-08 0.3420E-03
0.7244E-08 0.3228E-02 0.7413E-08 0.1124E-02 0.7586E-08 0.3008E-02 0.7762E-08 0.2236E-03 0.7943E-08 0.1863E-02
0.8128E-08 0.5596E-03 0.8318E-08 0.2342E-02 0.8511E-08 0.3190E-03 0.8710E-08 0.1758E-02 0.8913E-08 0.2790E-02
0.9120E-08 0.3918E-02 0.9333E-08 0.5916E-03 0.9550E-08 0.3340E-02 0.9772E-08 0.2618E-02 0.1000E-07 0.3062E-02
0.1023E-07 0.1270E+00 0.1047E-07 0.6442E-03 0.1072E-07 0.1078E-02 0.1096E-07 0.5606E-03 0.1122E-07 0.2598E-02
0.1148E-07 0.2752E-02 0.1175E-07 0.1178E-04 0.1202E-07 0.1045E-02 0.1230E-07 0.1158E-02 0.1259E-07 0.1140E-02
0.1288E-07 0.2826E-02 0.1318E-07 0.1260E+00 0.1349E-07 0.2382E-02 0.1380E-07 0.3700E-01 0.1413E-07 0.3036E-02
0.1445E-07 0.1112E-02 0.1479E-07 0.9954E-03 0.1514E-07 0.2184E-03 0.1549E-07 0.1833E-02 0.1585E-07 0.6456E-04
0.1622E-07 0.8640E-03 0.1660E-07 0.4830E-02 0.1698E-07 0.1344E-03 0.1738E-07 0.6752E-03 0.1778E-07 0.1223E-02
0.1820E-07 0.3424E-03 0.1862E-07 0.1528E-02 0.1905E-07 0.1833E-02 0.1950E-07 0.7168E-03 0.1995E-07 0.1422E-03
0.2042E-07 0.1451E-02 0.2089E-07 0.2426E-02 0.2138E-07 0.3748E-01 0.2188E-07 0.1132E-02 0.2239E-07 0.1074E-02
0.2291E-07 0.9126E-04 0.2344E-07 0.4358E-03 0.2399E-07 0.1862E-02 0.2455E-07 0.9126E-03 0.2512E-07 0.2612E-05
0.2570E-07 0.7914E-03 0.2630E-07 0.2740E-03 0.2692E-07 0.2042E-03 0.2754E-07 0.3746E-01 0.2818E-07 0.5952E-03
0.2951E-07 0.2242E-02 0.3020E-07 0.1136E-03 0.3090E-07 0.5182E-03 0.3162E-07 0.5368E-03 0.3236E-07 0.2582E-03
0.3311E-07 0.1199E-04 0.3388E-07 0.6038E-03 0.3467E-07 0.1223E-02 0.3548E-07 0.7092E-03 0.3631E-07 0.1691E-03
0.3715E-07 0.1921E-03 0.3802E-07 0.6072E-08 0.3981E-07 0.4028E-03 0.4074E-07 0.7496E-04 0.4169E-07 0.1356E-03
0.4266E-07 0.3234E-03 0.4365E-07 0.3038E-03 0.4571E-07 0.4460E-03 0.4786E-07 0.2122E-03 0.5012E-07 0.9166E-04
0.5129E-07 0.3068E-03 0.5248E-07 0.1618E-03 0.5370E-07 0.1265E-03 0.5495E-07 0.7276E-05 0.5754E-07 0.6762E-05
0.6166E-07 0.4008E-03 0.6607E-07 0.1344E-03 0.6761E-07 0.1080E-03 0.7079E-07 0.1773E-03 0.7244E-07 0.4384E-04
0.7413E-07 0.6836E-04 0.7586E-07 0.4074E-04

The discrete distributions for frequency of intersection in the same format used for each of the calculation modules listed above.

G.3 REFERENCE

Press, W.H., Flannery, B.P., Teukolsky, S.A., and Vettering, W.T., 1992, Numerical Recipies, the Art of Scientific Computing, Cambridge University Press, 818 p.

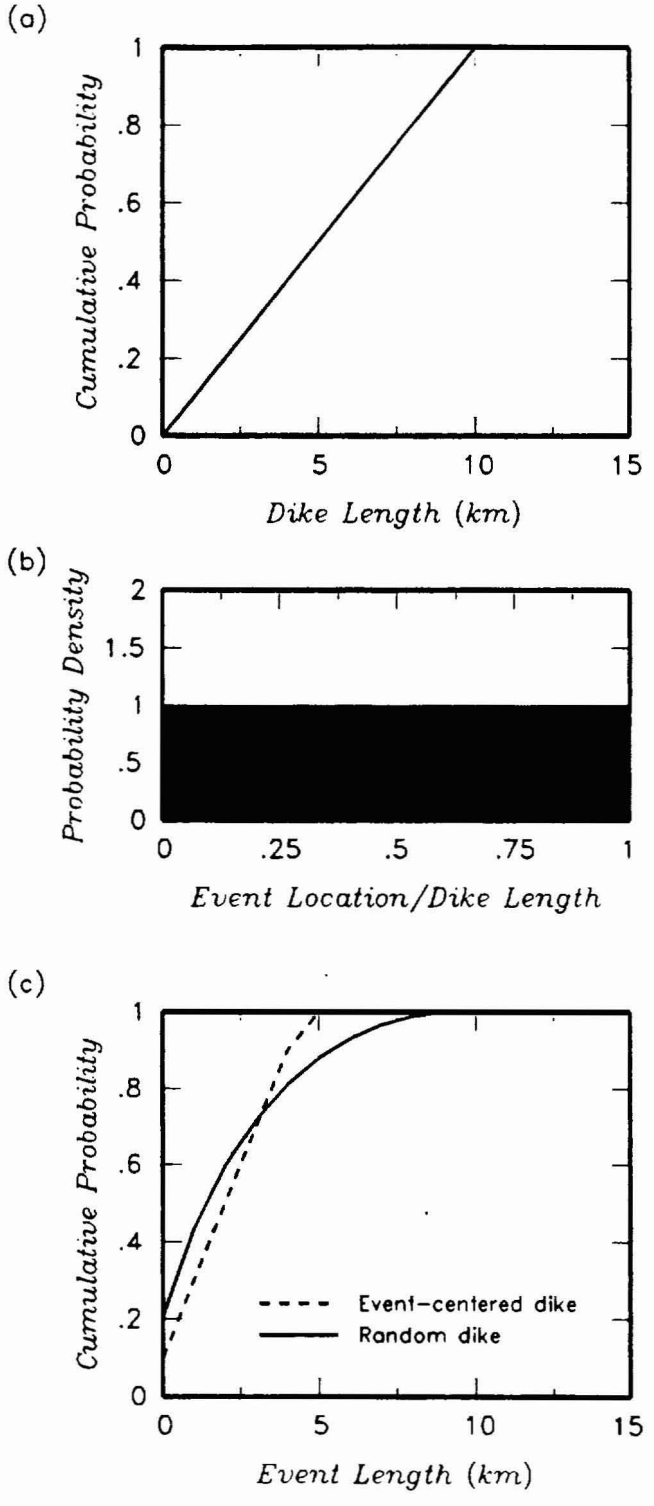

Figure G-1 Development of event length distributions. (a) Expert specified cumulative distribution for total dike length. (b) Expert specified distribution for location of point event on dike. (c) Derived distributions for event length.

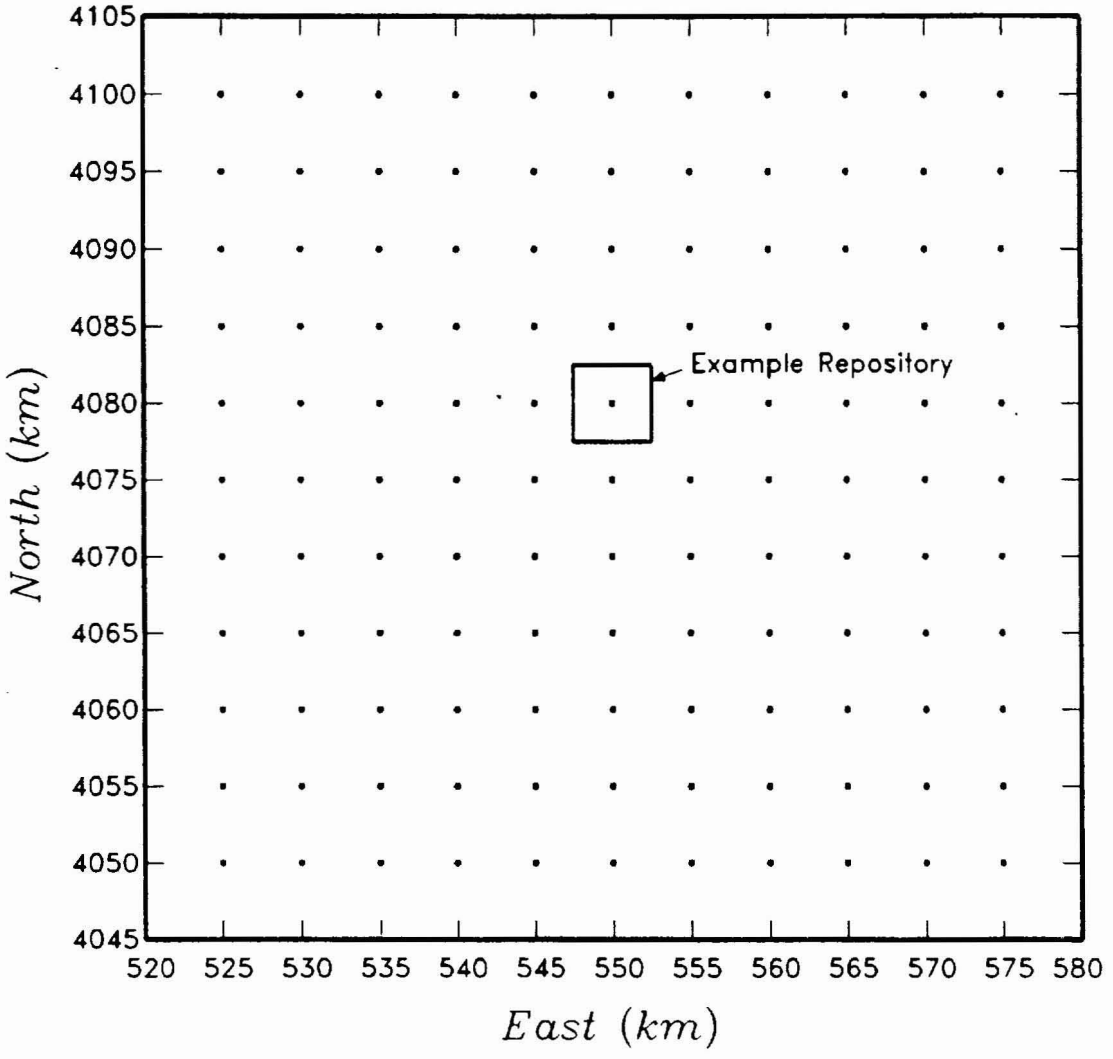

Figure G-2 Example calculation grid with $\Delta x = \Delta y = 5$ km.

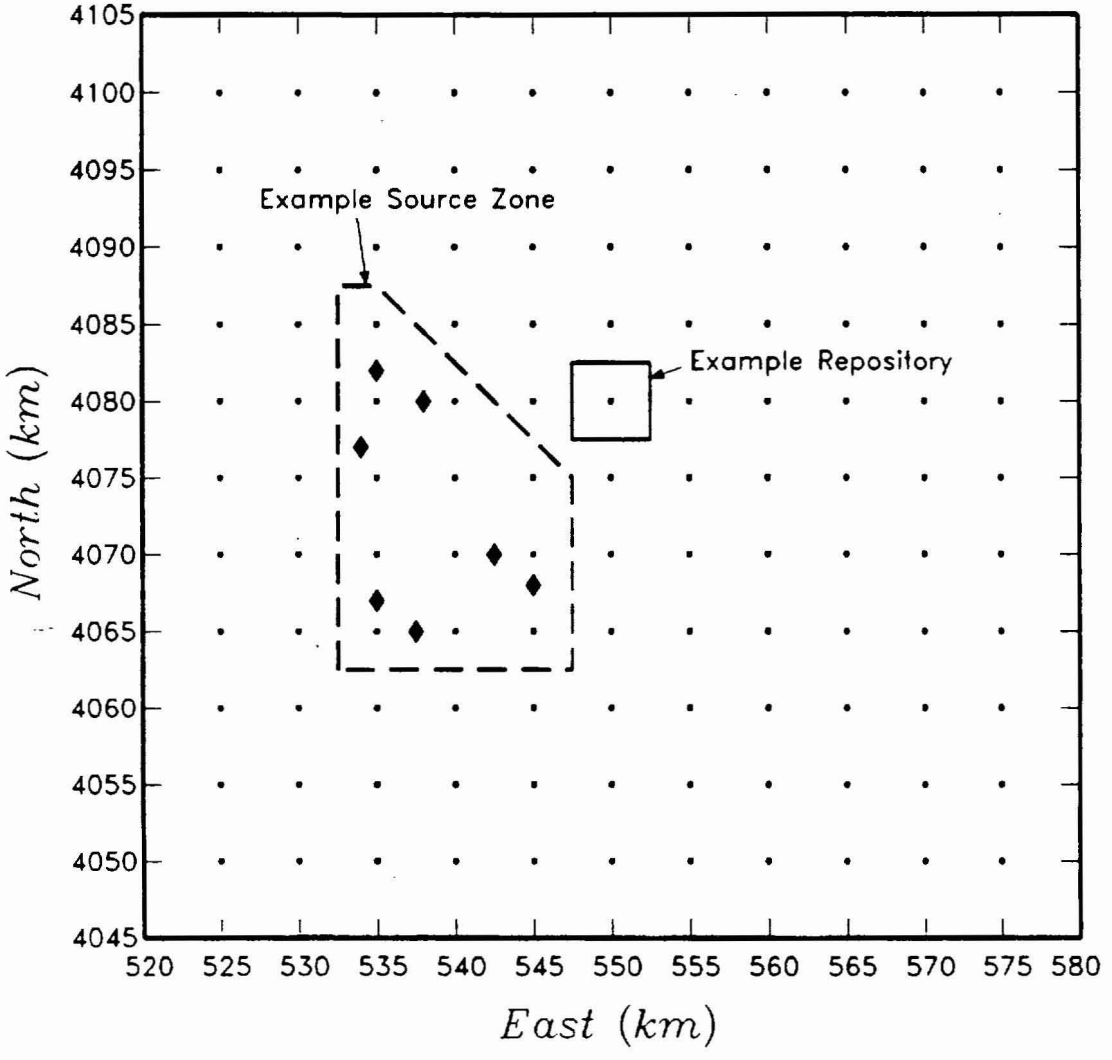

Figure G-3 Example source zone. Diamonds show locations of events, separated into a northern group of three and a southern group of four.

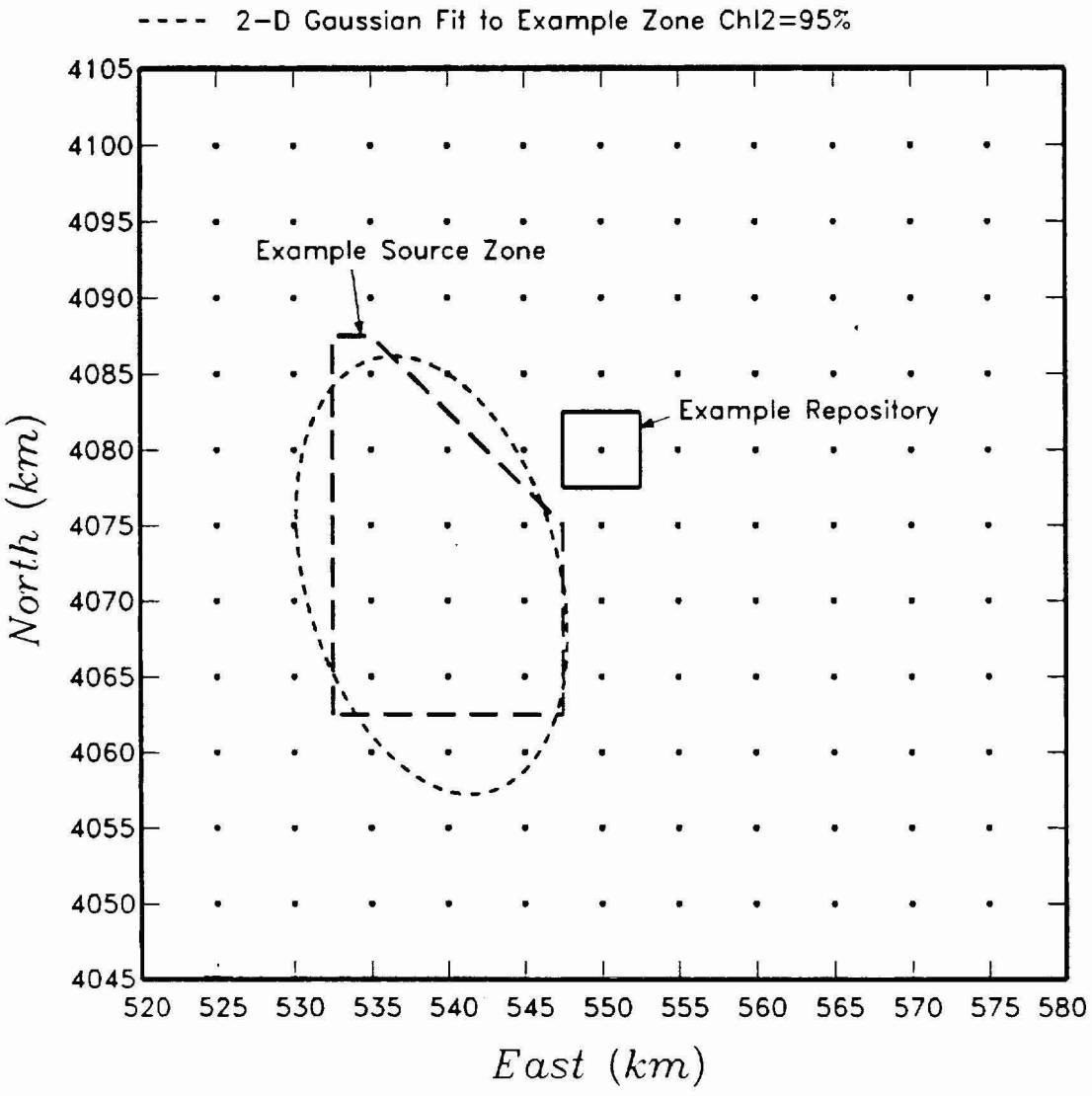

Figure G-4 Fit of a bivariate Gaussian field shape to the example source zone boundary assuming the boundary is an approximate 95 percent density contour.

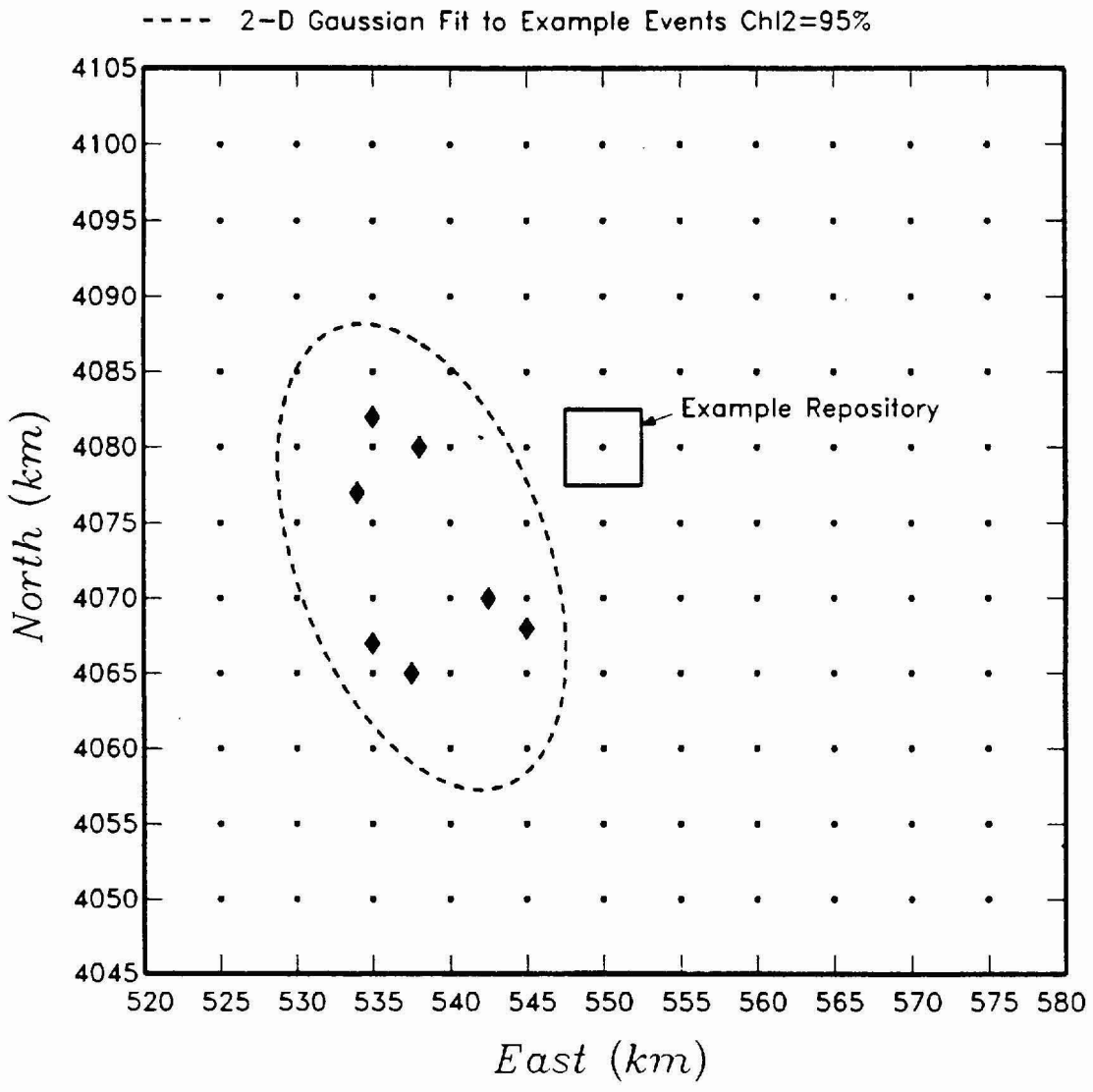

Figure G-5 Fit of a bivariate Gaussian field shape to the events shown on Figure G-3. The ellipse defines the 95-percent density contour.

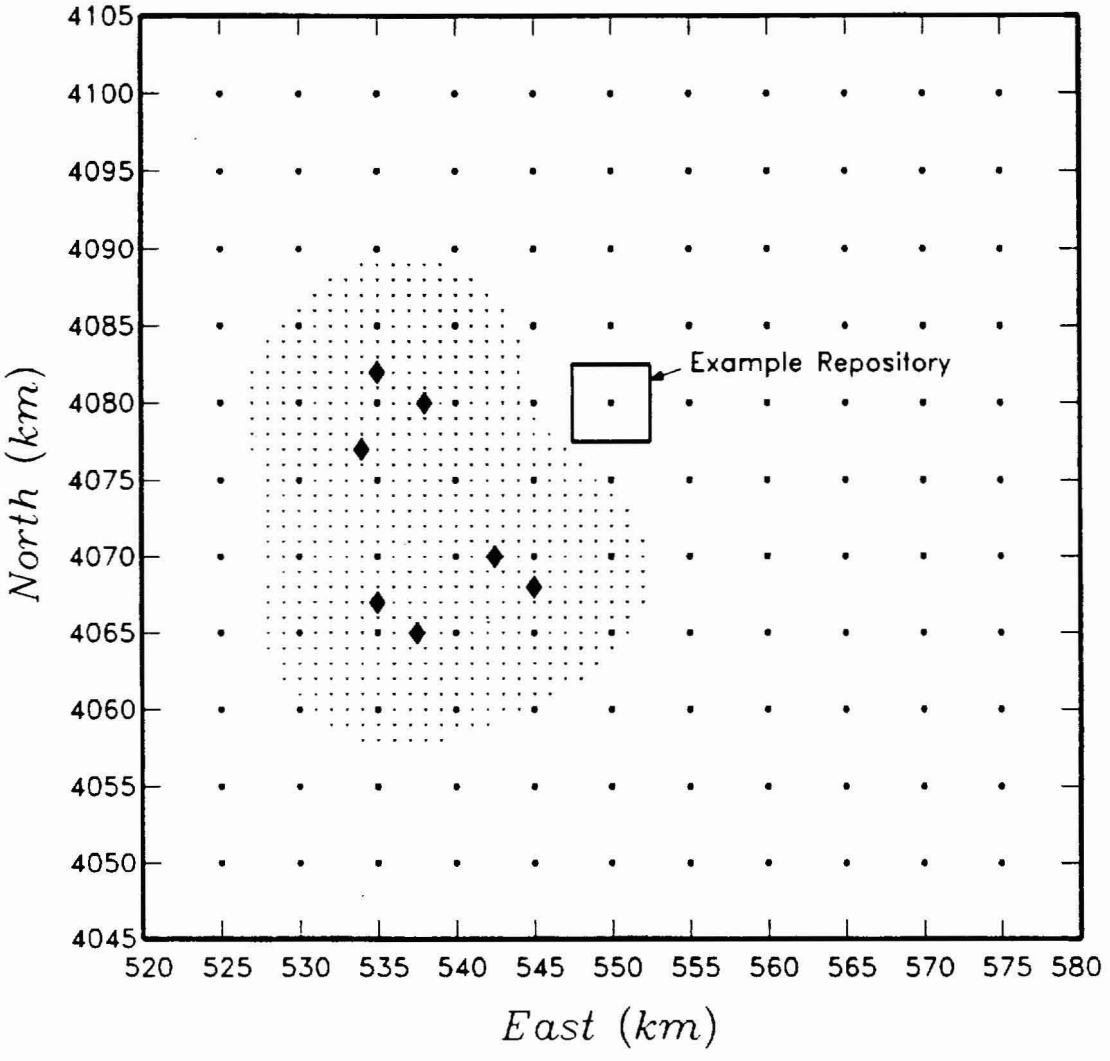

Figure G-6 Example kernel density estimation with fixed h. Stippled area defines the 95 percent density contour computed with an Epanechnikov kernel and h = 10 km.

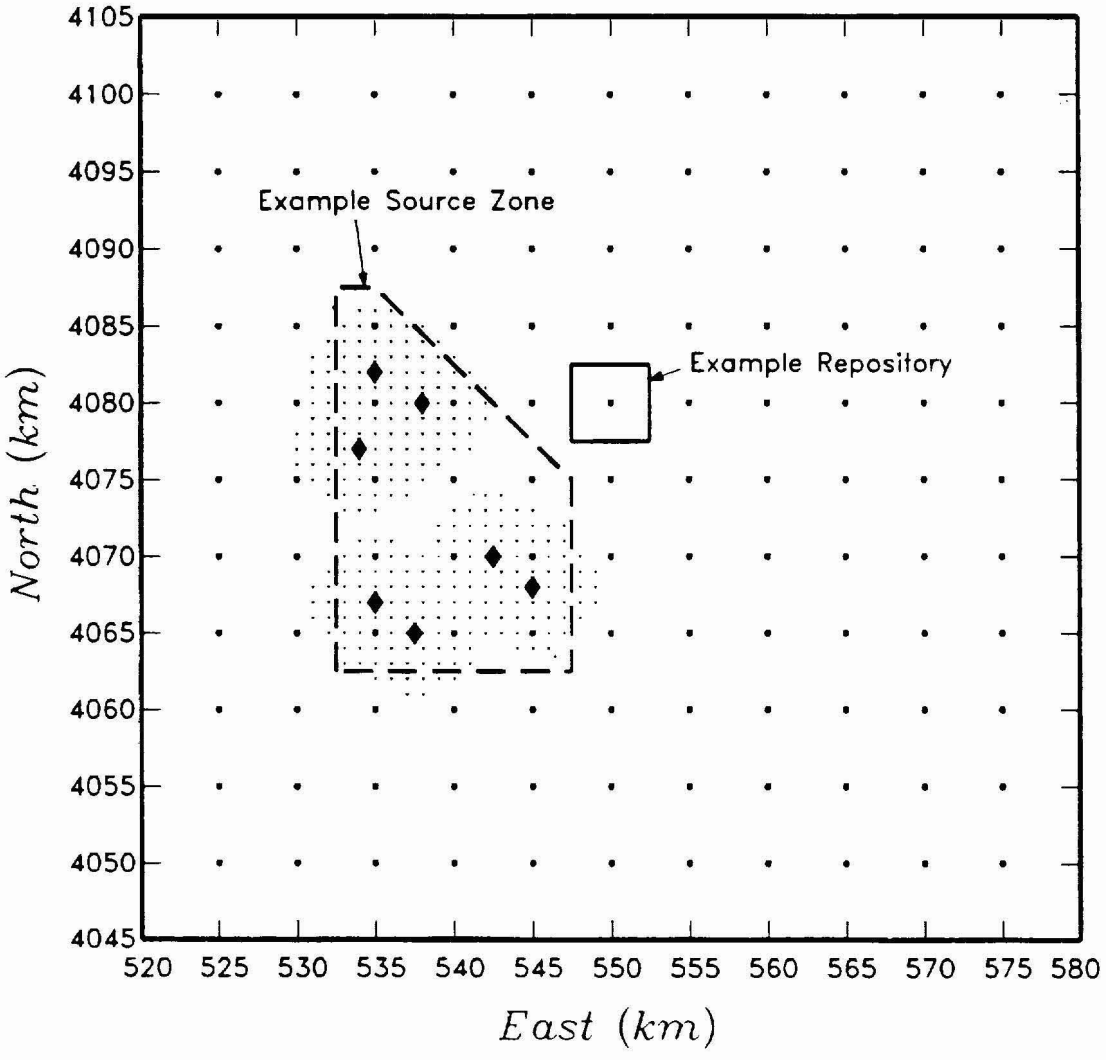

Figure G-7 Fit of a kernel density function to the example source zone boundary assuming the boundary is an approximate 95 percent density contour. The resulting value of h is 5.2 km.

APPENDIX H

QUALITY ASSURANCE

APPENDIX H
QUALITY ASSURANCE

The OCRWM Quality Assurance program is applicable to this document. Preparation of the document was consistent with Civilian Radioactive Waste Management System Management and Operating Contractor (M&O) Quality Administrative Procedure (QAP) QAP-3-5, Revision 6, "Development of Technical Documents." This procedure defines the requirements for preparation of technical documents that are subject to the requirements of the Quality Assurance Requirements and Description (QARD; DOE/RW-0333P, Revision 5). QAP-3-5 is the QA program vehicle used to control and document the PVHA task. This appendix to the Probabilistic Volcanic Hazard Analysis (PVHA) presents the relevant discussion of the QA program requirements from Section 5.2.C of the procedure which are not specifically addressed in other sections of the document.

An M&O QAP-2-0, "Control of Activities," Activity Evaluation was prepared specifically for the PVHA task and is maintained as a controlled document under Document Identifier B00000000-01717-2200-00112. This Activity Evaluation described the purpose of the PVHA, evaluated the applicability of the QARD, and established the procedures that applied to this task. "Classification of Permanent Items," M&O QAP-2-3, does not apply to this activity since the report does not address any permanent items as defined under this procedure. No determination of importance evaluations were necessary under M&O Nevada Line Procedure (NLP) NLP-2-0 as the PVHA involved only analysis of existing data which was generated during previous activities.

Qualification of PVHA Inputs and Outputs

Section 5.2.C.4 of QAP-3-5 requires identification of unqualified design input and data. As is summarized in Section 2.1.1 of the report, the required inputs for the PVHA task are any available pertinent or corroborating data, regardless of source. The sources of all input used in

the PVHA are identified as standard scientific bibliographic citations in the references sections. The data themselves do not provide an interpretation of the volcanic hazard at the site. Rather, it is the expert elicitation process that evaluates, integrates and interprets the data (inputs), and results in a qualified analysis of the hazard. Therefore, it is unnecessary to discriminate between qualified data and unqualified data in this report.

As discussed in Section 2.1.2, formal guidance for the expert elicitation process has been developed and established, and the methods have been successfully applied in other comparable analyses. The expert elicitation methods developed and applied in this analysis are clearly and carefully documented in Section 2.0 of the report.

The purpose of the expert elicitation was to characterize uncertainties in the hazard analysis. The results of the PVHA describe the expected annual frequency of a volcanic event intersecting the potential Mined Geological Disposal System repository footprint. Despite variations in interpretations and analytical assumptions between the experts, the hazard estimates are consistent among the experts.